



# Single Cell Genomics Identifies Unique Cardioprotective Phenotype of Stem Cells derived from Epicardial Adipose Tissue under Ischemia

Finosh G. Thankam<sup>1</sup> · Devendra K. Agrawal<sup>1</sup>

Accepted: 28 September 2021 / Published online: 18 October 2021

© The Author(s), under exclusive licence to Springer Science+Business Media, LLC, part of Springer Nature 2021

## Abstract

The conventional management strategies of myocardial infarction (MI) are effective to sustain life; however, myocardial regeneration has not been achieved owing to the inherently poor regenerative capacity of the native myocardium. Stem cell-based therapies are promising; however, lineage specificity and undesired differentiation profile are challenging. Herein, we focused on the epicardial fat (EF) as an ideal source for mesenchymal stem cells (MSCs) owing to the proximity and same microvasculature with cardiac muscle. Unfortunately, the epicardial adipose tissue derived stem cells (EATDS) remain understudied regarding their phenotype heterogeneity and cardiac regeneration potential. As EF closely reflects the cardiac pathology during ischemia, the present study aims to determine the EATDS subpopulations under simulated ischemic and reperfused conditions employing single cell RNA sequencing (scRNAseq). EATDS were isolated from three hyperlipidemic Yucatan microswine and were divided into Control, Ischemia (ISC), and Ischemia/reperfusion (ISC/R). The scRNAseq analysis was performed using 10 genomics platform which revealed 18 unique cell clusters suggesting the existence of heterogeneous phenotypes. The upregulated genes were taken into consideration and subsequent functional assessment revealed the cardioprotective phenotypes with diverse mechanisms including epigenetic regulation (Cluster 1), myocardial homeostasis (Cluster 1), cell integrity and cell cycle (Clusters 2 and 3), prevention of fibroblast differentiation (Cluster 4), differentiation to myocardial lineage (Cluster 6), anti-inflammatory responses (Clusters 5, 8, and 11), prevention of ER-stress (Cluster 9), and increasing the energy metabolism (Cluster 10). These unique phenotypes of heterogeneous EATDS population open significant translational opportunities for myocardial regeneration and cardiac management.

**Keywords** Cardiac ischemia · scRNAseq · Epicardial adipose tissue derived stem cells · Stem cell heterogeneity · Myocardial regeneration

## Introduction

Myocardial infarction results in the permanent loss of cardiomyocytes (CM) in the ischemic myocardium significantly affecting the functional performance of the surviving heart and ultimately contributes to heart failure (HF). Every year, the myocardial ischemia results in the death of more than seven million sufferers globally and remarkably impacts the quality of life of the survivors [1]. Current therapeutic interventions including revascularization, drugs and medications, and cardiac resynchronization have been widely practiced

which benefitted millions of sufferers across the globe. However, current management strategies are far from myocardial regeneration owing to the inherently poor regenerative capacity of the native heart tissue [1, 2]. Hence, the cell-based therapies have gained global interest for myocardial regeneration where diverse cell types including mesenchymal stem cells (MSCs) and fibroblasts have been attempted [3]. Among them, adipose-derived mesenchymal stem cells (ADMSCs) have been hailed as a practical source owing to the ease and minimal invasiveness of harvesting, autologous resources, excellent plasticity, and superior cardiac differentiation potential [4].

Interestingly, early reports unveiled the existence of resident stem cell population in the myocardium which represent less than 1% of the total cell population in the heart. These resident stem cell population possesses immense translational potential as they accelerate cardiac

✉ Finosh G. Thankam  
FThankam@westernu.edu

<sup>1</sup> Department of Translational Research, Western University of Health Sciences, 309 E. Second Street, Pomona, CA 91766-1854, USA

regeneration following an injury and maintain the cardiac lineage specificity; however, their limited numbers, difficulty in isolation and unavailability of myocardial tissue source offer roadblocks [5]. Importantly, the possibility of cardiac regenerative responses facilitated by adjacent tissues especially epicardial fat (EF) cannot be ignored as EF shares same microvasculature and exist in proximity with myocardium supporting normal cardiac function. In contrast, EF-derived proinflammatory milieu is intimately associated with coronary artery diseases and myocardial ischemia [6, 7]. However, EF remains to be an abundant repository for MSCs eliciting cardiac protective responses via paracrine and vasocrine signaling [8]. Unfortunately, the cardiac regeneration potential of epicardial adipose tissue derived stem cells (EATDS) warrants careful investigation with identification of specific stem cell phenotype.

MSCs are heterogeneous population and the identification of ideal phenotype is crucial in regenerative medicine to obtain reproducible outcomes; however, is challenging [9]. Moreover, information regarding the subpopulations and cardiac regenerative potential of EATDS are currently unavailable despite the recent advancements in adipobiology. In addition, the single cell genomics data regarding the heterogeneity of EATDS have not been reported yet. As EF closely reflects the cardiac pathology during ischemia, the present study aims to determine the EATDS subpopulations under in vitro simulated ischemic and reperfused conditions employing single cell RNA sequencing (scRNAseq) with a focus on the upregulated genes in distinct clusters.

## Methodology

### Isolation and Maintenance of EATDS

EATDS were isolated employing collagenase digestion method from three hyperlipidemic Yucatan microswine (*Sus scrofa*, Sinclair bioresources) post-sacrifice. Hyperlipidemia was induced to the animals (8–10 months of age, weighing 60–80 pound) by feeding with high cholesterol high fat diet, and the weight gain and blood chemistry were monitored regularly as reported in our previous study [10]. The harvested stem cells were maintained in DMEM with 10% fetal bovine serum (FBS) (Cat# 30–2020, ATCC) and antibiotics. The stem cells in passage 0–2 were used for the study and were characterized by the expression status for the biomarkers including CD90, CD105,  $\alpha$ SMA, vimentin, Sox2, Oct3/4 CD34, CD44 and CD31 following our previously published reports [11].

### Ischemia and Reperfusion

The isolated EATDS were grouped into Group I (Control), Group II (Ischemia only) (ISC), and Group III (Ischemia and reperfusion) (ISC/R). Ischemia was simulated by treating the cells in ischemic buffer (118 mM NaCl, 24 mM Na<sub>2</sub>HCO<sub>3</sub>, 1 mM Na<sub>2</sub>HPO<sub>4</sub>, 2.5 mM CaCl<sub>2</sub>, 1.2 mM, MgCl<sub>2</sub>, 20 mM sodium lactate, 16 mM KCl, 10 mM 2-deoxyglucose and pH 6.2) for 2 h and reperfusion was attained by replacing the ischemic buffer with complete culture media overnight. The treatment with ischemic buffer results in hypoxia and the reoxygenation was achieved using complete media and the experimental groups were defined accordingly. ISC group tolerated hypoxia/anoxia due to treatment with ischemic buffer, ISC/R group received reoxygenation following ischemia due to the treatment with complete media, and the cells grown in complete media served as control.

### Single Cell RNA Sequencing (scRNA-seq)

EATDS were pooled from three swine and used for scRNAseq analysis. Single-cell library preparation was performed in the commercially available 10× Genomics Chromium System (Children's Hospital Los Angeles SC2 Core, CA) exploiting the droplet method. The library generation was performed using the Chromium Single Cell 5' v2 chemistry to capture ~ 10,000 cells per sample. For the analysis, the cells from three pigs were pooled in each experimental group. Reagents and cells were combined to generate GEMs (Gel Beads-in-Emulsion) in such a way that single cells were partitioned with unique, cell-linked molecular barcodes following the cell sorting and counting which were loaded on the microfluidics Chip K. The samples were sequenced on the Illumina HiSeq 2500 and the Illumina NextSeq 500 high output at ~ 20,000 reads/cell. The generated raw scRNA-seq data was processed using the 10× Genomics Cell Ranger pipeline and the data obtained from the Illumina NextSeq platform was processed to Fastq files using the Cell Ranger mkfastq program. Then, the Fastq files were mapped to the *sus\_scrofa\_11* database ([https://uswest.ensembl.org/Sus\\_scrofa/Info/Index](https://uswest.ensembl.org/Sus_scrofa/Info/Index)). The Cell Ranger count program was run on individual Fastq datasets from the different treatment conditions and Cell Ranger aggr was employed to generate aggregated unique molecular identifier (UMI) count matrices for the experimental datasets generated from the study.

Statistical analysis for the expression status of the scRNA-seq data was performed by the statistical program associated with the 10× platform [12]. The processed data revealing the cell clusters was examined in the Loupe

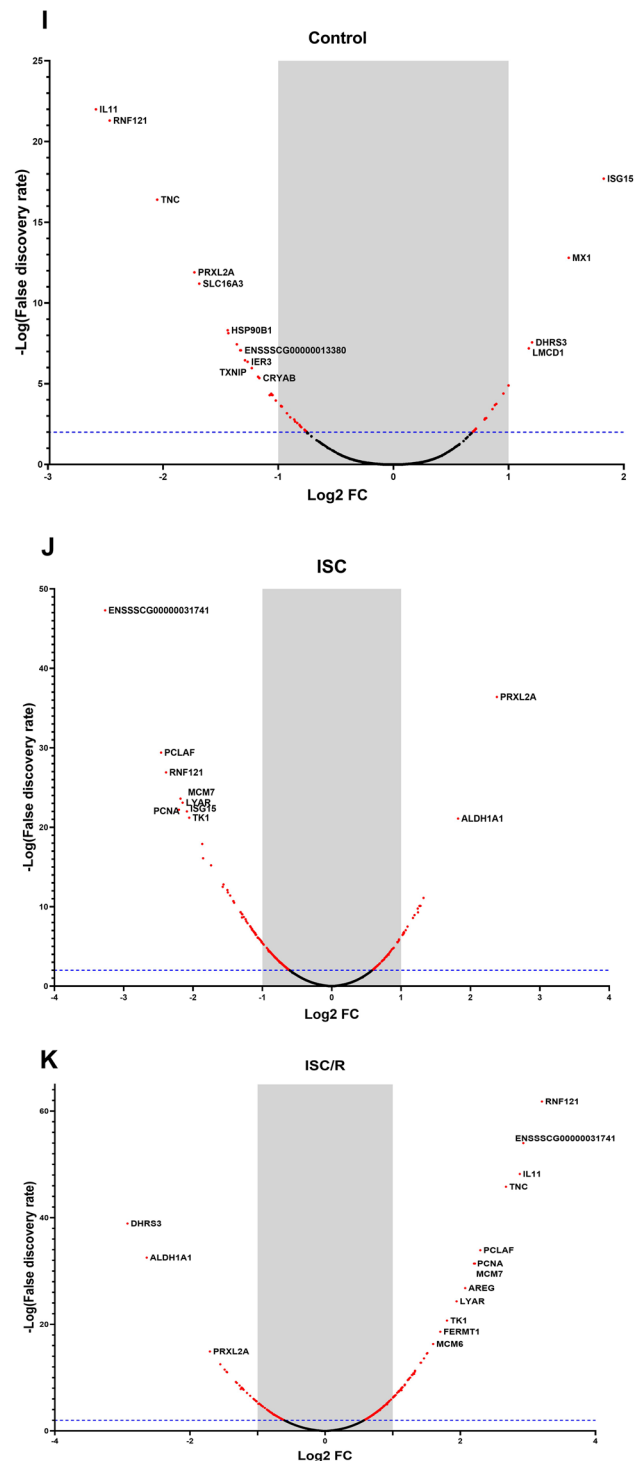
**Fig. 1** (A) Immunofluorescence analysis for the protein expression of biomarkers in cultured EATDS. Images in the top panel show overlaid images of biomarkers with the nuclear stain DAPI. Images were acquired at 20× magnification using CCD camera attached to the Leica Thunder microscope. The images right to the overlaid images reveal the UMAP analysis of the scRNAseq data revealing the expression status of each gene in the total cell population. Images in the lower panel show the violin plots showing the distribution of gene expression in each cluster. Distribution of cell populations and altered genes in ISC-EATDS: (B) UMAP analysis revealing three distinct population of cells as evident by green (ISC), orange (control) and blue (ISC/R) spots. (C) Heat map showing the spatial expression of 763 genes identified from EATDS based on the upregulation in ISC group. (D) Scatter plot showing the FC expression indicating the upregulation of genes in ISC than control and ISC/R. (E) Violin plot showing the distribution of upregulated genes in which the ISC group showing trend towards >1 FC. (F) Heat map of highly altered 16 genes (FC > 2) revealing the upregulation in ISC group. (G) Scatterplot of highly expressed genes showing the minimal level of expression in control and ISC/R group and increased expression in ISC group. (H) Violin plot for highly expressed genes revealing the distribution towards upregulation in ISC compared to control and ISC/R. Volcano plots displaying the differential expression (both upregulated and downregulated) of key genes in (I) control, (J) ISC and (K) ISC/R groups

Browser 5.0.1. using graph-based analysis mode. The clusters of interests were analyzed in LibraryId mode to assess the gene expression and cell count in each experimental group. The comparison was performed based on the number of cells mapped in each cluster and the locally upregulated genes were listed compared to the control. The genes were sorted based on the fold-change of upregulation where  $FC < 2$  was omitted from the listing. Similarly, the cell clusters/populations < 2% of the total population was omitted to obtain reliable data. Also, the biomarker expression was assessed from the scRNAseq data based on the gene/feature expression mode.

## Results

### Single Cell Genomics

Web-summary of the scRNAseq data profile for the spatial gene expression using barcoding-based transcriptomics technology of 10 Genomics platform revealed > 91% Fraction Reads in Cells (FRC) and > 98% valid barcodes in control, ISC and ISC/R groups suggesting the effective sample preparation providing healthy cells for the analysis. Estimated number of cells, mean reads per cell, and median genes per cell obtained were 6922, 49,027 and 4066, 9791, 28,912 and 3151 and 8808, 30,135 and 3483, respectively for control, ISC and ISC/R groups with a total estimate of 25,521 cells, 711,958,422 total sequencing reads (Post-normalization), 27,897 mean reads per cell (Post-normalization), and 3,299 mean genes per cells throughout all three samples. Overall,



the Loupe analysis revealed heterogeneous cell clusters in ISC, and ISC/R groups compared to the control cells.

The EATDS were positive for the mesenchymal markers, vimentin and  $\alpha$ SMA, and the stem cell markers, SOX2, CD90 and Oct3/4 and the adipocyte marker adiponectin, as evident from the immunostaining. The cells were negative for CD105, CD14, CD44, and CD34 (Fig. 1A). Similar trend

was obtained from scRNAseq data where the transcriptomics of vimentin and  $\alpha$ SMA was evident from the mean fold change  $> 100$  in the violin plots (Fig. 1A). Similarly, the negative biomarkers displayed the fold change  $\leq 1$  as displayed in the violin plots (Fig. 1A). However, the details for SOX2 and Oct3/4 were unavailable in the database. Based on the characterization, the EATDS were defined to be Vim + /  $\alpha$ SMA + / SOX2 + / Oct3/4 / CD90- / CD105- / CD14- / CD44- / CD34- / ADIPOQ-.

UMAP analysis revealed three unique population of cells each representing control, ISC and ISC/R (Fig. 1B). The cells from control and ISC/R were clustered together whereas ISC cells were distinct from the other two groups. Also, 763 genes were highly altered in the global population of EATDS cells where the sorting was performed based on the extent of upregulation in the ISC group (Supplementary Table 1, Fig. 1C and D). The violin plot revealed that the distribution of cells, based on the expression of these genes, were trending to be FC  $> 1$  whereas the cells in the control and ISC groups were clustered around FC = 1 displaying uniform distribution. However, a few genes in control cells tend towards FC  $> 1$  (Fig. 1D and E). Sixteen genes (FC  $> 2$ ) were significantly increased in ISC group on comparison with the control and ISC/R where PRXL2A (Peroxiredoxin like 2A) exhibited maximum FC of 5.21 ( $P < 0.0001$ ) (Table 1, Fig. 1F–H). The FC values of these 16 genes in the control and ISC/R groups were distributed mostly around 1 whereas FC  $> 2$  was evident in ISC group (Fig. 1F–H). Apart from the 16 genes in ISC, DHRS3 gene was only one to be upregulated (FC = 2.30,  $P < 0.0001$ ) in the other two groups. Overall, the data suggest a unique population of ISC cells which tend to revert towards control lineage upon reperfusion. The

volcano plot revealed the of downregulation IL-11, TNC, PRXL2A, and RNF121 (Ring Finger Protein 121) in the control cells with a concomitant upregulation of ISG15 (Interferon-stimulated gene 15), MX1 (MX dynamin like GTPase 1), DHRS3, and LMCD1 (LIM and Cysteine Rich Domains 1) (Fig. 1I). The ISC cells revealed the downregulation of ENSG00000171848 (RRM2, ribonucleotide reductase regulatory subunit M2), PCNA, MCM7 (mini chromosome maintenance function 7), TK1 (Thymidine Kinase 1) and PCLAF (PCNA Clamp Associated Factor) and the upregulation of PRXL2A and ALDH1A1 (Aldehyde dehydrogenase Family Member A1) (Fig. 1J). Reperfusion resulted in the downregulation of PRXL2A, DHRS3 and ALDH1A1 with an upregulation of IL-11, RRM2, TNC, PRXL2A, PCNA, MCM7, PCLAF, TK1 and RNF121 (Fig. 1K). The t-SNE plot revealed 18 unique clusters of cells overall representing control, ISC and ISC/R (Fig. 2A and B). The number of cells in each cluster and sub-clusters are displayed in Table 2.

**Cluster 1 Cells Favored ISC/R** Cluster 1 exhibited a total number of 3,300 cells where  $\sim 95\%$  cells were mapped in ISC/R group with  $\sim 4\%$  in control groups and  $\sim 0.7\%$  cells in ISC group (Table 2). This suggests the existence of a predominant population of cells in ISC/R which is distinct from control and ISC group. Also, 959 genes were highly altered in the local population of EATDS cells in the cluster 1 where the sorting was based on the extent of gene expression in ISC group (Supplementary Table 2, Fig. 2B–E). The violin and scatter plots revealed that the distribution of cells, based on the expression of these genes, were trending to be FC  $> 1$  in ISC group whereas the cells in the control

**Table 1** The list of genes globally upregulated (FC  $> 2$ ) in ISC group

SI/No	Feature ID	Genes	Control FC	P-value	ISC FC	P-value	ISC/R FC	P-value
1	ENSSSCG00000010340	PRXL2A	0.30	1.16E-12	5.21	4.221E-37	0.31	1.183E-15
2	ENSSSCG00000028996	ALDH1A1	0.85	0.76686	3.53	7.102E-22	0.16	3.112E-33
3	ENSSSCG00000035430	YPEL3	0.72	0.211028	2.50	7.428E-12	0.43	1.252E-08
4	ENSSSCG00000037158	MTURN	0.75	0.366985	2.40	7.78E-11	0.43	1.858E-08
5	ENSSSCG00000008072	ASPN	0.54	0.001191	2.43	7.816E-11	0.59	0.000712
6	ENSSSCG00000026981	MRPS6	0.39	3.64E-08	2.36	1.684E-10	0.75	0.1020607
7	ENSSSCG00000035249	GADD45G	0.79	0.545466	2.37	5.176E-10	0.42	1.378E-08
8	ENSSSCG00000006321	FAM78B	0.67	0.0882	2.29	1.129E-09	0.52	2.199E-05
9	ENSSSCG00000025924	IGFBP5	0.94	0.987756	2.25	2.596E-09	0.37	1.072E-11
10	ENSSSCG00000023298	SRXN1	0.51	0.000255	2.13	3.156E-08	0.72	0.0508004
11	ENSSSCG00000026082	DNAJC3	0.57	0.004895	2.09	9.092E-08	0.67	0.0168039
12	ENSSSCG00000005055	LGALS3	0.73	0.266855	2.06	1.589E-07	0.56	0.0001643
13	ENSSSCG00000000857	IGF1	0.74	0.297713	2.06	1.893E-07	0.56	0.0001438
14	ENSSSCG00000036724	CRYAB	0.45	4.42E-06	2.04	2.109E-07	0.82	0.3226654
15	ENSSSCG00000006308	CREG1	0.73	0.277911	2.04	2.903E-07	0.57	0.0002524
16	ENSSSCG00000005601	HSPA5	0.65	0.060315	2.03	3.514E-07	0.63	0.0041015

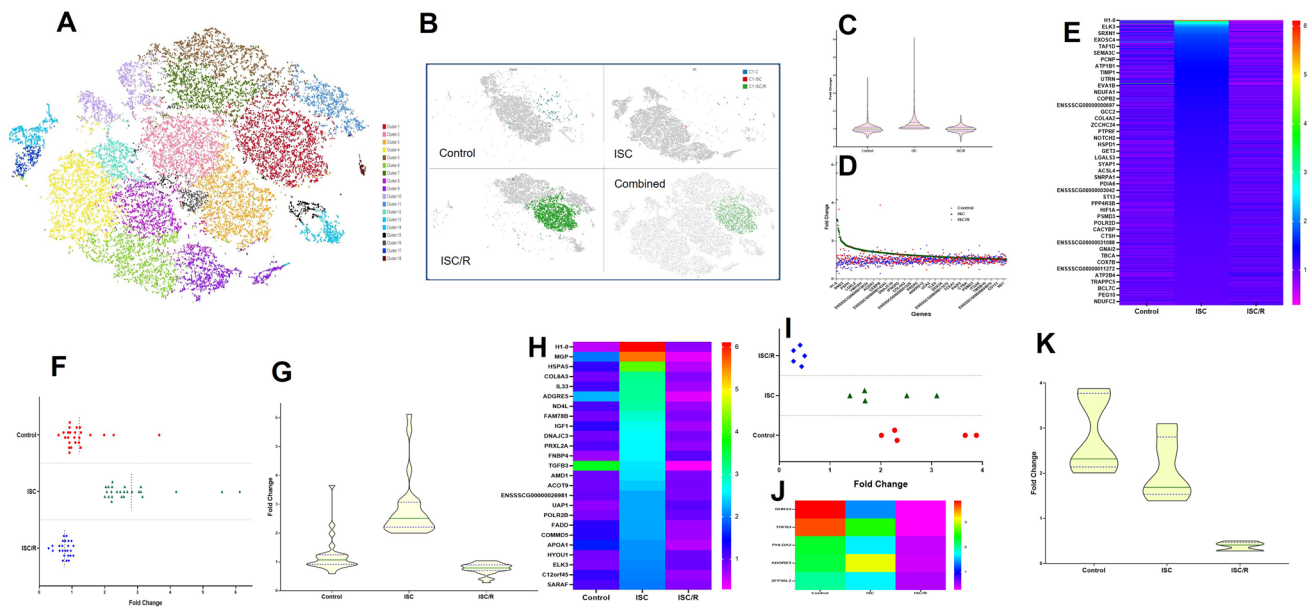


**Fig. 2** Distribution of cell populations and altered genes in Cluster 1: (A) t-SNE plot revealing 18 distinct clusters of cells in the global population of EATDS. (B) Split view of Control, ISC and ISC/R groups and combined view of t-SNE plot showing the distribution of cells within the Cluster 1 based on the local expression of 959 genes. (C) Violin plot showing the distribution of upregulated genes in which the ISC group showing trend towards > 1 FC. (D) Scatter plot showing the FC expression indicating the upregulation of genes in ISC than control and ISC/R. (E) Heat map showing the local expression of 959 genes identified from EATDS based on the upregulation in ISC group. (F) Scatterplot of highly expressed 25 genes in ISC group showing the minimal level of expression in control and ISC/R

group where the dotted lines indicate mean FC of 25 genes. (G) Violin plot for highly expressed 5 genes in Control group revealing the trend towards upregulation in ISC and downregulation in ISC/R. (H) Heat map of highly altered 5 genes (FC > 2) in Control group compared to ISC and ISC/R groups. (I) Scatterplot of highly expressed 5 genes (FC > 2) in the Control group showing the minimal level of expression in ISC/R and similar level of expression in ISC. (J) Heat map of highly altered 5 genes (FC > 2) in Control group compared to ISC and ISC/R groups. (K) Violin plot for highly expressed 5 genes in Control group revealing the trend towards upregulation in ISC and downregulation in ISC/R

**Table 2** Cell density in each cluster

Clusters	No. of cells	Control	ISC	ISC/R	% Control	% ISC	% ISC/R
Cluster 1	3300	139	22	3139	4.21	0.67	95.12
Cluster 2	2617	2454	29	134	93.77	1.11	5.12
Cluster 3	2612	2489	50	73	95.29	1.91	2.79
Cluster 4	2585	13	2570	2	0.50	99.42	0.08
Cluster 5	1998	79	3	1915	3.95	0.15	95.85
Cluster 6	1947	33	1911	3	1.69	98.15	0.15
Cluster 7	1746	125	15	1606	7.16	0.86	91.98
Cluster 8	1721	109	1607	5	6.33	93.38	0.29
Cluster 9	1286	29	1229	28	2.26	95.57	2.18
Cluster 10	1261	713	507	40	56.54	40.21	3.17
Cluster 11	1191	15	2	1174	1.26	0.17	98.57
Cluster 12	824	6	816	1	0.73	99.03	0.12
Cluster 13	605	93	128	388	15.37	21.16	64.13
Cluster 14	590	55	418	117	9.32	70.85	19.83
Cluster 15	395	176	89	130	44.56	22.53	32.91
Cluster 16	377	366	6	5	97.08	1.59	1.33
Cluster 17	371	5	349	17	1.35	94.07	4.58
Cluster 18	95	23	40	31	24.21	42.11	32.63



and ISC groups were clustered around  $FC = 1$  and displayed uniform distribution. However, a few genes in control cells tend towards  $FC > 1$  (Fig. 2C–E). Twenty-five genes ( $FC > 2$ ) were increased in ISC group on comparison with the control and ISC/R. The DNA binding protein H1-0 (Histone H1.0) exhibited maximum FC of 6.12 followed by the ECM component protein MGP (Matrix Gla Protein) with a FC of 5.58 whereas the FC of other three genes were less than 5 (Table 3, Fig. 2F–H). The FC values of these 25 genes in the control groups were distributed mostly around 1 whereas that of ISC/R were tend mostly towards  $FC < 1$  (Fig. 2F–H). Five genes ( $FC > 2$ ) were increased in Control group on comparison with the ISC and ISC/R where DHRS3 (Short-chain dehydrogenase/reductase 3) and TGF $\beta$ 3

(Transforming growth factor beta 3) were highly upregulated (Table 3, Fig. 2I–K). The violin and scatter plots revealed that the distribution of cells was trending to be  $FC > 2$  in control group and  $FC > 1$  in ISC group whereas the cells in the ISC/R groups were clustered around  $FC < 1$ ; however, displayed uniform distribution (Fig. 2I–K). The genes with  $FC > 2$  was completely absent in ISC/R group suggesting the unique population of cells with basal level of expression.

**Cluster 2 and 3 Tend Towards Normal** Cluster 2 displayed 2,454 cells where ~94% cells were mapped in control group with ~1% in ISC group and ~5% cells in ISC/R group (Fig. 3A, Table 2). This suggests the existence of a predominant population of cells in the control which is distinct from

**Table 3** The list of genes locally upregulated ( $FC > 2$ ) in each group based on Cluster-1 cells

Sl/No	Feature ID	Gene	C1C FC	C1 ISC FC	C1 ISC/R FC
ISC					
1	ENSSSCG00000039348	H1-0	0.59	6.12	0.79
2	ENSSSCG00000037697	MGP	1.98	5.58	0.40
3	ENSSSCG00000005601	HSPA5	1.22	4.18	0.62
4	ENSSSCG00000027331	COL6A3	0.92	3.15	0.83
5	ENSSSCG00000005203	IL33	1.14	3.10	0.71
6	ENSSSCG00000013775	ADGRE5	2.27	3.10	0.41
7	ENSSSCG00000018086	ND4L	1.10	3.04	0.75
8	ENSSSCG00000006321	FAM78B	0.92	2.83	0.86
9	ENSSSCG00000000857	IGF1	1.24	2.69	0.70
10	ENSSSCG00000026082	DNAJC3	0.92	2.61	0.89
11	ENSSSCG00000010340	PRXL2A	1.07	2.59	0.79
12	ENSSSCG00000030610	FNBP4	0.74	2.58	1.04
13	ENSSSCG00000002385	TGFB3	3.66	2.51	0.28
14	ENSSSCG00000004392	AMD1	0.94	2.47	0.88
15	ENSSSCG00000012172	ACOT9	0.93	2.37	0.90
16	ENSSSCG00000026981	ENS- SSCG00000026981	0.97	2.23	0.88
17	ENSSSCG00000006340	UAP1	0.79	2.22	1.04
18	ENSSSCG00000022955	POLR2B	0.88	2.22	0.96
19	ENSSSCG00000030888	FADD	1.26	2.21	0.72
20	ENSSSCG00000035123	COMMD5	1.27	2.20	0.72
21	ENSSSCG00000030921	APOA1	1.56	2.12	0.61
22	ENSSSCG00000015106	HYOU1	0.91	2.11	0.95
23	ENSSSCG00000023803	ELK3	0.88	2.06	0.98
24	ENSSSCG00000027792	C12orf45	1.21	2.03	0.76
25	ENSSSCG00000033402	SARAF	1.09	2.00	0.83
Control					
1	ENSSSCG00000003439	DHRS3	3.88	1.39	0.28
2	ENSSSCG00000002385	TGFB3	3.66	2.51	0.28
3	ENSSSCG00000021597	PHLDA2	2.32	1.68	0.44
4	ENSSSCG00000013775	ADGRE5	2.27	3.10	0.41
5	ENSSSCG00000038549	ZFP36L2	2.01	1.69	0.50
ISC/R					
–	–	–	–	–	–

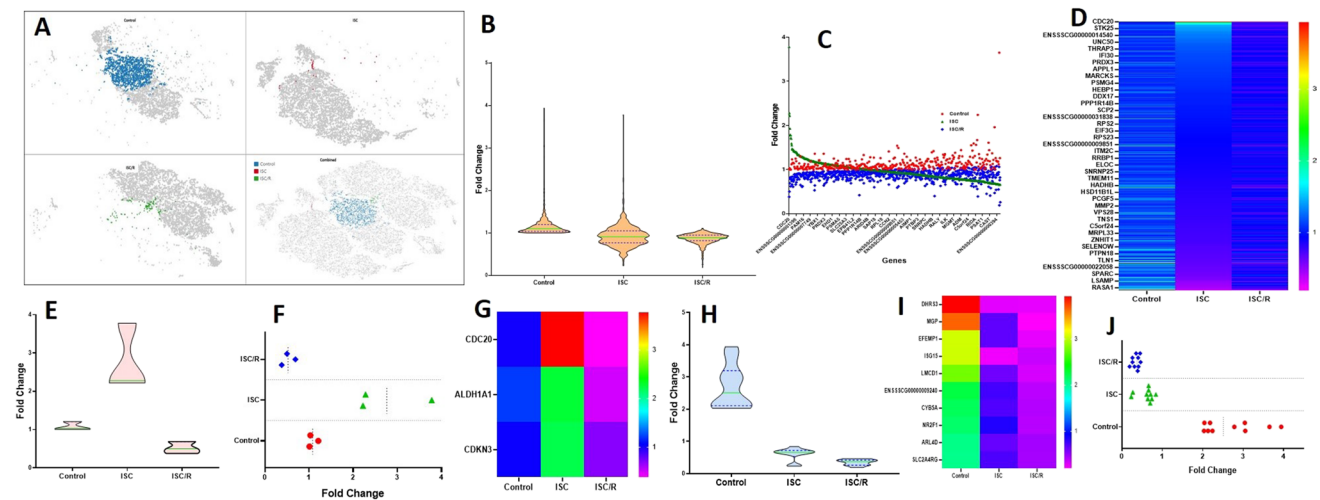


**Fig. 3** Distribution of cell populations and altered genes in Cluster 2: **(A)** Split view of Control, ISC and ISC/R groups and combined view of t-SNE plot showing the distribution of cells within the Cluster 2 based on the local expression of 789 genes. **(B)** Violin plot showing the distribution of upregulated genes in which the ISC group showing uniform distribution around  $FC=1$  whereas the control cells tend towards  $FC>1$ . **(C)** Scatter plot showing the FC expression indicating the upregulation of genes in ISC than control and ISC/R. **(D)** Heat map showing the local expression of 789 genes identified from EATDS based on the upregulation in ISC group. **(E)** Violin plot for highly expressed 3 genes revealing the distribution towards upregu-

lation in ISC compared to control and ISC/R. **(F)** Scatterplot of highly expressed 3 genes in ISC group showing the minimal level of expression in control and ISC/R group where the dotted lines indicate mean FC. **(G)** Heat map of highly altered 3 genes ( $FC>2$ ) revealing the upregulation in ISC group. **(H)** Violin plot for highly expressed 10 genes in Control group revealing the trend towards upregulation whereas downregulation and uniform distribution in ISC and ISC/R. **(I)** Scatterplot of highly expressed 10 genes ( $FC>2$ ) in the Control group showing the minimal level of expression in ISC/R and similar level of expression in ISC. **(J)** Heat map of highly altered 10 genes ( $FC>2$ ) in Control group compared to ISC and ISC/R groups

ISC and ISC/R groups. Interestingly, 789 genes were highly altered in the local population of EATDS cells in the Cluster 2 where the sorting was based on the extent of gene expression in ISC group (Supplementary Table 3, Fig. 3B–D). The violin and scatter plots revealed that the distribution of cells, based on the expression of these genes, were trending to be  $FC>1$  in control group whereas the cells in the ISC and ISC/R groups were clustered around  $FC=1$ . However, a few genes in ISC cells tend towards  $FC>1$  (Fig. 3B–D). Three genes ( $FC>2$ ) were increased in ISC group on comparison with the control and ISC/R. The cell cycle mediator CDC20 (Cell division cycle protein 20 homolog) exhibited maximum FC of 3.28 whereas the FC of other two genes were less than 3 (Table 4, Fig. 3E–G). The FC values of these 3 genes in the control groups were distributed mostly around 1 whereas that of ISC/R were tend mostly towards  $FC<1$  (Table 4, Fig. 3E–G). Ten genes ( $FC>2$ ) were increased in control group on comparison with the ISC and ISC/R. The highly expressed genes were DHRS3 ( $FC=3.94$ ), and MGP ( $FC=3.65$ ) whereas the remaining 8 genes displayed  $FC\leq 3$  (Table 4, Fig. 3H–J). The violin and scatter plots revealed that the distribution of cells was trending to be  $FC>2$  in control group and  $FC<1$  in ISC and ISC/R groups which displayed distribution around the median FC. The genes with  $FC>2$  was completely absent in ISC/R group suggesting the unique population of cells with basal level of expression.

Similarly, the cluster 3 displayed 2,612 cells where ~95% cells were mapped in control group with ~2% in the ISC group and ~3% cells in ISC/R group (Fig. 4A–D, Table 2) (Supplementary Table 4). This suggests the existence of a predominant population of cells in the control which is distinct from ISC and ISC/R group. Interestingly, 970 genes were detected to be highly altered in the local population of EATDS cells in the cluster 3 where the sorting was based on the extent of gene expression in ISC group. However, all genes except CCN5 (Cellular Communication Network Factor 5) in the control group exhibited  $FC<2$ .

**Cluster 4 Cells Tend Toward Ischemia** Cluster 4 displayed 2,585 cells where ~99.5% cells were mapped in the ISC group, and control group with ~0.5%; however, ISC/R group displayed negligible cells (Fig. 4E, Table 2). Hence, the comparison was between ISC and control groups. This suggests the existence of a predominant population of cells in the ISC group which is distinct from the control. Interestingly, 1,431 genes were detected in the locally in the Cluster 4 where the sorting was based on the extent of gene expression in control group (Supplementary Table 5, Fig. 4E–H). The violin and scatter plots revealed that the distribution of cells trending to be  $FC>1$  in control group whereas the cells in the ISC group were clustered around  $FC=1$  (Fig. 4F–H). Interestingly, 95 genes ( $FC>2$ ) were

**Table 4** The list of genes locally upregulated (FC > 2) in each group based on Cluster 2 cells

Sl/No	Feature ID	Gene	C1 C FC	C1 ISC FC	C1 ISC/R FC
ISC					
1	ENSSSCG00000003949	CDC20	1.01	3.78	0.38
2	ENSSSCG00000028996	ALDH1A1	1.21	2.28	0.50
3	ENSSSCG00000005047	CDKN3	1.03	2.22	0.69
Control					
4	ENSSSCG00000003439	DHRS3	3.94	0.27	0.26
5	ENSSSCG00000037697	MGP	3.65	0.66	0.19
6	ENSSSCG00000008397	EFEMP1	3.05	0.66	0.26
7	ENSSSCG00000040575	ISG15	3.04	0.23	0.35
8	ENSSSCG00000011538	LMCD1	2.78	0.61	0.31
9	ENSSSCG00000009240	ENS- SSCG00000009240	2.24	0.74	0.39
10	ENSSSCG00000004875	CYB5A	2.18	0.70	0.41
11	ENSSSCG00000014157	NR2F1	2.13	0.84	0.40
12	ENSSSCG00000017380	ARL4D	2.04	0.64	0.46
13	ENSSSCG00000037562	SLC2A4RG	2.03	0.71	0.45
ISC/R					
	–	–	–	–	–

downregulated in ISC group on comparison with the control. The FC values of these 95 genes in the control groups were distributed mostly around 2 whereas that of ISC were tend mostly towards FC < 1 (Table 5). Similarly, the violin and scatter plots revealed that the distribution of cells was trending to be FC > 2 in control group and FC < 1 in ISC (Fig. 4I–K). The fibroblast differentiation protein NREP (Neuronal Regeneration-Related Protein) exhibited maximum FC of 6.13 whereas the FC RAMP1 (Receptor Activity Modifying Protein 1), PICK1 (Protein Interacting with PRKCA1) and ISG15 (Interferone Simulated Gene 15) were 4.59, 4.31, and 4.36 respectively (Table 5, Fig. 4I–K). FC for the remaining 91 genes were between 2 and 3 (Table 5). The genes with FC > 2 was completely absent in ISC group suggesting that this unique population of cells lineaging from the control cells by the downregulation of at least 95 genes in response to ischemia.

**Cluster 5 Cells Favor Reperfusion** Cluster 5 displayed 1,998 cells where ~96% cells were mapped in ISC/R group, and control group contains ~4% cells; however, ISC group displayed negligible cells (Fig. 5A, Table 2). Hence, the comparison was between ISC/R and control groups. The data suggests the existence of a predominant population of cells in the ISC/R group which is distinct from the control. Interestingly, 2,768 genes were detected locally in the cluster 5 where the sorting was based on the extent of gene expression in ISC/R group (Supplementary Table 6, Fig. 5A–D). The violin and scatter plots revealed that the distribution of cells trending to be FC > 1 in both the groups (Fig. 5A–D). Interestingly, 28 genes (FC > 2) were upregulated in ISC/R

group on comparison with the control (Table 6). The FC values of these 28 genes in the ISC/R group were distributed around 2 whereas that of control group were tend mostly towards FC < 1 (Table 6). Similarly, the violin and scatter plots revealed that the distribution of cells was trending to FC > 2 in ISC/R group and FC < 1 in control (Fig. 5E–G). Hematopoietic cytokine, IL-11, (FC = 8.10) and the DNA binding protein RNF121 (Ring Finger Protein 121) (FC = 8.03) were highly expressed in ISC/R cells and the FC of remaining 27 proteins were less than 5 (Table 6). Similarly, 21 genes (FC > 2) were upregulated in control group on comparison with the ISC/R (Table 6). The violin and scatter plots revealed that the distribution of cells was trending to be FC > 2 in control group and FC < 1 in ISC/R (Fig. 5I–K). MI associated protein PROCR (Protein C Receptor) exhibited maximum FC of 7.93 whereas the FC of remaining 27 proteins were less than 4 (Table 6). The data suggests that the unique population of cells in ISC/R group lineages from the control cells by the downregulation of at least 21 and upregulation of at least 28 genes in response to ischemia.

**Cluster 6 Cells Favors Ischemia** Cluster 6 displayed 1,947 cells where ~98% cells were mapped in ISC group, and control group contains ~2% cells; however, ISC/R group displayed negligible cells (Fig. 6A, Table 2). Hence, the comparison was between ISC and control groups. The data suggests the existence of a predominant population of cells in the ISC group which is distinct from the control. Interestingly, 2,908 genes were detected locally in cluster 6 where the sorting was based on the extent of gene expression in ISC group (Supplementary Table 7, Fig. 6A–D). The violin and



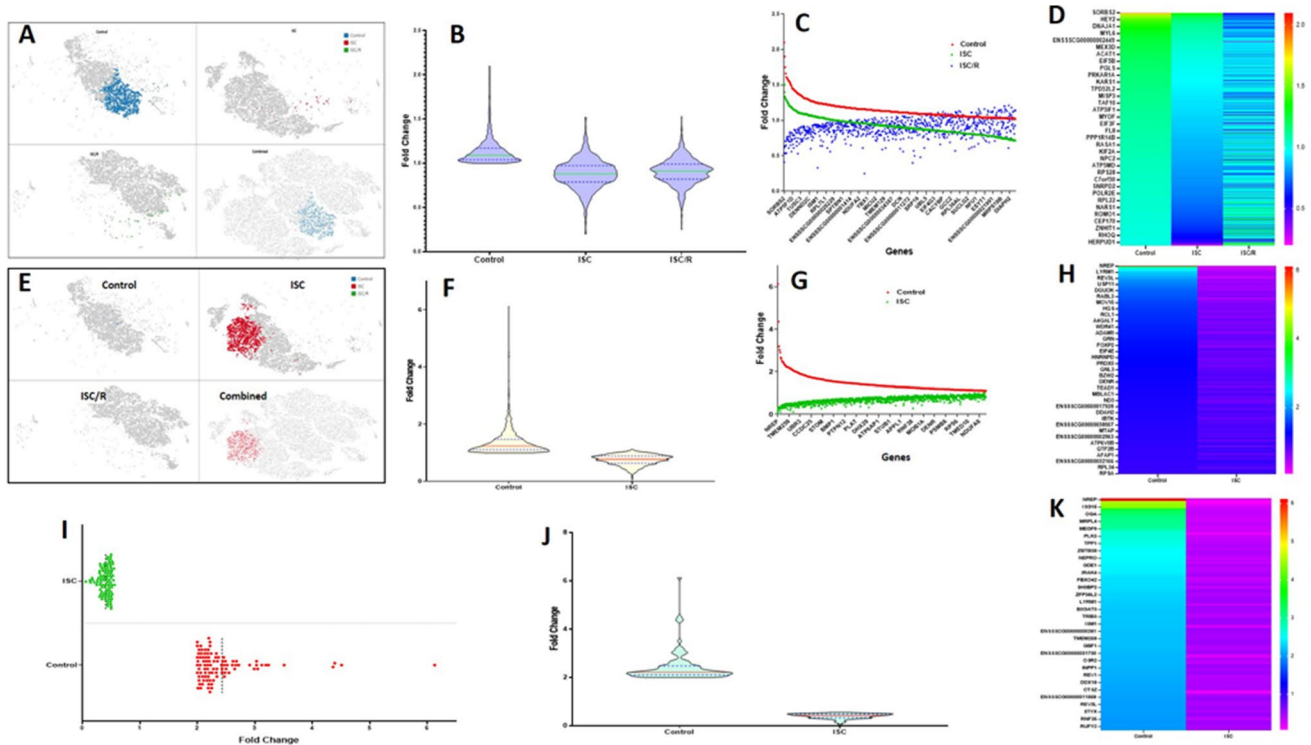


**Fig. 4** Distribution of cell populations and altered genes in Cluster 3 and 4: **(A)** Split view of Control, ISC and ISC/R groups of Cluster 3 cells and combined view of t-SNE plot showing the distribution of cells within the Cluster 3 tending towards the control based on the local expression of 970 genes. **(B)** Violin plot showing the distribution of upregulated genes in which the ISC and ISC/R groups showing the distribution around  $FC=1$  whereas the control cells tend towards  $FC>1$ . **(C)** Scatter plot showing the FC expression indicating the upregulation of genes in control than ISC and ISC/R. **(D)** Heat map showing the local expression of 970 genes identified from EATDS based on the upregulation in ISC group. **(E)** Split view Control, ISC and ISC/R groups of Cluster 4 cells and combined view of t-SNE plot showing the distribution of cells within the Cluster

4 based on the local expression of 1431 genes. **(F)** Violin plot for highly expressed 1431 genes revealing the distribution towards upregulation in control and ISC group. **(G)** Scatterplot of highly expressed 1431 genes in Control group showing the minimal level of expression in ISC group where the dotted lines indicate mean FC. **(H)** Heat map of highly altered 1431 genes ( $FC>2$ ) revealing the upregulation in Control group. **(I)** Scatterplot of highly expressed 95 genes in Control group showing the minimal level of expression in ISC group where the dotted lines indicate mean FC. **(J)** Violin plot for highly expressed 95 genes revealing the distribution towards upregulation in control and ISC group. **(K)** Heat map of highly altered 95 genes ( $FC>2$ ) revealing the upregulation in Control group

scatter plots revealed that the overall distribution of cells was tending to be around  $FC=1$  in both the groups (Fig. 6A–D). Interestingly, 37 genes ( $FC>2$ ) were upregulated in ISC group on comparison with the control (Table 7). FC values of these 37 genes in the ISC group were distributed around  $FC>2$  whereas that of control group tend towards  $FC<1$  (Table 7). Similarly, the violin and scatter plots revealed that the distribution of cells was tending to  $FC>2$  in ISC group and  $FC<1$  in control (Fig. 6E–G). The contractile protein MYH11 (Myosin Heavy Chain 11) ( $FC=4.9$ ) and the calcium binding protein CRELD2 (Cysteine Rich with EGF Like Domains 2) ( $FC=4.35$ ) were highly expressed in ISC cells and the FC of remaining 35 proteins were less than 4 (Table 7). Similarly, 52 genes ( $FC>2$ ) were upregulated in the Control group on comparison with the ISC (Table 7). The violin and scatter plots revealed that the distribution of cells was towards  $FC>2$  in Control group and  $FC<1$

in ISC (Fig. 6I–K). The immunomodulatory protein OAS2 (2'-5'-Oligoadenylate Synthetase 2) exhibited maximum FC of 5.35 whereas the FC of remaining 51 proteins were less than 5 (Table 7). The data suggest that the unique population of cells in ISC group lineages from the control cells by the downregulation of at least 52 and upregulation of at least 37 genes in response to ischemia.

**Cluster 7 Cells Tend Towards Reperfusion** Cluster 7 displayed 1,746 cells where  $\sim 92\%$  cells were mapped in ISC/R group, ISC group contain  $\sim 1\%$  cells and control group contain  $\sim 7\%$  cells (Fig. 7A, Table 2). The comparison was between ISC/R, ISC and control groups and the data suggest the existence of a predominant population of cells in the ISC/R group which is distinct from the control and ISC. Interestingly, 2,037 genes were detected locally in cluster 7 where the sorting was based on the extent of gene expression

**Table 5** The list of locally downregulated genes in ISC group with respect to control (FC > 2) group in Cluster 4 cells

Control				
No	Feature ID	Genes	C FC	ISC FC
1	ENS-SSCG00000034993	NREP	6.13	0.18
2	ENS-SSCG00000016331	RAMP1	4.51	0.06
3	ENS-SSCG00000000114	PICK1	4.39	0.17
4	ENS-SSCG00000040575	ISG15	4.36	0.26
5	ENS-SSCG00000001053	TBC1D7	3.51	0.32
6	ENS-SSCG00000023653	GLIS2	3.24	0.35
7	ENS-SSCG00000010569	OGA	3.19	0.33
8	ENS-SSCG00000003112	ENS-SSCG00000003112	3.12	0.31
9	ENS-SSCG00000015951	METAP1D	3.05	0.28
10	ENS-SSCG00000013656	MRPL4	3.03	0.31
11	ENS-SSCG00000009077	PLK4	3.03	0.37
12	ENS-SSCG00000012173	SAT1	2.99	0.32
13	ENS-SSCG00000005506	MEGF9	2.91	0.26
14	ENS-SSCG00000009491	TGDS	2.72	0.32
15	ENS-SSCG00000040095	GPR35	2.68	0.14
16	ENS-SSCG00000003928	PLK3	2.67	0.34
17	ENS-SSCG00000012880	CPT1A	2.65	0.32
18	ENS-SSCG00000024312	ID4	2.62	0.37
19	ENS-SSCG00000023080	TPP1	2.61	0.37
20	ENS-SSCG00000018092	ND6	2.55	0.44
21	ENS-SSCG00000003339	INTS11	2.52	0.36
22	ENS-SSCG00000022073	ZBTB38	2.50	0.43
23	ENS-SSCG00000015080	CEP164	2.49	0.45
24	ENS-SSCG00000013249	CKAP5	2.48	0.38
25	ENS-SSCG00000011923	NEPRO	2.47	0.30
26	ENS-SSCG00000032728	EFNB1	2.47	0.38

**Table 5** (continued)

Control				
No	Feature ID	Genes	C FC	ISC FC
27	ENS-SSCG00000039580	FOXJ2	2.46	0.30
28	ENS-SSCG00000029212	GDE1	2.44	0.46
29	ENS-SSCG00000011415	MAPKAPK3	2.43	0.36
30	ENS-SSCG00000007738	ENS-SSCG00000007738	2.43	0.38
31	ENS-SSCG00000000799	IRAK4	2.42	0.41
32	ENS-SSCG00000033844	CYP1B1	2.37	0.47
33	ENS-SSCG00000024876	TMEM181	2.35	0.32
34	ENS-SSCG00000024794	FBXO42	2.34	0.34
35	ENS-SSCG00000002458	TMEM251	2.34	0.41
36	ENS-SSCG00000015776	RWDD4	2.33	0.48
37	ENS-SSCG00000022004	SH3BP2	2.33	0.34
38	ENS-SSCG00000014806	ANAPC15	2.32	0.49
39	ENS-SSCG00000015962	SP3	2.29	0.49
40	ENS-SSCG00000038549	ZFP36L2	2.28	0.40
41	ENS-SSCG00000027530	TAF12	2.28	0.49
42	ENS-SSCG00000033703	FAM111A	2.26	0.50
43	ENS-SSCG00000007853	LYRM1	2.25	0.50
44	ENS-SSCG00000035775	BCS1L	2.25	0.31
45	ENS-SSCG00000026006	KLF13	2.24	0.50
46	ENS-SSCG00000020809	B3GAT3	2.23	0.51
47	ENS-SSCG00000030002	C18orf21	2.22	0.47
48	ENS-SSCG00000005651	ODF2	2.22	0.40
49	ENS-SSCG00000039862	TRIB3	2.22	0.40
50	ENS-SSCG00000022230	CD9	2.22	0.51
51	ENS-SSCG00000009876	DDX54	2.21	0.51
52	ENS-SSCG00000007073	ISM1	2.21	0.49
53	ENS-SSCG00000033509	SAMD11	2.20	0.25

**Table 5** (continued)

Control				
No	Feature ID	Genes	C FC	ISC FC
54	ENS-SSCG00000034260	GDF15	2.20	0.51
55	ENS-SSCG00000000261	ENS-SSCG00000000261	2.20	0.49
56	ENS-SSCG00000035686	CS	2.19	0.50
57	ENS-SSCG00000004822	ALDH1A3	2.19	0.44
58	ENS-SSCG00000027779	TMEM259	2.19	0.48
59	ENS-SSCG00000004018	AFDN	2.18	0.52
60	ENS-SSCG00000007077	ESF1	2.18	0.52
61	ENS-SSCG00000010579	GBF1	2.18	0.44
62	ENS-SSCG00000007530	PPP1R3D	2.17	0.40
63	ENS-SSCG00000024614	ITSN1	2.16	0.50
64	ENS-SSCG00000031730	ENS-SSCG00000031730	2.15	0.46
65	ENS-SSCG00000039909	ICAM2	2.14	0.21
66	ENS-SSCG00000024904	SEC22A	2.14	0.39
67	ENS-SSCG00000006073	OSR2	2.14	0.43
68	ENS-SSCG00000016613	AASS	2.13	0.30
69	ENS-SSCG00000038506	ENS-SSCG00000038506	2.13	0.53
70	ENS-SSCG00000016050	INPP1	2.13	0.50
71	ENS-SSCG00000037791	ENS-SSCG00000037791	2.11	0.43
72	ENS-SSCG00000005646	COQ4	2.11	0.54
73	ENS-SSCG00000008179	REV1	2.10	0.42
74	ENS-SSCG00000008096	ZC3H6	2.09	0.42
75	ENS-SSCG00000004979	MYO9A	2.09	0.42
76	ENS-SSCG00000015712	DDX18	2.08	0.45
77	ENS-SSCG00000001907	UBL7	2.07	0.43
78	ENS-SSCG00000011047	FAM171A1	2.06	0.45
79	ENS-SSCG00000007522	CTSZ	2.06	0.39
80	ENS-SSCG00000014800	RNF121	2.06	0.13

**Table 5** (continued)

Control				
No	Feature ID	Genes	C FC	ISC FC
81	ENS-SSCG00000006087	CPQ	2.05	0.44
82	ENS-SSCG00000011859	ENS-SSCG00000011859	2.05	0.49
83	ENS-SSCG00000029262	GOSR1	2.04	0.55
84	ENS-SSCG00000006365	DEDD	2.03	0.44
85	ENS-SSCG00000025703	REV3L	2.03	0.44
86	ENS-SSCG00000009565	GAS6	2.03	0.50
87	ENS-SSCG00000006561	SLC39A1	2.03	0.50
88	ENS-SSCG00000005039	STYX	2.02	0.44
89	ENS-SSCG00000023142	GAMT	2.01	0.56
90	ENS-SSCG00000015044	NKAPD1	2.01	0.47
91	ENS-SSCG00000016202	RNF25	2.00	0.34
92	ENS-SSCG00000049172	ENS-SSCG00000049172	2.00	0.53
93	ENS-SSCG00000010062	CABIN1	2.00	0.47
94	ENS-SSCG00000010239	RUFY2	2.00	0.46
95	ENS-SSCG00000031073	BABAM1	2.00	0.46

in ISC/R group (Supplementary Table 8, Fig. 7A–D). The violin and scatter plots revealed that the overall distribution of cells was tending to be around FC = 1 in both the groups (Fig. 7A–D). Interestingly, 15 genes (FC > 2) were upregulated in ISC/R group on comparison with the control and ISC (Table 8). FC values of these 15 genes in the ISC/R group were distributed around FC > 2 whereas that of control and ISC groups tend towards FC < 1 (Table 8). Similarly, the violin and scatter plots revealed that the distribution of cells was tending to FC > 2 in ISC/R group, and FC = 1 in ISC and FC < 1 in control groups (Fig. 7E–G). Hematopoietic cytokine, IL-11, (FC = 10.27) and the DNA binding protein RNF121 (Ring Finger Protein 121) (FC = 7.27) were highly expressed in ISC/R cells and the FC of remaining 13 proteins were less than 4 (Table 8). Similarly, 49 genes (FC > 2) were upregulated in ISC group on comparison with the ISC/R and control (Table 8). The violin and scatter plots revealed that the distribution of cells was towards FC > 2 in ISC group and FC < 1 in ISC/R and control group (Fig. 7I–J). Histone protein H1.0 exhibited maximum expression

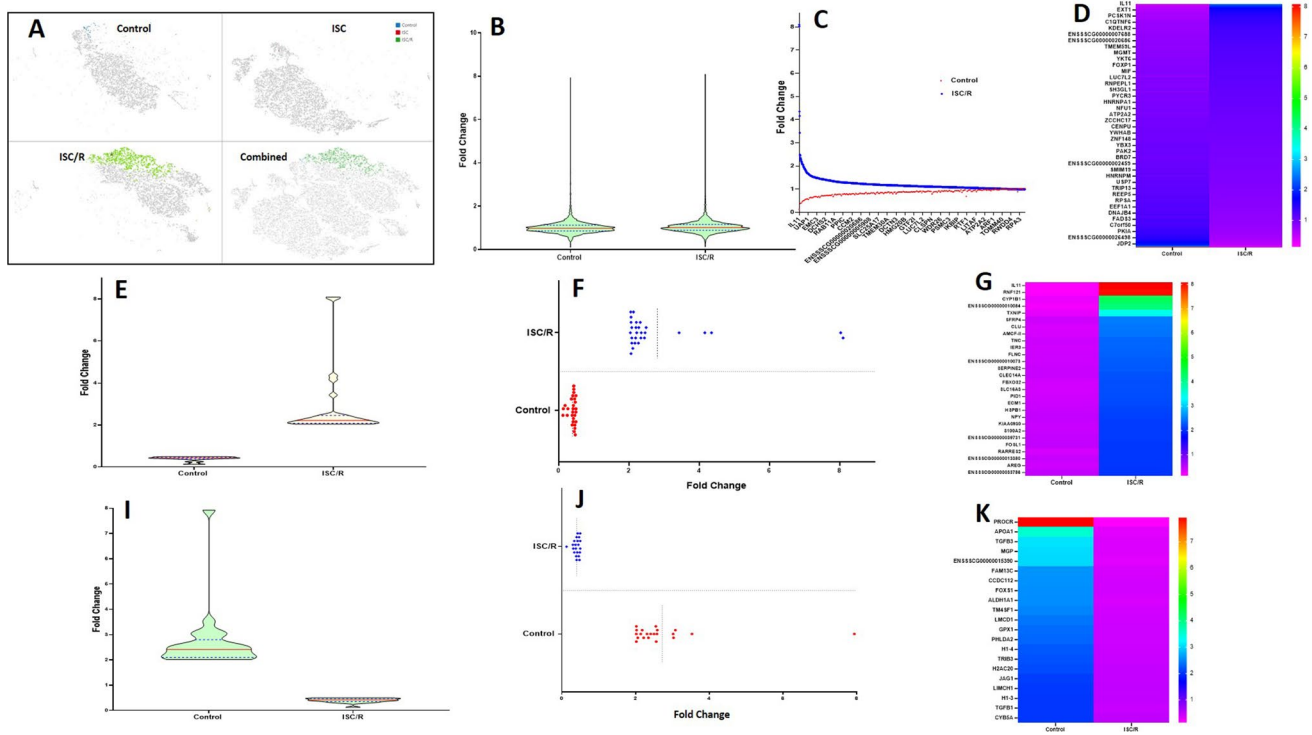


**Fig. 5** Distribution of cell populations and altered genes in Cluster 5: (A) Split view of Control, ISC and ISC/R groups of Cluster 5 cells and combined view of t-SNE plot showing the distribution of cells within the Cluster 5 tending towards the ISC/R group based on the local expression of 2,768 genes. (B) Violin plot for highly expressed 2,768 genes revealing the distribution towards upregulation in control and ISC/R group. (C) Scatterplot of highly expressed 2,768 genes in Control group showing the downregulation trend compared to ISC/R group. (D) Heat map of highly altered 2,768 genes ( $FC > 2$ ) revealing the upregulation in ISC/R group. (E) Violin plot for highly expressed 28 genes revealing the distribution towards upregulation in

ISC/R group compared to control. (F) Scatterplot of highly expressed 28 genes in ISC/R group showing the minimal level of expression in control group where the dotted lines indicate mean FC. (G) Heat map of highly altered 28 genes ( $FC > 2$ ) revealing the upregulation in ISC/R group. (H) Violin plot for highly expressed 21 genes revealing the distribution towards upregulation in Control group compared to ISC/R group. (I) Scatterplot of highly expressed 21 genes in Control group showing the minimal level of expression in ISC/R group where the dotted lines indicate mean FC. (K) Heat map of highly altered 21 genes ( $FC > 2$ ) revealing the upregulation in Control group

( $FC = 4.06$ ) followed by the chaperon protein HSPA5 (Heat Shock Protein 70 Family Protein 5) ( $FC = 3.89$ ) whereas the  $FC$  of other 47 genes were between 3.61 and 2 (Table 7). The membrane transporter protein, ABCB1 (ATP-binding cassette, sub-family B (MDR/TAP), member 1) ( $FC = 2.55$ ) and the transcriptional regulator LMCD1 (LIM and Cysteine Rich Domains 1) ( $FC = 2.28$ ) were the two genes upregulated in the control group compared with ISC/R and ISC group (Table 7). The data suggests that the unique population of cells in ISC/R group lineaging from the control cells by the downregulation of at least 49 genes in ischemia and 2 genes in control and the upregulation of at least 15 genes regarding ischemia and control.

**Cluster 8 Cells Tend Towards Ischemia** Cluster 8 displayed 1,721 cells where ~94% cells were mapped in ISC group, control group contain ~7% cells; however, ISC/R displayed negligible cells (~0.2%) (Fig. 8A, Table 2). The comparison was between ISC, and control groups and the data suggest

the existence of a predominant population of cells in the ISC group which is distinct from the control. Interestingly, 1,895 genes were detected locally in cluster 8 where the sorting was based on the extent of gene expression in ISC group (Supplementary Table 9, Fig. 8A–D). The violin and scatter plots revealed that the overall distribution of cells was tending to be around  $FC = 1$  in both the groups (Fig. 8A–D). Interestingly, 37 genes ( $FC > 2$ ) were upregulated in ISC group on comparison with the control (Table 9).  $FC$  values of these 37 genes in the ISC group were distributed around  $FC > 2$  whereas that of control tend towards  $FC < 1$  (Table 8). Similarly, the violin and scatter plots revealed that the distribution of cells was tending to  $FC > 2$  in ISC and  $FC < 1$  in control groups (Fig. 8E–G). The chaperone protein, HSP90B1 (Heat Shock Protein 90 Beta Family Member 1) ( $FC = 4.29$ ) and CRELD2 (Cysteine Rich with EGF Like Domains 2) ( $FC = 4.25$ ) were highly expressed in ISC cells and the  $FC$  of remaining 35 proteins were less than 4 (Table 9). Similarly, 13 genes ( $FC > 2$ ) were upregulated in

**Table 6** The list of genes locally upregulated genes (FC > 2) in ISC/R and control groups with respect to each other group in Cluster 5 cells

SI/No	Feature ID	Genes	Control FC	ISC/R FC
Control				
1	ENSSSCG00000026585	PROCR	7.93	0.13
2	ENSSSCG00000030921	APOA1	3.53	0.30
3	ENSSSCG00000002385	TGFB3	3.08	0.34
4	ENSSSCG000000037697	MGP	3.03	0.34
5	ENSSSCG00000015390	ENSSSCG00000015390	3.02	0.31
6	ENSSSCG00000010209	FAM13C	2.59	0.38
7	ENSSSCG00000029866	CCDC112	2.58	0.39
8	ENSSSCG000000033613	FOXS1	2.56	0.40
9	ENSSSCG000000028996	ALDH1A1	2.55	0.37
10	ENSSSCG000000033018	TM4SF1	2.50	0.40
11	ENSSSCG00000011538	LMCD1	2.41	0.42
12	ENSSSCG000000033727	GPX1	2.35	0.43
13	ENSSSCG000000021597	PHLDA2	2.31	0.43
14	ENSSSCG000000033672	H1-4	2.22	0.45
15	ENSSSCG000000039862	TRIB3	2.18	0.46
16	ENSSSCG000000034598	H2AC20	2.14	0.48
17	ENSSSCG00000007067	JAG1	2.06	0.49
18	ENSSSCG000000008799	LIMCH1	2.03	0.50
19	ENSSSCG000000001137	H1-3	2.02	0.50
20	ENSSSCG000000003017	TGFB1	2.02	0.47
21	ENSSSCG000000004875	CYB5A	2.02	0.50
ISC/R				
1	ENSSSCG000000040725	IL11	0.13	8.10
2	ENSSSCG00000014800	RNF121	0.12	8.03
3	ENSSSCG000000033844	CYP1B1	0.24	4.35
4	ENSSSCG00000010084	ENSSSCG00000010084	0.18	4.16
5	ENSSSCG000000031262	TXNIP	0.26	3.43
6	ENSSSCG000000035299	SFRP4	0.41	2.49
7	ENSSSCG000000009668	CLU	0.36	2.46
8	ENSSSCG000000008957	AMCF-II	0.38	2.44
9	ENSSSCG000000005494	TNC	0.43	2.35
10	ENSSSCG000000027607	IER3	0.42	2.34
11	ENSSSCG00000016578	FLNC	0.43	2.32
12	ENSSSCG00000010073	ENSSSCG00000010073	0.43	2.28
13	ENSSSCG00000016233	SERPINE2	0.45	2.27
14	ENSSSCG000000023760	CLEC14A	0.47	2.22
15	ENSSSCG000000005981	FBXO32	0.40	2.21
16	ENSSSCG000000024018	SLC16A3	0.40	2.20
17	ENSSSCG000000035058	PID1	0.41	2.19
18	ENSSSCG000000029230	ECM1	0.44	2.17
19	ENSSSCG000000039962	HSPB1	0.46	2.13
20	ENSSSCG00000016718	NPY	0.49	2.11
21	ENSSSCG000000000018	KIAA0930	0.46	2.08
22	ENSSSCG000000006580	S100A2	0.46	2.08
23	ENSSSCG000000039731	ENSSSCG000000039731	0.49	2.08
24	ENSSSCG00000012967	FOSL1	0.49	2.06
25	ENSSSCG000000035419	RARRES2	0.38	2.06
26	ENSSSCG00000013380	ENSSSCG00000013380	0.47	2.06
27	ENSSSCG000000008963	AREG	0.42	2.05
28	ENSSSCG000000033786	ENSSSCG000000033786	0.49	2.04



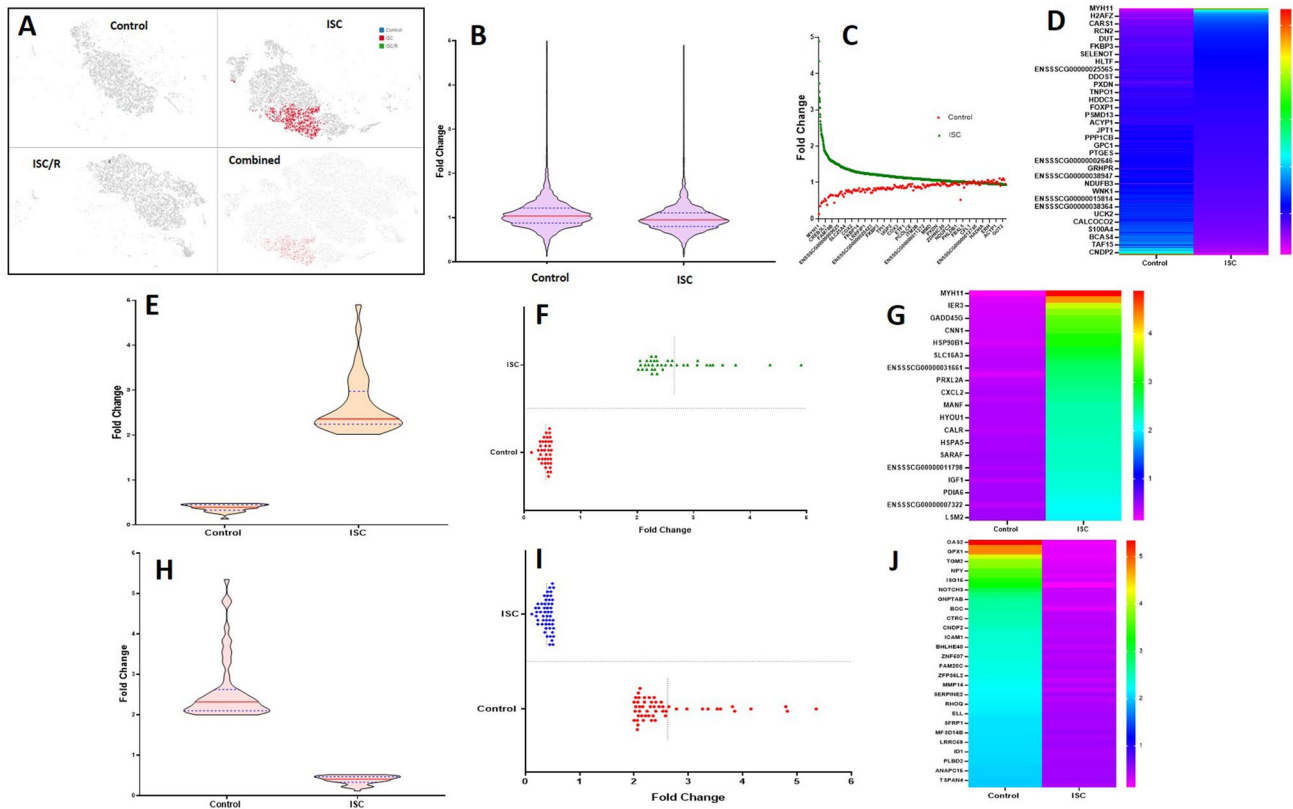


**Fig. 6** Distribution of cell populations and altered genes in Cluster 6: (A) Split view of Control, ISC and ISC/R groups of Cluster 6 cells and combined view of t-SNE plot showing the distribution of cells within the Cluster 6 tending towards the ISC group based on the local expression of 2,908 genes. (B) Violin plot for highly expressed 2,908 genes revealing the distribution towards upregulation in control and ISC groups. (C) Scatterplot of highly expressed 2,908 genes in Control group showing the downregulation trend compared to ISC group. (D) Heat map of highly altered 2,908 genes ( $FC > 2$ ) revealing the upregulation in ISC group. (E) Violin plot for highly expressed 37 genes revealing the distribution towards upregulation in ISC group

compared to control. (F) Scatterplot of highly expressed 37 genes in ISC group showing the minimal level of expression in control group where the dotted lines indicate mean FC. (G) Heat map of highly altered 37 genes ( $FC > 2$ ) revealing the upregulation in ISC group. (H) Violin plot for highly expressed 52 genes revealing the distribution towards upregulation in Control group compared to ISC group. (I) Scatterplot of highly expressed 52 genes in Control group showing the minimal level of expression in ISC group where the dotted lines indicate mean FC. (K) Heat map of highly altered 52 genes ( $FC > 2$ ) revealing the upregulation in Control group

Control group on comparison with the ISC (Table 9). The violin and scatter plots revealed that the distribution of these 13 genes was towards  $FC > 2$  in control group and  $FC < 1$  in ISC group (Fig. 8H–J). The extracellular cytokine, ISG15 (Interferon-stimulated gene 15) exhibited maximum expression ( $FC = 4.60$ ) whereas the FC of other 14 genes were below 3 (Table 9). The data suggests that the unique population of cells in ISC group lineaging from the control cells by the downregulation of at least 13 and the upregulation of at least 37 genes in response to ischemia.

**Cluster 9 Cells Tend Towards Ischemia** Cluster 9 displayed 1,286 cells where ~96% cells were mapped in ISC group, control and ISC/R groups contain ~2% cells each (Fig. 9A, Table 2). The comparison was between ISC, ISC/R and control groups and the data suggests the existence of a predominant population of cells in the ISC group which is distinct

from the control. Interestingly, 3,093 genes were detected locally in cluster 9 where the sorting was based on the extent of gene expression in ISC group (Supplementary Table 10, Fig. 9A–D). The violin and scatter plots revealed that the overall distribution of cells was tending to be around  $FC = 1$  in all the three groups (Fig. 9A–D). Interestingly, 37 genes ( $FC > 2$ ) were upregulated in ISC group on comparison with the control (Table 10). FC values of these 25 genes in the ISC group were distributed around  $FC > 2$  whereas that of control tend towards  $FC < 1$  and ISC/R tend towards  $FC > 1$  (Table 10). Similarly, the violin and scatter plots revealed that the distribution of cells was tending to  $FC > 2$  in ISC and  $FC < 1$  in the control and  $FC > 1$  in ISC/R groups (Fig. 9E–G). Similar to the Cluster 8, CRELD2 ( $FC = 4.12$ ) was highly expressed in ISC cells and the FC of remaining 24 proteins were less than 4 (Table 10). Similarly, 32 genes ( $FC > 2$ ) were upregulated in the control group on

**Table 7** The list of genes locally upregulated genes (FC > 2) in control and ISC groups with respect to each other group in Cluster 6 cells

SL/No	Feature ID	Genes	Control FC	ISC FC
Control				
1	ENSSSCG00000009881	OAS2	5.35	0.19
2	ENSSSCG00000007391	MATN4	4.82	0.21
3	ENSSSCG000000033727	GPX1	4.79	0.23
4	ENSSSCG000000008963	AREG	4.15	0.20
5	ENSSSCG000000023522	TGM2	3.85	0.25
6	ENSSSCG000000014924	CTSC	3.81	0.28
7	ENSSSCG000000016718	NPY	3.59	0.30
8	ENSSSCG000000030300	ENSSSCG000000030300	3.53	0.23
9	ENSSSCG000000040575	ISG15	3.36	0.31
10	ENSSSCG000000016199	CYP27A1	3.26	0.12
11	ENSSSCG000000025176	NOTCH3	2.97	0.33
12	ENSSSCG000000036213	FGF2	2.78	0.35
13	ENSSSCG000000000862	GNPTAB	2.64	0.36
14	ENSSSCG000000013723	DHPS	2.59	0.33
15	ENSSSCG000000025826	BOC	2.58	0.23
16	ENSSSCG000000017584	PPP1R9B	2.53	0.40
17	ENSSSCG000000003458	CTRC	2.53	0.38
18	ENSSSCG000000000094	SUN2	2.50	0.41
19	ENSSSCG000000004870	CNDP2	2.46	0.40
20	ENSSSCG000000023611	TNXB	2.40	0.38
21	ENSSSCG000000013655	ICAM1	2.40	0.41
22	ENSSSCG000000035357	BCL2L1	2.39	0.43
23	ENSSSCG000000036136	BHLHE40	2.37	0.36
24	ENSSSCG000000040317	SOD2	2.37	0.45
25	ENSSSCG000000025139	ZNF507	2.35	0.38
26	ENSSSCG00000001565	CDKN1A	2.32	0.42
27	ENSSSCG000000020813	FAM20C	2.32	0.47
28	ENSSSCG000000038587	CRNKL1	2.30	0.41
29	ENSSSCG000000038549	ZFP36L2	2.28	0.44
30	ENSSSCG000000003839	ENSSSCG000000003839	2.27	0.35
31	ENSSSCG000000002039	MMP14	2.24	0.45
32	ENSSSCG000000015284	MDM4	2.21	0.36
33	ENSSSCG000000016233	SERPINE2	2.19	0.49
34	ENSSSCG000000032428	ARSA	2.19	0.39
35	ENSSSCG000000031261	RHOQ	2.17	0.45
36	ENSSSCG00000007737	TPST1	2.16	0.45
37	ENSSSCG000000040181	ELL	2.14	0.49
38	ENSSSCG000000008443	EPAS1	2.11	0.50
39	ENSSSCG000000025822	SFRP1	2.10	0.47
40	ENSSSCG000000049524	ENSSSCG000000049524	2.10	0.48
41	ENSSSCG000000026552	MFSD14B	2.09	0.52
42	ENSSSCG000000008171	NPAS2	2.08	0.47
43	ENSSSCG000000028019	LRRC59	2.08	0.52
44	ENSSSCG000000008645	ID2	2.07	0.51
45	ENSSSCG000000037016	ID1	2.07	0.46
46	ENSSSCG000000037355	RNF115	2.06	0.46
47	ENSSSCG000000009872	PLBD2	2.06	0.50
48	ENSSSCG000000008480	MORN2	2.03	0.51
49	ENSSSCG000000014806	ANAPC15	2.03	0.50
50	ENSSSCG000000036723	EMP1	2.02	0.50

**Table 7** (continued)

SL/No	Feature ID	Genes	Control FC	ISC FC
51	ENSSSCG00000012838	TSPAN4	2.00	0.52
52	ENSSSCG00000033509	SAMD11	2.00	0.44
ISC				
1	ENSSSCG00000000146	MYH11	0.13	4.90
2	ENSSSCG000000000981	CRELD2	0.25	4.35
3	ENSSSCG000000027607	IER3	0.29	3.74
4	ENSSSCG000000043781	RHOB	0.29	3.51
5	ENSSSCG000000035249	GADD45G	0.31	3.34
6	ENSSSCG000000013380	ENSSSCG000000013380	0.31	3.29
7	ENSSSCG000000013614	CNN1	0.33	3.23
8	ENSSSCG000000038077	PPP1R14A	0.32	3.07
9	ENSSSCG000000000849	HSP90B1	0.28	3.06
10	ENSSSCG00000002383	FOS	0.35	2.89
11	ENSSSCG000000024018	SLC16A3	0.36	2.82
12	ENSSSCG00000002754	NQO1	0.38	2.70
13	ENSSSCG000000031661	ENSSSCG000000031661	0.37	2.62
14	ENSSSCG000000010493	PDLIM1	0.26	2.60
15	ENSSSCG000000010340	PRXL2A	0.37	2.54
16	ENSSSCG000000026981	ENSSSCG000000026981	0.41	2.50
17	ENSSSCG000000008959	CXCL2	0.43	2.45
18	ENSSSCG000000035344	UBE2S	0.38	2.43
19	ENSSSCG000000032914	MANF	0.43	2.36
20	ENSSSCG000000021973	GPX8	0.43	2.35
21	ENSSSCG000000015106	HYOU1	0.42	2.35
22	ENSSSCG000000036724	CRYAB	0.42	2.33
23	ENSSSCG000000013746	CALR	0.39	2.31
24	ENSSSCG000000010016	MORC2	0.45	2.30
25	ENSSSCG000000005601	HSPA5	0.45	2.27
26	ENSSSCG000000011046	ITGA8	0.45	2.26
27	ENSSSCG000000033402	SARAF	0.48	2.26
28	ENSSSCG000000006088	SDC2	0.47	2.25
29	ENSSSCG000000011798	ENSSSCG000000011798	0.42	2.24
30	ENSSSCG000000026082	DNAJC3	0.47	2.20
31	ENSSSCG000000000857	IGF1	0.39	2.17
32	ENSSSCG000000011575	ATG7	0.46	2.17
33	ENSSSCG000000008633	PDIA6	0.46	2.14
34	ENSSSCG000000011972	FILIP1L	0.46	2.09
35	ENSSSCG000000007322	ENSSSCG000000007322	0.38	2.06
36	ENSSSCG000000011676	ENSSSCG000000011676	0.47	2.05
37	ENSSSCG000000039021	LSM2	0.48	2.02

comparison with the ISC (Table 10). The violin and scatter plots revealed that the distribution of these 32 genes was towards  $FC > 2$  in control and ISC/R groups and  $FC < 1$  in ISC group (Fig. 9H–J). The cytoskeletal protein ACTA1 (Actin Alpha 1, Skeletal Muscle) ( $FC = 9.84$ ) exhibited maximum expression whereas the FC of other 21 genes were below 4 (Table 10). Additionally, 375 genes ( $FC > 2$ ) were upregulated in ISC/R group on comparison with the ISC and control (Table 10). The violin and scatter plots

revealed that the distribution of these 375 genes was towards  $FC > 2$  in control and ISC/R groups and  $FC < 1$  in ISC group (Fig. 9H–M). The DNA replication machinery component MCM3 (Minichromosome Maintenance Complex Component 3) ( $FC = 31.05$ ) and the motor protein (Myosin XIX) ( $FC = 10.38$ ) exhibited maximum expression whereas the FC of other 27 genes were between 10 and 4 and the remaining 346 genes were below 4 (Table 10). The data suggests that the unique population of cells in ISC group lineaging from

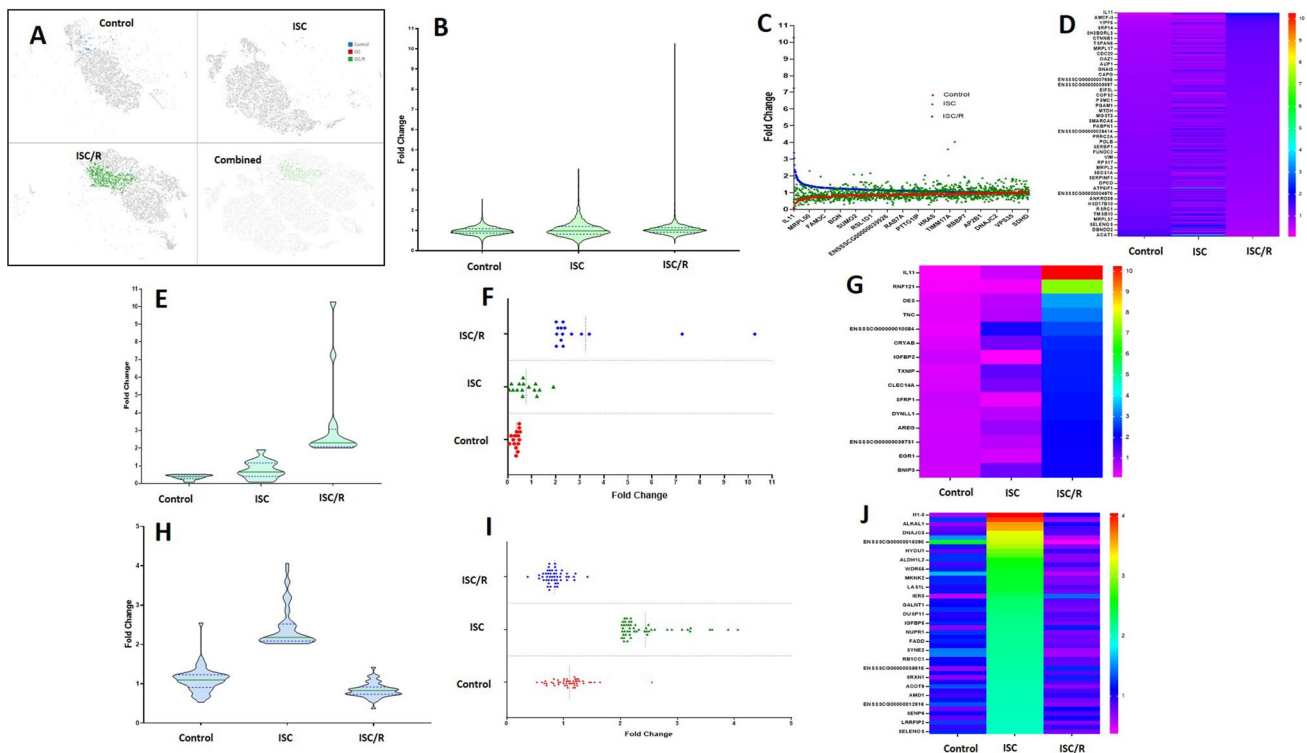


**Fig. 7** Distribution of cell populations and altered genes in Cluster 7: (A) Split view of Control, ISC and ISC/R groups of Cluster 7 cells and combined view of t-SNE plot showing the distribution of cells within the Cluster 7 tending towards the ISC/R group based on the local expression of 2,037 genes. (B) Violin plot for highly expressed 2,037 genes revealing the distribution towards upregulation in ISC and ISC/R groups. (C) Scatterplot of highly expressed 2,037 genes in ISC/R and ISC group showing the upregulation trend compared to Control group. (D) Heat map of highly altered 2,037 genes (FC > 2) revealing the upregulation in ISC/R and ISC group. (E) Violin plot for highly expressed 15 genes revealing the distribution towards

upregulation in ISC/R group compared to control. (F) Scatterplot of highly expressed 15 genes in ISC group showing the minimal level of expression in control group and FC > 1 in ISC where the dotted lines indicate mean FC. (G) Heat map of highly altered 15 genes (FC > 2) revealing the upregulation in ISC/R group. (H) Violin plot for highly expressed 49 genes revealing the distribution towards upregulation in ISC group compared to Control and ISC/R groups. (I) Scatterplot of highly expressed 49 genes in ISC group showing the minimal level of expression in control and ISC/R group where the dotted lines indicate mean FC. (J) Heat map of highly altered 49 genes (FC > 2) revealing the upregulation in ISC group

the control cells by the downregulation of at least 32 and the upregulation of at least 25 genes in response to ischemia and the ischemic response was elicited by the upregulation of 375 genes as evident in ISC/R group.

**Cluster 10 Cells Tend Towards Control and Ischemia** Cluster 10 displayed 1,261 cells where ~40% cells were mapped in ISC group, ~57% in control group and ISC/R groups contain ~3% cells (Fig. 10A, Table 2). The comparison was between ISC, ISC/R and control groups and the data suggests the existence of a predominant population of cells in the ISC group and control group which is distinct from the ISC/R. Interestingly, 2,546 genes were detected locally in cluster 10 where the sorting was based on the extent of gene expression in ISC group (Supplementary Table 10, Fig. 10A–D). The violin and scatter plots revealed that the overall distribution of cells was tending to be around FC > 1 in ISC and ISC/R groups and FC = 1 in the control group

(Fig. 10A–D). Interestingly, 25 genes (FC > 2) were upregulated in ISC group on comparison with the control and ISC/R groups (Table 11). FC values of these 25 genes in the ISC group were distributed around FC > 2 whereas that of control and ISC/R tend towards FC ≤ 1 (Table 11). Similarly, the violin and scatter plots revealed that the distribution of cells was tending to FC > 2 in ISC and FC ≤ 1 in the control and ISC/R groups (Fig. 10–G). SLC16A3 (FC = 8.49) and PRXL2A (FC = 7.02) were highly expressed in ISC cells and the FC of remaining 23 proteins were less than 4 (Table 11). Similarly, 7 genes (FC > 2) were upregulated in the control group on comparison with the ISC (Table 11). The violin and scatter plots revealed that the distribution of these 7 genes was towards FC > 2 in control and FC ≤ 1 in the ISC and ISC/R groups (Fig. 10H–J). The ISG15 (FC = 7.55) exhibited maximum expression whereas the FC of other 6 genes were below 3 (Table 11). Additionally, 30 genes (FC > 2) were upregulated in ISC/R group on comparison

**Table 8** The list of genes locally upregulated genes (FC > 2) in control and ISC groups with respect to each other group in Cluster 7 cells

SI/No	Feature ID	Genes	Control FC	ISC FC	ISC/R FC
Control					
1	ENSSSCG00000015390	ENSSSCG00000015390	2.55	3.18	0.37
2	ENSSSCG00000011538	LMCD1	2.28	0.54	0.48
ISC					
1	ENSSSCG00000039348	H1-0	0.62	4.06	1.05
2	ENSSSCG00000005601	HSPA5	1.26	3.89	0.64
3	ENSSSCG00000033922	ALKAL1	0.66	3.61	1.06
4	ENSSSCG00000010340	PRXL2A	0.83	3.57	0.90
5	ENSSSCG00000026082	DNAJC3	0.91	3.23	0.87
6	ENSSSCG00000002959	FAM98C	1.54	3.22	0.57
7	ENSSSCG00000015390	ENSSSCG00000015390	2.55	3.18	0.37
8	ENSSSCG00000008959	CXCL2	1.17	3.08	0.72
9	ENSSSCG00000015106	HYOU1	0.84	2.90	0.95
10	ENSSSCG00000024591	ETV1	1.23	2.82	0.71
11	ENSSSCG00000000839	ALDH1L2	1.23	2.60	0.72
12	ENSSSCG00000033115	IFNAR1	0.90	2.54	0.94
13	ENSSSCG00000032062	WDR55	1.19	2.50	0.75
14	ENSSSCG000000008207	RPIA	1.64	2.49	0.57
15	ENSSSCG00000013448	MKNK2	1.20	2.47	0.75
16	ENSSSCG00000012654	ENSSSCG00000012654	1.21	2.46	0.74
17	ENSSSCG00000012366	LAS1L	1.01	2.45	0.86
18	ENSSSCG00000006153	FABP5	1.17	2.42	0.76
19	ENSSSCG00000027607	IER3	0.53	2.32	1.42
20	ENSSSCG00000006321	FAM78B	1.05	2.28	0.85
21	ENSSSCG00000003743	GALNT1	1.11	2.26	0.80
22	ENSSSCG00000011194	ANKRD28	1.24	2.24	0.74
23	ENSSSCG00000008298	DUSP11	1.00	2.23	0.89
24	ENSSSCG00000032914	MANF	1.06	2.19	0.84
25	ENSSSCG00000025924	IGFBP5	1.19	2.18	0.76
26	ENSSSCG00000000981	CRELD2	0.70	2.18	1.18
27	ENSSSCG00000040162	NUPR1	1.24	2.18	0.74
28	ENSSSCG00000015328	SGCE	1.13	2.16	0.80
29	ENSSSCG00000030888	FADD	1.19	2.16	0.77
30	ENSSSCG00000024563	CEP83	1.08	2.16	0.84
31	ENSSSCG00000005110	SYNE2	1.45	2.15	0.65
32	ENSSSCG00000026153	ACAT1	1.48	2.14	0.63
33	ENSSSCG00000028902	RB1CC1	1.07	2.12	0.85
34	ENSSSCG00000011843	PAK2	1.10	2.12	0.83
35	ENSSSCG00000038616	ENSSSCG00000038616	0.68	2.11	1.21
36	ENSSSCG00000027135	PPM1G	1.06	2.10	0.85
37	ENSSSCG00000023298	SRXN1	0.70	2.09	1.19
38	ENSSSCG00000014043	ENSSSCG00000014043	1.02	2.08	0.88
39	ENSSSCG00000012172	ACOT9	1.35	2.07	0.69
40	ENSSSCG00000036883	FABP3	1.00	2.07	0.89
41	ENSSSCG00000004392	AMD1	0.91	2.06	0.97
42	ENSSSCG00000040663	HERPUD1	1.16	2.06	0.79
43	ENSSSCG00000012916	ENSSSCG00000012916	1.34	2.06	0.70
44	ENSSSCG00000027293	TNPO1	0.79	2.05	1.09
45	ENSSSCG00000020702	SENP6	1.05	2.04	0.87
46	ENSSSCG00000002414	SEL1L	0.82	2.04	1.06
47	ENSSSCG00000027738	LRRFIP2	1.28	2.03	0.73



**Table 8** (continued)

SI/No	Feature ID	Genes	Control FC	ISC FC	ISC/R FC
48	ENSSSCG00000033278	ATP6V1D	0.94	2.02	0.95
49	ENSSSCG00000004826	SELENOS	1.20	2.02	0.77
ISC/R					
1	ENSSSCG00000040725	IL11	0.07	0.48	10.27
2	ENSSSCG00000014800	RNF121	0.14	0.15	7.25
3	ENSSSCG00000020785	DES	0.27	0.60	3.39
4	ENSSSCG00000005494	TNC	0.30	0.65	3.07
5	ENSSSCG00000010084	ENSSSCG00000010084	0.23	1.90	2.65
6	ENSSSCG00000036724	CRYAB	0.35	1.16	2.38
7	ENSSSCG00000035392	IGFBP2	0.48	0.07	2.30
8	ENSSSCG00000031262	TXNIP	0.35	1.32	2.30
9	ENSSSCG00000023760	CLEC14A	0.38	1.11	2.28
10	ENSSSCG00000025822	SFRP1	0.48	0.22	2.22
11	ENSSSCG00000009904	DYNLL1	0.43	0.62	2.22
12	ENSSSCG00000008963	AREG	0.44	0.88	2.08
13	ENSSSCG00000039731	ENSSSCG00000039731	0.48	0.64	2.04
14	ENSSSCG00000014336	EGR1	0.51	0.39	2.02
15	ENSSSCG00000024388	BNIP3	0.42	1.21	2.01

with the ISC and control (Table 11). The violin and scatter plots revealed that the distribution of these 30 genes was towards  $FC \leq 1$  in control and ISC groups (Fig. 10H–M). The Ring Finger protein (RNF121) ( $FC = 17.16$ ) and the ECM protein Tenascin C (TNC) ( $FC = 5.22$ ) exhibited maximum expression whereas the FC of other 28 genes were between were below 4 (Table 11). The data suggests that the unique population of cells in ISC group lineaging from the control cells by the downregulation of at least 25 and the upregulation of at least 7 genes in response to ischemia and the ischemic response was elicited by the upregulation of 30 genes as evident in ISC/R group.

**Cluster 11 Cells Tend Towards Reperfusion** Cluster 11 displayed 4,134 cells where  $\sim 0.16\%$  cells were mapped in ISC group,  $\sim 1.26\%$  in control group and ISC/R groups contain  $\sim 98.58\%$  cells (Fig. 11A, Table 2). The comparison was between ISC/R and control groups and the data suggests the existence of a predominant population of cells in the ISC/R group which is distinct from the control. Interestingly, 4,134 genes were detected locally in cluster 11 where the sorting was based on the extent of gene expression in ISC/R group (Supplementary Table 11, Fig. 11A–D). The violin and scatter plots revealed that the overall distribution of cells was tending to be around  $FC > 1$  ISC/R group and Control group (Fig. 11A–D). Interestingly, 51 genes ( $FC > 2$ ) were upregulated in ISC/R group on comparison with the control (Table 12). FC values of these 51 genes in the ISC/R group were distributed around  $FC > 2$  whereas that of control tend towards  $FC \leq 1$  (Table 12). Similarly, the violin and scatter plots revealed that the distribution of cells was tending

to  $FC > 2$  in ISC/R and  $FC \leq 1$  in the control (Fig. 11E–G). RCAN1 (Regulator of Calcineurin 1) ( $FC = 5.81$ ) was the highly expressed gene in ISC/R cells and the FC of remaining 50 proteins were less than 4 (Table 12). Similarly, 126 genes ( $FC > 2$ ) were upregulated in the control group on comparison with the ISC/R (Table 12). The violin and scatter plots revealed that the distribution of these 126 genes was towards  $FC > 2$  in control and  $FC \leq 1$  in the ISC/R group (Fig. 11H–J). The Protein phosphatase 4 regulatory subunit 4 (PPP4R4) ( $FC = 7.17$ ) exhibited maximum expression followed by the G-protein-coupled neuro peptide receptor, NPFFR2 (Neuropeptide FF receptor 2) ( $FC = 6.61$ ) whereas the FC for the remaining 124 genes were below 6 (Table 12). The data suggest that the unique population of cells in ISC/R group lineaging from the control cells by the downregulation of at least 51 and the upregulation of at least 126 genes in response to ischemia.

## Discussion

Despite the heterogeneous population of MSCs, the passaging of subpopulations results in clonal expansion and alterations in their stemness hurdling their regenerative function. Hence, the thorough understanding regarding the heterogeneous nature of MSCs is necessary for harvesting/expanding unique subpopulations to sustain their regenerative potential for ensuring reproducibility of the outcomes [13]. Interestingly, scRNAseq offers a powerful tool to dissect and quantify the heterogeneous subpopulation by assessing the gene expression patterns in individual cells

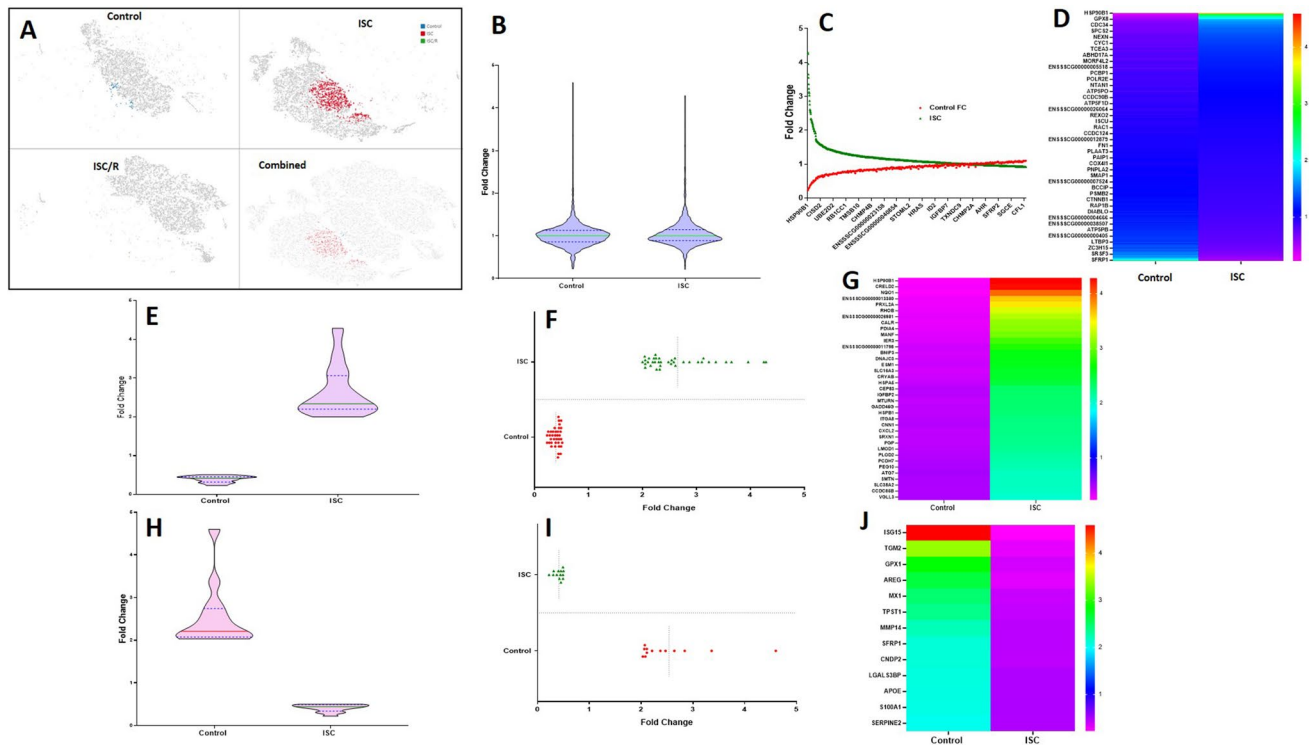


**Fig. 8** Distribution of cell populations and altered genes in Cluster 8: (A) Split view of Control, and ISC groups of Cluster 8 cells and combined view of t-SNE plot showing the distribution of cells within the Cluster 8 tending towards the ISC group based on the local expression of 1,895 genes. (B) Violin plot for highly expressed 1,895 genes revealing the distribution towards upregulation in ISC. (C) Scatterplot of highly expressed 1,895 genes in ISC group showing the upregulation trend compared to Control group. (D) Heat map of highly altered 1,895 genes ( $FC > 2$ ) revealing the upregulation in ISC group. (E) Violin plot for highly expressed 37 genes revealing the distribution towards upregulation in ISC group compared to control. (F)

Scatterplot of highly expressed 37 genes in ISC group showing the minimal level of expression in control group and  $FC > 2$  in ISC where the dotted lines indicate mean FC. (G) Heat map of highly altered 37 genes ( $FC > 2$ ) revealing the upregulation in ISC/R group. (H) Violin plot for highly expressed 13 genes revealing the distribution towards upregulation in Control compared to ISC group. (I) Scatterplot of highly expressed 13 genes in Control group showing the minimal level of expression in ISC group where the dotted lines indicate mean FC. (K) Heat map of highly altered 13 genes ( $FC > 2$ ) revealing the upregulation in ISC group

[14]. The scarcity of relevant information regarding cardiac regeneration and immense translational potential of EATDS encouraged us to explore the existing subpopulations based on single cell genomics. Excitingly, 18 unique clusters of cells were unveiled in our study which were further screened by the upregulation status of signature genes in each cluster based on the treatment (Control, ISC and ISC/R). Ischemia being the primary trigger for myocardial infarction, our major focus was emphasized on the upregulated genes in the ISC group (considering the number of cells,  $> 2\%$ ) in each cluster despite the bulk of data.

Cardiac ischemia activates the asymmetric division of diverse stem cell population resulting in the progenitors/pre-cursors cells to cardiac lineage. Hence, the adverse events underlying the pathology stimulates the stem cell activation as a protective mechanism [15]. EF being at the close proximity and sharing same micro niche as cardiac muscle, the ischemic insults possibly activate the EATDS; however, the underlying mechanism is scarce [16–18]. As expected, the

UMAP analysis revealed a distinct cluster of EATDS in ISC group where the reperfusion tends the cells towards the control group suggesting the existence of a unique population of EATDS in response to ischemia. Overall, the genes associated with tissue regeneration were downregulated/expressed constitutively in the control cells which were significantly upregulated under ischemic insults and reperfusion. IL-11 is a key mediator in promoting cell proliferation and differentiation of ADMSCs and IL-11 signaling has been involved in antioxidant responses [19]. Apart from maintaining ECM integrity, TNC plays a significant role in tissue regeneration by facilitating the mobilization of stem cells from their respective niche [20]. Similarly, PRXL2A is intimately involved in redox signaling offering the protection from oxidative injury [21]. The downregulation of IL-11, TNC and PRXL2A in the control cells suggest the basal level of these genes reflecting the cellular homeostasis. Interestingly, immune responsive mediator ISG15, the antiviral gatekeeper gene MX1 [22], and the metabolic and redox sensor DHRS3

**Table 9** The list of genes locally upregulated genes (FC > 2) in control and ISC groups with respect to each other group in Cluster 8 cells

SI/No	Feature ID	Genes	Control FC	ISC FC	ISC/R FC
Control					
1	ENSSSCG00000040575	ISG15	4.60	0.22	1.35
2	ENSSSCG00000023522	TGM2	3.36	0.30	2.70
3	ENSSSCG00000033727	GPX1	2.84	0.37	0.37
4	ENSSSCG00000008963	AREG	2.64	0.31	11.61
5	ENSSSCG00000012077	MX1	2.47	0.40	2.74
6	ENSSSCG00000007737	TPST1	2.37	0.42	1.83
7	ENSSSCG00000002039	MMP14	2.21	0.45	2.10
8	ENSSSCG00000025822	SFRP1	2.11	0.45	3.17
9	ENSSSCG00000004870	CNDP2	2.11	0.44	4.76
10	ENSSSCG00000036383	LGALS3BP	2.08	0.49	1.35
11	ENSSSCG00000003088	APOE	2.07	0.49	1.08
12	ENSSSCG00000031053	S100A1	2.06	0.50	0.68
13	ENSSSCG00000016233	SERPINE2	2.03	0.49	1.57
ISC					
1	ENSSSCG00000000849	HSP90B1	0.23	4.29	0.30
2	ENSSSCG00000000981	CRELD2	0.25	4.25	0.13
3	ENSSSCG00000002754	NQO1	0.23	3.96	0.98
4	ENSSSCG00000013380	ENSSSCG00000013380	0.27	3.65	0.30
5	ENSSSCG00000010340	PRXL2A	0.28	3.55	0.33
6	ENSSSCG00000043781	RHOB	0.30	3.36	0.35
7	ENSSSCG00000026981	ENSSSCG00000026981	0.31	3.23	0.26
8	ENSSSCG00000013746	CALR	0.30	3.13	0.61
9	ENSSSCG00000015453	PDIA4	0.31	3.10	0.62
10	ENSSSCG00000032914	MANF	0.33	3.03	0.36
11	ENSSSCG00000027607	IER3	0.34	2.87	0.62
12	ENSSSCG00000011798	ENSSSCG00000011798	0.38	2.76	0.12
13	ENSSSCG00000024388	BNIP3	0.36	2.61	0.94
14	ENSSSCG00000026082	DNAJC3	0.38	2.60	0.50
15	ENSSSCG00000016900	ESM1	0.39	2.58	0.43
16	ENSSSCG00000024018	SLC16A3	0.37	2.54	0.97
17	ENSSSCG00000036724	CRYAB	0.39	2.53	0.50
18	ENSSSCG00000005601	HSPA5	0.41	2.48	0.30
19	ENSSSCG00000024563	CEP83	0.45	2.34	0.18
20	ENSSSCG00000035392	IGFBP2	0.45	2.33	0.09
21	ENSSSCG00000037158	MTURN	0.42	2.32	0.65
22	ENSSSCG00000035249	GADD45G	0.44	2.31	0.51
23	ENSSSCG00000039962	HSPB1	0.43	2.30	0.45
24	ENSSSCG00000011046	ITGA8	0.45	2.26	0.28
25	ENSSSCG00000013614	CNN1	0.46	2.25	0.17
26	ENSSSCG00000008959	CXCL2	0.43	2.24	0.79
27	ENSSSCG00000023298	SRXN1	0.44	2.23	0.67
28	ENSSSCG00000036614	PGP	0.44	2.21	0.82
29	ENSSSCG00000031201	LMOD1	0.45	2.19	0.60
30	ENSSSCG00000011689	PLOD2	0.46	2.15	0.53
31	ENSSSCG00000008765	PCDH7	0.48	2.12	0.40
32	ENSSSCG00000036049	PEG10	0.49	2.10	0.22
33	ENSSSCG00000011575	ATG7	0.51	2.05	0.16
34	ENSSSCG00000010017	SMTN	0.49	2.05	0.50
35	ENSSSCG00000000808	SLC38A2	0.49	2.05	0.43
36	ENSSSCG00000012968	CCDC85B	0.48	2.04	0.70

**Table 9** (continued)

SI/No	Feature ID	Genes	Control FC	ISC FC	ISC/R FC
37	ENSSSCG00000032398	VGLL3	0.49	2.00	0.68

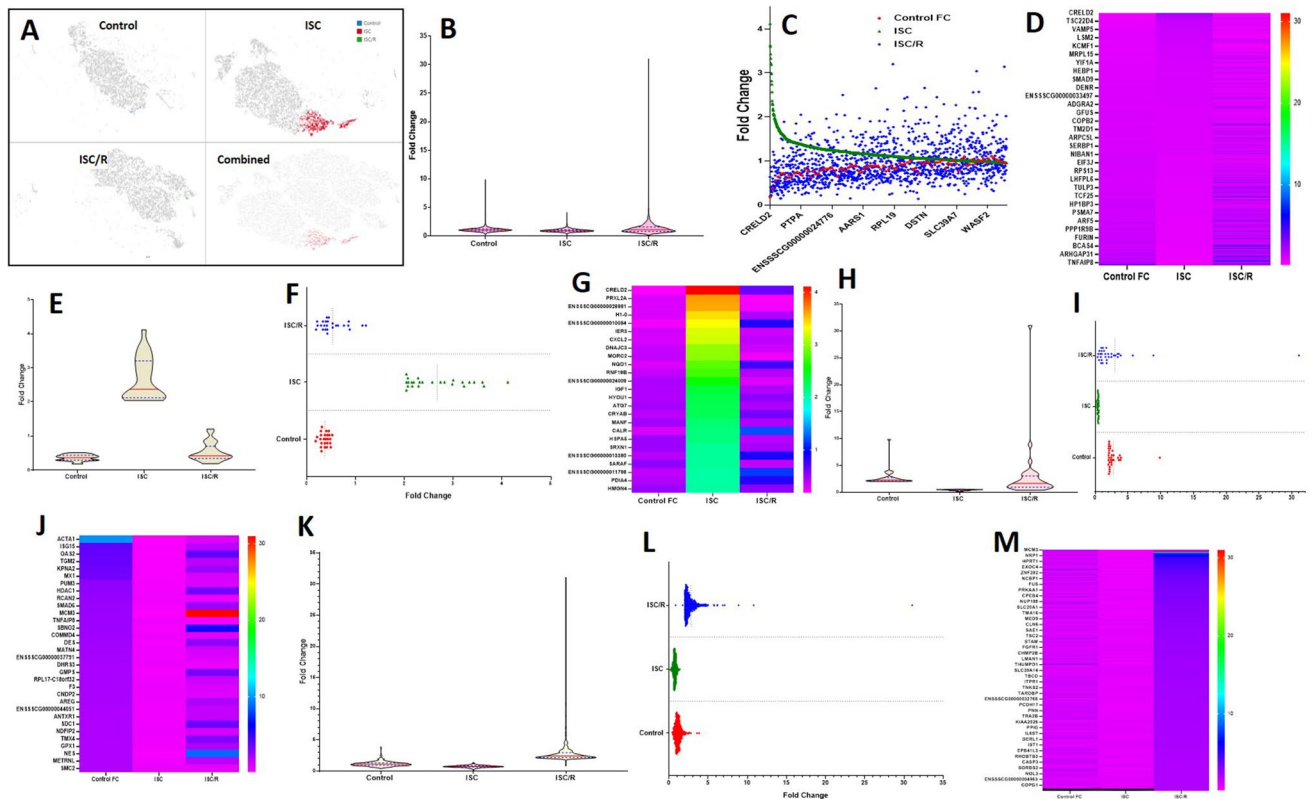


**Fig. 9** Distribution of cell populations and altered genes in Cluster 9: (A) Split view of Control, ISC and ISC/R groups of Cluster 9 cells and combined view of t-SNE plot showing the distribution of cells within the Cluster 9 tending towards the ISC group based on the local expression of 3,093 genes. (B) Violin plot for highly expressed 3,093 genes revealing the distribution towards upregulation in ISC/R group. (C) Scatterplot of highly expressed 3,093 genes in ISC group showing the upregulation trend compared to ISC and ISC/R groups. (D) Heat map of highly altered 3,093 genes ( $FC > 2$ ) revealing the upregulation in ISC and ISC/R groups. (E) Violin plot for highly expressed 25 genes revealing the distribution towards upregulation in ISC group compared to control and ISC/R. (F) Scatterplot of highly expressed 25 genes in ISC group ( $FC > 2$ ) showing the minimal level of expression in control group where the dotted lines indicate mean

FC. (G) Heat map of highly altered 25 genes ( $FC > 2$ ) revealing the upregulation in ISC group. (H) Violin plot for highly expressed 32 genes revealing the distribution towards upregulation in Control and ISC/R compared to ISC group. (I) Scatterplot of highly expressed 32 genes in Control group showing the minimal level of expression in ISC group where the dotted lines indicate mean FC. (J) Heat map of highly altered 32 genes ( $FC > 2$ ) revealing the upregulation in Control and ISC/R group. (K) Violin plot for highly expressed 375 genes revealing the distribution towards upregulation in ISC/R compared to Control and ISC groups. (L) Scatterplot of highly expressed 375 genes in ISC/R group showing the minimal level of expression in ISC group where the dotted lines indicate mean FC. (M) Heat map of highly altered 375 genes ( $FC > 2$ ) revealing the upregulation in ISC/R group

[23] were upregulated in the control contributing to the cellular homeostasis. Moreover, PRXL2A was significantly upregulated in ISC EATDS along with the antioxidant responsive enzyme ALDH1A1 with a concomitant downregulation of cell cycle mediators. This points that the EATDS under ischemia prefers non-proliferative phenotypes. Importantly, upon reperfusion the cellular homeostasis and healing mediators, (downregulated in control cells) and cell cycle mediators (downregulated in ISC cells) were significantly upregulated with a concomitant downregulation of redox

and antioxidant signals vividly suggesting the switch of ISC cells to proliferative and healing phenotype. Evidently, the highly upregulated gene in ISC cells, PRXL2A, is a potent cardioprotective mediator which plays a key role in antioxidant response, angiogenesis, and post-ischemic inflammation via the activation of TLR4 signaling [24]. Importantly, PRXL2A is crucial for the activation, maintenance and proliferation of MSCs through the activation of the pathways including AKT/glycogen synthase kinase 3 beta/ $\beta$ -catenin axis and peroxiredoxin/JNK axis [24, 25] suggesting its

**Table 10** The list of genes locally upregulated genes (FC > 2) in control, ISC and ISC/R groups with respect to each other group in Cluster 9 cells

Sl/No	Feature ID	Genes	Control FC	ISC FC	ISC/R FC
Control					
1	ACTA1	ACTA1	9.84	0.12	0.84
2	ENSSSCG00000040575	ISG15	3.91	0.28	1.74
3	ENSSSCG00000009881	OAS2	3.85	0.25	3.88
4	ENSSSCG00000023522	TGM2	3.74	0.29	1.68
5	ENSSSCG00000029005	KPNA2	3.58	0.29	2.46
6	ENSSSCG00000012077	MX1	3.47	0.33	1.00
7	ENSSSCG00000005227	PUM3	2.80	0.40	0.97
8	ENSSSCG00000003613	HDAC1	2.78	0.34	3.42
9	ENSSSCG00000001716	RCAN2	2.62	0.44	0.57
10	ENSSSCG00000004948	SMAD6	2.58	0.38	2.45
11	ENSSSCG00000025488	MCM3	2.50	0.14	31.05
12	ENSSSCG00000040617	TNFAIP8	2.47	0.48	0.35
13	ENSSSCG00000030042	SBNO2	2.45	0.33	5.72
14	ENSSSCG00000001884	COMMD4	2.43	0.47	0.77
15	ENSSSCG00000020785	DES	2.36	0.39	2.83
16	ENSSSCG00000007391	MATN4	2.29	0.48	1.16
17	ENSSSCG00000037791	ENSSSCG00000037791	2.27	0.48	0.92
18	ENSSSCG00000003439	DHRS3	2.18	0.52	0.46
19	ENSSSCG00000028855	GMPS	2.18	0.41	3.37
20	ENSSSCG00000035007	RPL17-C18orf32	2.17	0.48	1.33
21	ENSSSCG00000022447	F3	2.16	0.51	0.97
22	ENSSSCG00000004870	CNDP2	2.12	0.53	0.88
23	ENSSSCG00000008963	AREG	2.12	0.47	2.05
24	ENSSSCG00000044051	ENSSSCG00000044051	2.10	0.49	1.56
25	ENSSSCG00000008601	SDC1	2.10	0.42	3.60
26	ENSSSCG00000008340	ANTXR1	2.10	0.50	1.53
27	ENSSSCG00000009480	NDFIP2	2.07	0.52	1.12
28	ENSSSCG00000021353	TMX4	2.05	0.44	3.07
29	ENSSSCG00000033727	GPX1	2.03	0.49	1.96
30	ENSSSCG00000006474	NES	2.03	0.31	8.87
31	ENSSSCG00000017137	METRNL	2.03	0.50	1.74
32	ENSSSCG00000005403	SMC2	2.00	0.57	0.61
ISC					
1	ENSSSCG00000000981	CRELD2	0.18	4.12	0.64
2	ENSSSCG00000010340	PRXL2A	0.29	3.63	0.19
3	ENSSSCG00000026981	ENSSSCG00000026981	0.29	3.60	0.21
4	ENSSSCG00000039348	H1-0	0.28	3.43	0.41
5	ENSSSCG00000010084	ENSSSCG00000010084	0.21	3.33	0.86
6	ENSSSCG00000027607	IER3	0.31	3.22	0.33
7	ENSSSCG00000008959	CXCL2	0.30	3.19	0.38
8	ENSSSCG00000026082	DNAJC3	0.35	3.00	0.33
9	ENSSSCG00000010016	MORC2	0.37	2.98	0.22
10	ENSSSCG00000002754	NQO1	0.29	2.82	0.76
11	ENSSSCG00000025206	RNF19B	0.37	2.74	0.41
12	ENSSSCG00000024009	ENSSSCG00000024009	0.43	2.57	0.29
13	ENSSSCG00000000857	IGF1	0.42	2.37	0.42
14	ENSSSCG00000015106	HYOU1	0.42	2.31	0.53
15	ENSSSCG00000011575	ATG7	0.45	2.29	0.43
16	ENSSSCG00000036724	CRYAB	0.39	2.28	0.60
17	ENSSSCG00000032914	MANF	0.46	2.19	0.42



**Table 10** (continued)

SI/No	Feature ID	Genes	Control FC	ISC FC	ISC/R FC
18	ENSSSCG00000013746	CALR	0.30	2.16	1.21
19	ENSSSCG00000005601	HSPA5	0.48	2.15	0.39
20	ENSSSCG00000023298	SRXN1	0.48	2.08	0.45
21	ENSSSCG00000013380	ENSSSCG00000013380	0.40	2.07	0.88
22	ENSSSCG00000033402	SARAF	0.52	2.07	0.36
23	ENSSSCG00000011798	ENSSSCG00000011798	0.37	2.04	1.14
24	ENSSSCG00000015453	PDIA4	0.41	2.04	0.85
25	ENSSSCG00000020696	HMGN4	0.49	2.04	0.53
ISC/R					
1	ENSSSCG00000025488	MCM3	2.50	0.14	31.05
2	ENSSSCG00000017682	MYO19	0.93	0.41	10.80
3	ENSSSCG00000006474	NES	2.03	0.31	8.87
4	ENSSSCG00000005946	CCN4	1.47	0.42	7.10
5	ENSSSCG00000011855	IQCG	1.00	0.52	6.86
6	ENSSSCG00000014331	ENSSSCG00000014331	0.90	0.58	6.18
7	ENSSSCG00000015784	ACSL1	1.11	0.52	6.15
8	ENSSSCG00000025775	TADA2A	0.59	0.72	5.75
9	ENSSSCG00000030042	SBNO2	2.45	0.33	5.72
10	ENSSSCG00000011102	NRP1	0.84	0.65	4.98
11	ENSSSCG00000009553	TUBGCP3	1.02	0.60	4.95
12	ENSSSCG00000018091	ND5	0.62	0.72	4.77
13	ENSSSCG00000027331	COL6A3	0.89	0.65	4.76
14	ENSSSCG00000009501	ENSSSCG00000009501	1.87	0.42	4.76
15	ENSSSCG00000014136	VCAN	0.66	0.74	4.71
16	ENSSSCG00000028805	PTPRM	1.49	0.49	4.61
17	ENSSSCG00000015045	NCAM1	1.89	0.41	4.58
18	ENSSSCG00000012425	UPRT	0.95	0.66	4.58
19	ENSSSCG00000034896	HPRT1	1.09	0.60	4.48
20	ENSSSCG00000008427	KCNK12	0.66	0.80	4.47
21	ENSSSCG00000007992	PIGQ	1.90	0.43	4.46
22	ENSSSCG00000016233	SERPINE2	1.68	0.44	4.40
23	ENSSSCG00000004921	ATP8B1	0.91	0.69	4.37
24	ENSSSCG00000025822	SFRP1	1.44	0.50	4.31
25	ENSSSCG00000035564	MCM6	1.09	0.62	4.20
26	ENSSSCG00000001925	ADPGK	1.20	0.59	4.19
27	ENSSSCG00000039996	FAM168A	1.17	0.60	4.11
28	ENSSSCG00000016543	EXOC4	0.56	0.90	4.05
29	ENSSSCG00000039862	TRIB3	1.22	0.58	4.02
30	ENSSSCG00000015214	STT3A	1.08	0.64	3.99
31	ENSSSCG00000038950	VAR51	1.08	0.64	3.89
32	ENSSSCG00000009881	OAS2	3.85	0.25	3.88
33	ENSSSCG00000001756	IREB2	1.29	0.58	3.85
34	ENSSSCG00000022656	SRFBP1	0.55	0.96	3.76
35	ENSSSCG00000012823	DKC1	1.00	0.68	3.76
36	ENSSSCG00000000837	CHST11	1.71	0.49	3.75
37	ENSSSCG00000016773	ZNF282	1.58	0.51	3.74
38	ENSSSCG00000015872	GPD2	1.07	0.67	3.73
39	ENSSSCG00000003403	CENPS	0.87	0.76	3.69
40	ENSSSCG00000008601	SDC1	2.10	0.42	3.60
41	ENSSSCG00000014082	POLK	1.28	0.61	3.56
42	ENSSSCG00000001372	GNL1	0.73	0.85	3.55

**Table 10** (continued)

SI/No	Feature ID	Genes	Control FC	ISC FC	ISC/R FC
43	ENSSSCG00000003088	APOE	1.16	0.65	3.52
44	ENSSSCG00000000757	ADIPOR2	1.26	0.61	3.51
45	ENSSSCG00000015712	DDX18	1.79	0.47	3.51
46	ENSSSCG00000005366	NCBP1	1.13	0.66	3.47
47	ENSSSCG00000004832	UBE3A	0.90	0.74	3.45
48	ENSSSCG00000010176	C1orf131	1.67	0.51	3.45
49	ENSSSCG00000010118	HIRA	1.08	0.68	3.44
50	ENSSSCG00000003613	HDAC1	2.78	0.34	3.42
51	ENSSSCG00000024300	TMEM254	1.19	0.64	3.41
52	ENSSSCG00000029998	KLF7	0.62	0.90	3.38
53	ENSSSCG00000028855	GMPS	2.18	0.41	3.37
54	ENSSSCG00000027689	SRM	1.30	0.60	3.37
55	ENSSSCG00000030798	FUS	1.34	0.59	3.36
56	ENSSSCG00000037305	TMEM33	1.10	0.69	3.35
57	ENSSSCG00000025821	C2CD2	0.88	0.77	3.33
58	ENSSSCG00000004958	PIAS1	0.69	0.90	3.32
59	ENSSSCG00000039568	SNAI2	1.14	0.66	3.32
60	ENSSSCG00000005478	ENSSSCG00000005478	0.99	0.73	3.30
61	ENSSSCG00000004825	CHSY1	1.65	0.51	3.29
62	ENSSSCG00000018069	ND2	0.90	0.74	3.27
63	ENSSSCG00000016841	SLC1A3	0.95	0.75	3.26
64	ENSSSCG00000011157	PITRM1	0.97	0.75	3.24
65	ENSSSCG00000024598	PRKAA1	1.27	0.63	3.24
66	ENSSSCG00000001498	BEND6	1.16	0.67	3.23
67	ENSSSCG00000001836	RLBP1	0.41	1.11	3.20
68	ENSSSCG00000010171	TSNAX	1.45	0.58	3.19
69	ENSSSCG00000008266	LOXL3	0.89	0.79	3.19
70	ENSSSCG00000008261	HK2	0.66	0.95	3.18
71	ENSSSCG00000016005	SESTD1	1.96	0.46	3.18
72	ENSSSCG00000016981	CPEB4	0.74	0.89	3.18
73	ENSSSCG00000009246	ENOPH1	0.83	0.83	3.18
74	ENSSSCG00000005212	PLGRKT	1.97	0.45	3.17
75	ENSSSCG000000035611	MGAT2	1.27	0.62	3.15
76	ENSSSCG000000030153	SMURF1	0.94	0.78	3.15
77	ENSSSCG00000009633	ENSSSCG00000009633	0.65	0.97	3.14
78	ENSSSCG000000031871	ENTPD4	0.65	0.95	3.13
79	ENSSSCG00000010555	HIF1AN	0.93	0.79	3.11
80	ENSSSCG00000010568	NPM3	0.97	0.74	3.11
81	ENSSSCG00000008756	DHX15	1.03	0.72	3.10
82	ENSSSCG00000005667	NUP188	1.11	0.70	3.10
83	ENSSSCG00000021353	TMX4	2.05	0.44	3.07
84	ENSSSCG000000036885	ZNF654	0.63	1.00	3.04
85	ENSSSCG00000014934	CHORDC1	1.52	0.56	3.01
86	ENSSSCG00000001053	TBC1D7	1.42	0.59	2.99
87	ENSSSCG00000013659	DNMT1	1.04	0.73	2.99
88	ENSSSCG00000018065	ND1	0.61	0.95	2.99
89	ENSSSCG00000004730	TMEM87A	1.35	0.62	2.99
90	ENSSSCG00000017273	PSMD12	1.01	0.75	2.98
91	ENSSSCG000000032288	SLC20A1	0.93	0.79	2.98
92	ENSSSCG00000000549	PPFIBP1	1.49	0.56	2.95
93	ENSSSCG00000000176	DDX23	1.08	0.72	2.95

**Table 10** (continued)

SI/No	Feature ID	Genes	Control FC	ISC FC	ISC/R FC
94	ENSSSCG00000018082	COX3	0.72	0.87	2.94
95	ENSSSCG00000003795	WLS	0.86	0.83	2.94
96	ENSSSCG00000022486	CBLB	0.97	0.75	2.93
97	ENSSSCG00000015380	CDCA7L	0.78	0.89	2.93
98	ENSSSCG00000008496	EIF2AK2	1.97	0.46	2.92
99	ENSSSCG00000025053	RYBP	1.67	0.52	2.91
100	ENSSSCG00000008890	TMA16	1.13	0.71	2.90
101	ENSSSCG00000024125	KPNA3	0.94	0.77	2.89
102	ENSSSCG00000011329	CCDC12	1.40	0.60	2.89
103	ENSSSCG00000038856	TRIM8	1.29	0.63	2.88
104	ENSSSCG00000026052	LSM14B	1.11	0.72	2.86
105	ENSSSCG00000037451	PPFIA1	0.97	0.79	2.84
106	ENSSSCG00000025447	MID1IP1	1.04	0.75	2.84
107	ENSSSCG00000020785	DES	2.36	0.39	2.83
108	ENSSSCG00000032996	SLC7A5	1.54	0.56	2.81
109	ENSSSCG00000009345	PDS5B	0.71	0.95	2.79
110	ENSSSCG00000018053	MED9	0.97	0.78	2.79
111	ENSSSCG00000001903	EDC3	1.17	0.69	2.79
112	ENSSSCG00000008400	CFAP36	0.74	0.93	2.78
113	ENSSSCG00000009061	NAA15	0.84	0.86	2.78
114	ENSSSCG00000022806	LIN7C	1.44	0.59	2.78
115	ENSSSCG00000039004	ENSSSCG00000039004	1.16	0.69	2.76
116	ENSSSCG00000041822	SMARCD2	0.72	0.96	2.76
117	ENSSSCG00000017419	DNAJC7	1.22	0.67	2.76
118	ENSSSCG00000004957	CLN6	1.23	0.67	2.75
119	ENSSSCG00000023105	NET1	0.74	0.93	2.74
120	ENSSSCG00000004624	MAPK6	1.48	0.58	2.73
121	ENSSSCG00000008398	PPP4R3B	1.01	0.75	2.72
122	ENSSSCG00000040642	LASP1	1.10	0.70	2.72
123	ENSSSCG00000009569	PSPC1	0.92	0.82	2.71
124	ENSSSCG00000003154	GYS1	1.38	0.61	2.71
125	ENSSSCG00000000625	LRP6	0.88	0.86	2.68
126	ENSSSCG00000003111	SAE1	1.13	0.71	2.68
127	ENSSSCG00000014291	AFF4	1.47	0.58	2.68
128	ENSSSCG00000033786	ENSSSCG00000033786	1.13	0.71	2.68
129	ENSSSCG00000030396	SETD7	0.90	0.82	2.68
130	ENSSSCG00000033753	UBXN2A	0.99	0.79	2.67
131	ENSSSCG00000005494	TNC	0.61	1.06	2.66
132	ENSSSCG00000011028	EPC1	0.80	0.90	2.66
133	ENSSSCG00000000202	MCRS1	1.37	0.63	2.66
134	ENSSSCG00000040435	STAT6	0.83	0.89	2.66
135	ENSSSCG00000029485	FBXO11	0.79	0.90	2.66
136	ENSSSCG00000008040	TSC2	1.12	0.73	2.65
137	ENSSSCG00000010829	ENSSSCG00000010829	0.55	1.14	2.65
138	ENSSSCG00000007739	GUSB	0.90	0.85	2.65
139	ENSSSCG00000006395	ENSSSCG00000006395	1.46	0.58	2.64
140	ENSSSCG00000033703	FAM111A	1.95	0.47	2.64
141	ENSSSCG00000014970	MTMR2	0.87	0.87	2.64
142	ENSSSCG00000038987	CCDC59	1.01	0.77	2.64
143	ENSSSCG00000026552	MFSD14B	0.98	0.79	2.63
144	ENSSSCG00000003722	CDH2	1.15	0.70	2.63

**Table 10** (continued)

SI/No	Feature ID	Genes	Control FC	ISC FC	ISC/R FC
145	ENSSSCG00000011036	STAM	0.99	0.79	2.62
146	ENSSSCG00000005037	ERO1A	1.25	0.67	2.62
147	ENSSSCG00000013771	PRKACA	1.52	0.58	2.60
148	ENSSSCG00000001873	CSPG4	0.83	0.88	2.59
149	ENSSSCG000000035827	CTDSPL2	1.01	0.79	2.58
150	ENSSSCG000000023983	AGPS	1.36	0.63	2.58
151	ENSSSCG000000003787	ZRANB2	1.38	0.62	2.58
152	ENSSSCG000000038025	NRBP2	1.40	0.63	2.58
153	ENSSSCG00000007366	MYBL2	0.69	1.00	2.57
154	ENSSSCG00000015815	FGFR1	1.08	0.75	2.56
155	ENSSSCG000000027349	ENSSSCG000000027349	0.69	1.00	2.56
156	ENSSSCG000000028516	LARP4	1.07	0.76	2.56
157	ENSSSCG00000010204	BICC1	1.07	0.74	2.56
158	ENSSSCG00000004927	CLPX	1.21	0.70	2.55
159	ENSSSCG00000000743	FKBP4	1.01	0.79	2.55
160	ENSSSCG00000016983	STC2	0.96	0.81	2.54
161	ENSSSCG000000032498	IDH3A	1.18	0.70	2.54
162	ENSSSCG00000014557	RIC8A	1.22	0.70	2.53
163	ENSSSCG000000003485	RCC2	1.00	0.79	2.52
164	ENSSSCG00000011997	CHMP2B	1.11	0.74	2.52
165	ENSSSCG00000000457	USP15	1.06	0.77	2.52
166	ENSSSCG00000015729	TSN	1.13	0.74	2.51
167	ENSSSCG00000017626	SRSF1	1.52	0.59	2.51
168	ENSSSCG000000003017	TGFB1	0.52	1.22	2.50
169	ENSSSCG000000029456	SLC7A1	1.76	0.53	2.50
170	ENSSSCG00000004253	ENSSSCG00000004253	1.39	0.63	2.50
171	ENSSSCG000000009777	KMT5A	1.87	0.50	2.50
172	ENSSSCG00000004908	LMAN1	1.04	0.76	2.48
173	ENSSSCG000000036136	BHLHE40	1.58	0.57	2.47
174	ENSSSCG00000010508	TM9SF3	1.10	0.73	2.47
175	ENSSSCG000000039285	MFN1	0.90	0.86	2.47
176	ENSSSCG000000038422	TMX1	1.30	0.65	2.47
177	ENSSSCG000000002429	FOXN3	1.08	0.75	2.46
178	ENSSSCG00000004595	ADAM10	1.17	0.72	2.46
179	ENSSSCG00000012400	SNX12	0.96	0.84	2.46
180	ENSSSCG000000029005	KPNA2	3.58	0.29	2.46
181	ENSSSCG000000024748	THUMPD1	1.34	0.66	2.45
182	ENSSSCG00000010059	GUCD1	0.66	1.04	2.45
183	ENSSSCG00000000587	AEBP2	1.33	0.65	2.45
184	ENSSSCG000000005170	DENND4C	0.64	1.08	2.45
185	ENSSSCG00000004948	SMAD6	2.58	0.38	2.45
186	ENSSSCG000000003673	CEP192	0.88	0.89	2.45
187	ENSSSCG000000029279	GNA11	1.07	0.76	2.43
188	ENSSSCG00000015435	NAMPT	0.80	0.95	2.43
189	ENSSSCG000000001817	FURIN	1.21	0.70	2.43
190	ENSSSCG000000000458	MON2	0.80	0.95	2.43
191	ENSSSCG000000032622	SLC39A14	0.94	0.85	2.43
192	ENSSSCG000000036488	KLF3	1.06	0.77	2.42
193	ENSSSCG00000013475	NCLN	0.65	1.09	2.42
194	ENSSSCG000000025028	XIAP	1.02	0.81	2.42
195	ENSSSCG00000011136	TASOR2	1.25	0.69	2.42

**Table 10** (continued)

SI/No	Feature ID	Genes	Control FC	ISC FC	ISC/R FC
196	ENSSSCG00000024419	RBBP8	1.25	0.69	2.41
197	ENSSSCG00000010604	SH3PXD2A	0.91	0.85	2.41
198	ENSSSCG00000025698	SERPINE1	1.64	0.54	2.41
199	ENSSSCG00000017136	TBCD	1.01	0.81	2.40
200	ENSSSCG00000014022	HNRNPH1	1.34	0.64	2.40
201	ENSSSCG00000007811	SPNS1	1.23	0.71	2.39
202	ENSSSCG00000024696	CCNYL1	1.05	0.78	2.39
203	ENSSSCG00000015808	ADAM9	1.08	0.75	2.39
204	ENSSSCG00000017953	FXR2	0.87	0.89	2.39
205	ENSSSCG00000012247	ATP6AP2	1.29	0.66	2.39
206	ENSSSCG00000035238	ELOVL1	0.83	0.92	2.38
207	ENSSSCG00000010437	PAPSS2	1.63	0.56	2.37
208	ENSSSCG00000023437	ITPR1	1.51	0.60	2.37
209	ENSSSCG00000003617	TXLNA	1.21	0.72	2.36
210	ENSSSCG00000032967	CACNB3	1.36	0.66	2.36
211	ENSSSCG00000026819	NID1	1.01	0.79	2.35
212	ENSSSCG00000012825	IKBKG	0.84	0.93	2.35
213	ENSSSCG00000009123	CAMK2D	1.26	0.68	2.35
214	ENSSSCG00000005232	SMARCA2	0.90	0.87	2.35
215	ENSSSCG00000025440	ELOA	1.37	0.65	2.35
216	ENSSSCG00000010288	DNAJB12	1.20	0.72	2.34
217	ENSSSCG00000010465	TNKS2	1.21	0.71	2.34
218	ENSSSCG000000031109	HILPDA	0.84	0.90	2.33
219	ENSSSCG00000001871	HMG20A	1.05	0.80	2.33
220	ENSSSCG00000016578	FLNC	0.90	0.86	2.32
221	ENSSSCG00000008358	ACTR2	1.23	0.69	2.32
222	ENSSSCG00000021610	CHPF	1.42	0.63	2.32
223	ENSSSCG00000002330	PCNX1	0.97	0.84	2.31
224	ENSSSCG00000025912	URI1	1.32	0.67	2.31
225	ENSSSCG00000012939	BRMS1	1.28	0.69	2.31
226	ENSSSCG00000023126	TARDBP	0.97	0.84	2.30
227	ENSSSCG00000038144	ENSSSCG00000038144	1.25	0.68	2.30
228	ENSSSCG00000030547	PIP5K1A	1.39	0.65	2.30
229	ENSSSCG00000031537	HAND2	1.09	0.76	2.30
230	ENSSSCG00000016882	PARP8	0.87	0.90	2.30
231	ENSSSCG00000015396	SEMA3D	1.92	0.50	2.30
232	ENSSSCG00000022900	SUPT16H	1.27	0.69	2.30
233	ENSSSCG00000035523	FUT11	0.72	1.03	2.29
234	ENSSSCG00000003194	AKT1S1	0.84	0.91	2.29
235	ENSSSCG00000030581	VGLL4	0.89	0.90	2.29
236	ENSSSCG00000032768	ENSSSCG00000032768	1.10	0.77	2.29
237	ENSSSCG00000023984	RSL1D1	1.34	0.65	2.29
238	ENSSSCG00000013297	CD44	1.11	0.75	2.29
239	ENSSSCG00000012328	HUWE1	0.90	0.88	2.29
240	ENSSSCG00000025298	POLR1F	1.25	0.69	2.28
241	ENSSSCG00000008788	RFC1	1.26	0.69	2.28
242	ENSSSCG00000035318	NUP58	1.02	0.82	2.28
243	ENSSSCG00000018084	ND3	1.38	0.63	2.28
244	ENSSSCG00000025114	FMNL3	0.75	1.02	2.27
245	ENSSSCG00000009446	PCDH17	1.00	0.82	2.27
246	ENSSSCG00000011471	FLNB	1.63	0.56	2.27

**Table 10** (continued)

SI/No	Feature ID	Genes	Control FC	ISC FC	ISC/R FC
247	ENSSSCG00000006324	ENSSSCG00000006324	1.20	0.72	2.27
248	ENSSSCG00000016968	BDP1	0.95	0.85	2.27
249	ENSSSCG00000009208	ENSSSCG00000009208	1.30	0.69	2.26
250	ENSSSCG00000004822	ALDH1A3	1.23	0.70	2.26
251	ENSSSCG00000012325	SMC1A	1.44	0.63	2.25
252	ENSSSCG00000015570	IVNS1ABP	0.80	0.94	2.25
253	ENSSSCG00000022828	PNN	1.19	0.72	2.25
254	ENSSSCG00000005625	ENG	1.28	0.67	2.25
255	ENSSSCG00000032728	EFNB1	1.02	0.80	2.25
256	ENSSSCG00000016520	CREB3L2	1.43	0.63	2.25
257	ENSSSCG00000011474	PXK	1.28	0.69	2.24
258	ENSSSCG00000002926	TBCB	1.33	0.67	2.24
259	ENSSSCG00000025406	PIK3C2A	1.55	0.59	2.24
260	ENSSSCG00000035058	PID1	0.89	0.89	2.24
261	ENSSSCG00000039390	EIF3B	1.26	0.69	2.24
262	ENSSSCG00000030225	TRA2B	1.32	0.67	2.23
263	ENSSSCG00000008508	FAM98A	1.24	0.70	2.23
264	ENSSSCG00000015960	MAP3K20	1.25	0.70	2.23
265	ENSSSCG00000004460	IBTK	1.30	0.69	2.23
266	ENSSSCG00000038549	ZFP36L2	1.73	0.54	2.22
267	ENSSSCG00000002774	RIPOR1	1.07	0.80	2.22
268	ENSSSCG00000046234	ENSSSCG00000046234	0.69	1.07	2.22
269	ENSSSCG00000017365	G6PC3	1.23	0.71	2.22
270	ENSSSCG00000018081	ATP6	0.65	1.06	2.22
271	ENSSSCG00000025130	KLF12	0.93	0.88	2.21
272	ENSSSCG00000005205	KIAA2026	1.41	0.64	2.21
273	ENSSSCG00000012703	RBMX	0.96	0.84	2.21
274	ENSSSCG00000038410	CPEB2	0.88	0.90	2.21
275	ENSSSCG00000016646	ENSSSCG00000016646	1.48	0.62	2.21
276	ENSSSCG00000012771	SLC6A8	0.93	0.88	2.21
277	ENSSSCG00000011825	ATP13A3	1.54	0.60	2.21
278	ENSSSCG00000006892	DNTTIP2	0.74	1.00	2.21
279	ENSSSCG00000016824	RAI14	1.80	0.52	2.20
280	ENSSSCG00000025214	TSHZ3	0.77	1.00	2.20
281	ENSSSCG00000031123	PPIG	1.20	0.72	2.20
282	ENSSSCG00000023709	PTPRJ	1.34	0.67	2.19
283	ENSSSCG00000008697	HTT	1.16	0.75	2.19
284	ENSSSCG00000023912	ORAI2	0.78	1.00	2.19
285	ENSSSCG00000039060	RASSF3	1.12	0.77	2.19
286	ENSSSCG00000011552	ARPC4	1.33	0.66	2.18
287	ENSSSCG00000002441	PPP4R3A	0.85	0.94	2.17
288	ENSSSCG00000018041	ALDH3A2	0.82	0.94	2.17
289	ENSSSCG00000016916	IL6ST	1.53	0.59	2.17
290	ENSSSCG00000033120	PALM2AKAP2	1.38	0.65	2.17
291	ENSSSCG00000008162	IL1R1	0.65	1.11	2.17
292	ENSSSCG00000008644	KIDINS220	1.04	0.82	2.16
293	ENSSSCG00000006115	RUNX1T1	1.47	0.62	2.16
294	ENSSSCG00000005084	PPM1A	1.05	0.81	2.16
295	ENSSSCG00000024149	ELOVL5	1.31	0.69	2.16
296	ENSSSCG00000000510	TMEM19	1.55	0.60	2.16
297	ENSSSCG00000037381	GET1	1.23	0.71	2.16



**Table 10** (continued)

SI/No	Feature ID	Genes	Control FC	ISC FC	ISC/R FC
298	ENSSSCG00000033690	DERL1	0.88	0.90	2.15
299	ENSSSCG00000027139	FYTTD1	1.30	0.68	2.15
300	ENSSSCG00000006074	STK3	1.24	0.72	2.15
301	ENSSSCG00000028663	RBM25	0.85	0.94	2.15
302	ENSSSCG00000006340	UAP1	0.94	0.87	2.15
303	ENSSSCG00000029594	WBP1L	1.04	0.80	2.15
304	ENSSSCG00000008909	CLOCK	0.90	0.91	2.15
305	ENSSSCG00000002863	LRP3	1.05	0.81	2.14
306	ENSSSCG00000033912	ATG12	1.25	0.71	2.14
307	ENSSSCG00000002743	IST1	0.67	1.09	2.14
308	ENSSSCG00000028420	EIF4E	0.85	0.94	2.14
309	ENSSSCG00000035987	EHD3	1.12	0.76	2.13
310	ENSSSCG00000015213	EI24	0.89	0.91	2.13
311	ENSSSCG00000028019	LRRC59	1.14	0.76	2.13
312	ENSSSCG00000005039	STYX	1.35	0.67	2.13
313	ENSSSCG00000039249	ENSSSCG00000039249	1.00	0.82	2.13
314	ENSSSCG00000017047	CLINT1	1.41	0.64	2.12
315	ENSSSCG00000003359	TPRG1L	1.54	0.60	2.12
316	ENSSSCG00000022942	PHF6	0.94	0.88	2.11
317	ENSSSCG00000003687	EPB41L3	1.11	0.78	2.11
318	ENSSSCG00000000118	MICALL1	1.19	0.74	2.11
319	ENSSSCG00000022659	CLTC	1.17	0.74	2.11
320	ENSSSCG00000007056	PLCB1	1.38	0.66	2.11
321	ENSSSCG00000009657	PPP2R2A	1.59	0.59	2.10
322	ENSSSCG00000024578	PHLDB1	0.92	0.87	2.10
323	ENSSSCG00000027898	ATP2B1	0.98	0.84	2.10
324	ENSSSCG00000005749	BRD3	0.88	0.91	2.10
325	ENSSSCG00000029805	RHOBTB3	1.02	0.82	2.10
326	ENSSSCG00000036321	TRADD	1.08	0.80	2.09
327	ENSSSCG00000013302	CAT	0.87	0.94	2.09
328	ENSSSCG00000038533	NAPG	1.43	0.64	2.08
329	ENSSSCG00000005959	ENSSSCG00000005959	1.19	0.74	2.08
330	ENSSSCG00000036549	DPYSL3	1.15	0.75	2.08
331	ENSSSCG00000007253	MAPRE1	1.18	0.74	2.07
332	ENSSSCG00000028755	EIPR1	1.58	0.60	2.07
333	ENSSSCG00000024486	HOOK3	1.20	0.72	2.07
334	ENSSSCG00000014240	CSNK1G3	1.03	0.83	2.07
335	ENSSSCG00000034012	CASP3	1.32	0.68	2.07
336	ENSSSCG00000004622	GNB5	1.11	0.78	2.07
337	ENSSSCG00000023409	TIA1	1.52	0.61	2.07
338	ENSSSCG00000009083	SPRY1	0.93	0.90	2.06
339	ENSSSCG00000029538	PPP2R1B	1.25	0.72	2.06
340	ENSSSCG00000012001	ROBO1	1.20	0.73	2.06
341	ENSSSCG00000002446	ATXN3	0.57	1.23	2.06
342	ENSSSCG00000025561	VASN	0.95	0.86	2.06
343	ENSSSCG00000036679	SORBS2	1.31	0.70	2.05
344	ENSSSCG00000000890	NEDD1	1.59	0.60	2.05
345	ENSSSCG00000040855	C5orf51	1.05	0.83	2.05
346	ENSSSCG00000017308	CDC27	0.48	1.38	2.05
347	ENSSSCG00000008963	AREG	2.12	0.47	2.05
348	ENSSSCG00000000262	SPRYD3	1.43	0.65	2.05

**Table 10** (continued)

Sl/No	Feature ID	Genes	Control FC	ISC FC	ISC/R FC
349	ENSSSCG00000010035	YWHAH	0.80	0.97	2.05
350	ENSSSCG00000032554	ENSSSCG00000032554	1.08	0.81	2.05
351	ENSSSCG00000015411	PTPN12	1.04	0.81	2.05
352	ENSSSCG00000040125	NOL3	1.18	0.75	2.04
353	ENSSSCG00000039635	ENSSSCG00000039635	0.57	1.21	2.04
354	ENSSSCG00000010904	NEK7	1.70	0.56	2.04
355	ENSSSCG00000009464	COMMD6	1.13	0.78	2.04
356	ENSSSCG00000014924	CTSC	0.98	0.85	2.03
357	ENSSSCG00000009018	SH3D19	1.24	0.72	2.03
358	ENSSSCG00000025966	EIF4H	1.00	0.83	2.03
359	ENSSSCG00000014828	RAB6A	1.07	0.80	2.03
360	ENSSSCG00000004963	ENSSSCG00000004963	0.80	1.01	2.03
361	ENSSSCG00000010686	BAG3	1.07	0.80	2.03
362	ENSSSCG00000014625	TRIM3	0.97	0.86	2.03
363	ENSSSCG00000007322	ENSSSCG00000007322	0.80	0.99	2.03
364	ENSSSCG00000003035	ENSSSCG00000003035	1.12	0.78	2.03
365	ENSSSCG00000005204	RANBP6	1.18	0.76	2.03
366	ENSSSCG00000017506	FBXL20	0.85	0.96	2.02
367	ENSSSCG00000004070	SCAF8	1.15	0.77	2.01
368	ENSSSCG000000031392	UBE2E2	1.22	0.74	2.01
369	ENSSSCG00000006009	EXT1	1.46	0.63	2.01
370	ENSSSCG00000011616	COPG1	0.84	0.95	2.01
371	ENSSSCG00000014387	DIAPH1	1.09	0.81	2.01
372	ENSSSCG00000039926	ENSSSCG00000039926	0.72	1.04	2.01
373	ENSSSCG000000034502	H6PD	1.16	0.77	2.00
374	ENSSSCG00000006089	PTDSS1	0.96	0.89	2.00
375	ENSSSCG00000008619	DDX1	1.22	0.74	2.00

pivotal role in the activation and proliferation of an unique subtype of EATDS following ischemia.

Even though the Cluster 1 cells favored reperfusion, two genes H1-0 and MGP were significantly upregulated in the ISC group. Interestingly, H1-0 is a key epigenetic regulator which is intimately associated with the activation, differentiation, and plasticity of stem cells [26, 27]. H1-0 drives the heterogeneity of cancer stem cells responding to the biochemical alterations in the micro niche [28]; however, information is unavailable regarding its role in EATDS. Therefore, it is logical that similar mode of operation is possible in EATDS as evident from the upregulation of H1-0 in the ISC group with a concomitant decrease following the reperfusion; however, warranting further examination. Similarly, MGP is an effective inhibitor for various BMPs (bone morphogenic proteins) and prevents the vascular calcification and angiogenesis [29]. Interestingly, MGP positive MSCs displayed protective effects on atherosclerosis and angiostenosis eliciting immunomodulatory responses [30]. Moreover, MGP is actively involved in the maintenance of myocardial homeostasis and cardiac performance where its role in EATDS is unknown [31]. The increased level of

MGP in Cluster 1 cells suggests the protective responses elicited by EATDS on encountering ischemia which was declined following reperfusion. Taken together, the ischemic insults result in a subpopulation of cells by upregulating the key mediators including H1-0 and MGP and further understanding of this subpopulation are required for regenerative cardiology.

Cluster 2 and 3 cells predominated in control group where the genes CDC20 and CCN5 were significantly upregulated in the ISC groups of Cluster 2 and 3, respectively. CDC20 is the cell cycle regulator which is crucial in determining the viability and proliferation status of cells [32]. The increased CDC20 reflects the actively proliferating cells despite the ischemia suggesting the adaptations of Cluster 2 cells to withstand the deleterious effects by increasing the cell density. Similarly, the matricellular protein CCN5 regulates the cellular integrity especially in responding to alterations in microenvironment [33]. Hence, the ischemic cells in the clusters 2 and 3 were survived respectively by increasing the cell cycle and maintaining the cellular integrity. Hence, it is reasonable to speculate that these subpopulations of cells exist in lower density acting as progenitors for specific

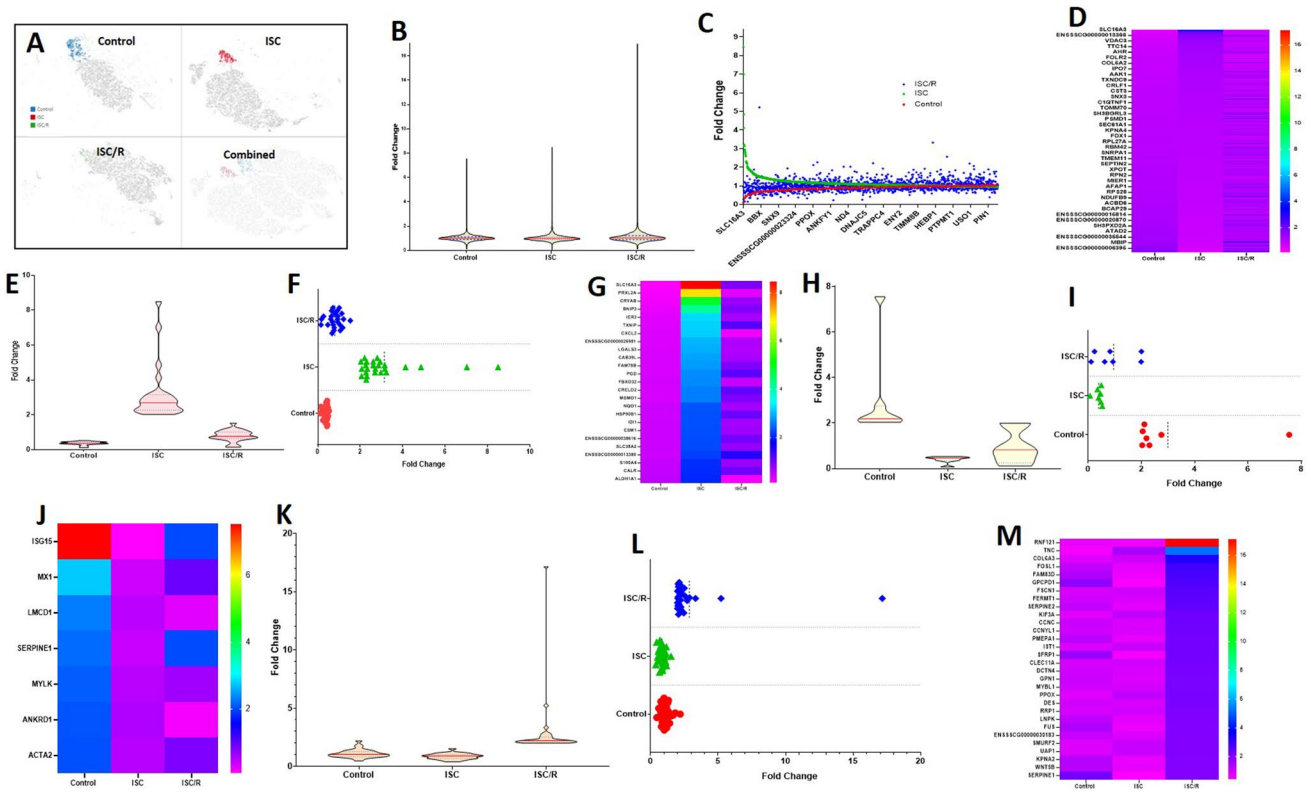


**Fig. 10** Distribution of cell populations and altered genes in Cluster 10 cells: (A) Split view of Control, ISC and ISC/R groups of Cluster 10 cells and combined view of t-SNE plot showing the distribution of cells within the Cluster 10 tending towards the ISC group based on the local expression of 2,546 genes. (B) Violin plot for highly expressed 2,546 genes revealing the distribution towards upregulation in ISC and ISC/R group. (C) Scatterplot of highly expressed 2,546 genes in ISC group showing the upregulation trend compared to control and ISC/R groups. (D) Heat map of highly altered 2,546 genes (FC>2) revealing the upregulation in ISC and ISC/R groups. (E) Violin plot for highly expressed 25 genes revealing the distribution towards upregulation in ISC group compared to control and ISC/R. (F) Scatterplot of highly expressed 25 genes in ISC group (FC>2) showing the decreased level of expression in control group where

the dotted lines indicate mean FC. (G) Heat map of highly altered 25 genes (FC>2) revealing the upregulation in ISC group. (H) Violin plot for highly expressed 7 genes revealing the distribution towards upregulation in Control and ISC/R compared to ISC group. (I) Scatterplot of highly expressed 7 genes in Control group showing the minimal level of expression in ISC group where the dotted lines indicate mean FC. (J) Heat map of highly altered 7 genes (FC>2) revealing the upregulation in Control and ISC/R group. (K) Violin plot for highly expressed 30 genes revealing the distribution towards upregulation in ISC/R compared to Control and ISC groups. (L) Scatterplot of highly expressed 30 genes in ISC/R group showing the minimal level of expression in ISC group where the dotted lines indicate mean FC. (M) Heat map of highly altered 30 genes (FC>2) revealing the upregulation in ISC/R group

cell lineage aiding in biological responses in cardiac tissue. Additionally, the exact functions of these EATDS in cardiac regeneration warrant further investigation.

Ischemia favored cluster 4 cells in which the downregulation of the major fibroblast differentiation protein, NREP was evident. NREP was highly upregulated in the control cells suggesting that the cluster 4 cells represent a predominant population of EATDS which aids in the prevention of fibrosis. Evidently, NREP expression was significantly increased in hypertrophic scars and its role in scarring mediated through TGF-β-Smad axis has been unveiled [34, 35]. Importantly, NREP accelerates the transdifferentiation of stem cells to fibroblasts [34]. However, the information of NREP on EATDS differentiation and cardiac fibrosis is limited. Additionally, the decreased level of NREP in EATDS

under ischemic environment suggests the existence of an antifibrotic subpopulation which maintains/preserves the stemness and possibly exhibiting cardioprotective functions. In addition, the cluster 6 cells favoring ischemia upregulated the cardiac muscle biomarker MYH11 suggesting a progenitor subpopulation differentiating towards myocardial lineage. Interestingly, MYH11 has been reported to be a crucial biomarker for adult cardiac precursor cells which are destined to be cardiomyocytes by the activation of NOTCH signaling [36].

The cluster 5 cells favoring reperfusion upregulated IL-11, which is a crucial anti-inflammatory cytokine which promotes the activation, proliferation, differentiation and commitment of various progenitor cells [37]. A recent study reported that IL-11 promoted the engraftment, maintenance,

**Table 11** The list of genes locally upregulated genes ( $FC > 2$ ) in control, ISC and ISC/R groups with respect to each other group in Cluster 10 cells

Sl/No	Feature ID	Feature name	Control FC	<i>P</i> -value	ISC FC	<i>P</i> -value	ISC/R FC	<i>P</i> -value
Control								
1	ENSSSCG00000040575	ISG15	7.55	1.9E-07	0.07	2E-11	1.99	1.0000
2	ENSSSCG00000012077	MX1	2.75	5.5E-05	0.35	3E-05	0.93	1.0000
3	ENSSSCG00000011538	LMCD1	2.30	3.5E-04	0.46	2E-03	0.24	1.0000
4	ENSSSCG00000025698	SERPINE1	2.19	2.3E-04	0.39	3E-06	2.00	1.0000
5	ENSSSCG00000011867	MYLK	2.11	2.6E-03	0.48	4E-03	0.62	1.0000
6	ENSSSCG00000010461	ANKRD1	2.05	6.5E-03	0.53	2E-02	0.11	1.0000
7	ENSSSCG00000010447	ACTA2	2.03	5.6E-04	0.49	6E-04	0.82	1.0000
ISC								
1	ENSSSCG00000024018	SLC16A3	0.11	4.1E-27	8.49	2.74E-26	0.94	1.0000
2	ENSSSCG00000010340	PRXL2A	0.15	1.4E-26	7.02	6.3E-28	0.27	1.0000
3	ENSSSCG00000036724	CRYAB	0.20	2.0E-19	4.86	1.8E-19	0.76	1.0000
4	ENSSSCG00000024388	BNIP3	0.24	2.5E-17	4.13	6.31E-17	0.92	1.0000
5	ENSSSCG00000027607	IER3	0.32	1.9E-10	3.23	6.62E-11	0.67	1.0000
6	ENSSSCG00000031262	TXNIP	0.31	3.2E-10	3.16	1.07E-09	1.21	1.0000
7	ENSSSCG00000008959	CXCL2	0.34	1.1E-06	3.15	8.77E-08	0.17	1.0000
8	ENSSSCG00000026981	ENSSSCG00000026981	0.34	1.2E-09	2.97	3.59E-10	0.64	1.0000
9	ENSSSCG00000005055	LGALS3	0.35	1.0E-09	2.93	2.64E-10	0.61	1.0000
10	ENSSSCG00000009397	CAB39L	0.36	2.2E-07	2.86	6.04E-08	0.65	1.0000
11	ENSSSCG00000006321	FAM78B	0.36	7.6E-08	2.80	6.04E-08	0.93	1.0000
12	ENSSSCG00000003402	PGD	0.36	2.7E-07	2.71	5.07E-07	1.17	1.0000
13	ENSSSCG00000005981	FBXO32	0.39	3.0E-05	2.69	6.96E-06	0.47	1.0000
14	ENSSSCG00000000981	CRELD2	0.38	3.3E-07	2.61	5.49E-07	1.13	1.0000
15	ENSSSCG00000008857	MSMO1	0.38	2.0E-06	2.61	1.8E-06	0.94	1.0000
16	ENSSSCG00000002754	NQO1	0.44	5.5E-05	2.33	2.38E-05	0.69	1.0000
17	ENSSSCG00000000849	HSP90B1	0.43	3.7E-06	2.31	4.5E-06	1.06	1.0000
18	ENSSSCG00000029066	IDI1	0.45	1.0E-04	2.30	4E-05	0.71	1.0000
19	ENSSSCG00000016900	ESM1	0.45	6.3E-05	2.28	3.08E-05	0.73	1.0000
20	ENSSSCG00000038616	ENSSSCG00000038616	0.44	3.0E-05	2.27	3.08E-05	1.01	1.0000
21	ENSSSCG00000000808	SLC38A2	0.45	2.1E-05	2.26	1.29E-05	0.80	1.0000
22	ENSSSCG00000013380	ENSSSCG00000013380	0.43	1.3E-05	2.20	6.01E-05	1.53	1.0000
23	ENSSSCG00000006578	S100A4	0.49	1.3E-03	2.07	0.000826	0.77	1.0000
24	ENSSSCG00000013746	CALR	0.48	1.4E-04	2.06	0.000179	1.04	1.0000
25	ENSSSCG00000028996	ALDH1A1	0.53	1.2E-02	2.03	0.002014	0.15	1.0000
ISC/R								
1	ENSSSCG00000014800	RNF121	0.61	8.1E-01	0.56	7E-01	17.16	0.0090
2	ENSSSCG00000005494	TNC	0.47	3.7E-03	1.51	4E-01	5.22	0.4018
3	ENSSSCG00000027331	COL6A3	0.81	1.0E+00	1.02	1E+00	3.33	1.0000
4	ENSSSCG00000012967	FOSL1	1.17	1.0E+00	0.72	6E-01	2.88	1.0000
5	ENSSSCG00000007351	FAM83D	1.41	6.3E-01	0.59	1E-01	2.76	1.0000
6	ENSSSCG00000007043	GPCPD1	1.83	4.2E-02	0.45	2E-03	2.70	1.0000
7	ENSSSCG00000007586	FSCN1	0.87	1.0E+00	1.00	1E+00	2.57	1.0000
8	ENSSSCG00000007052	FERMT1	1.00	1.0E+00	0.88	1E+00	2.50	1.0000
9	ENSSSCG00000016233	SERPINE2	1.19	1.0E+00	0.73	5E-01	2.46	1.0000
10	ENSSSCG00000014283	KIF3A	0.77	8.1E-01	1.17	1E+00	2.27	1.0000
11	ENSSSCG00000004353	CCNC	1.07	1.0E+00	0.84	1E+00	2.26	1.0000
12	ENSSSCG00000024696	CCNYL1	1.01	1.0E+00	0.88	1E+00	2.25	1.0000
13	ENSSSCG000000034259	PMEPA1	1.27	8.9E-01	0.70	4E-01	2.22	1.0000
14	ENSSSCG00000002743	IST1	0.84	1.0E+00	1.08	1E+00	2.22	1.0000

**Table 11** (continued)

SI/No	Feature ID	Feature name	Control FC	<i>P</i> -value	ISC FC	<i>P</i> -value	ISC/R FC	<i>P</i> -value
15	ENSSSCG00000025822	SFRP1	1.67	1.9E-01	0.52	4E-02	2.22	1.0000
16	ENSSSCG00000036814	CLEC11A	0.92	1.0E+00	0.98	1E+00	2.20	1.0000
17	ENSSSCG00000021427	DCTN4	1.02	1.0E+00	0.88	1E+00	2.17	1.0000
18	ENSSSCG00000008546	GPN1	1.05	1.0E+00	0.86	1E+00	2.13	1.0000
19	ENSSSCG00000027872	MYBL1	0.97	1.0E+00	0.94	1E+00	2.13	1.0000
20	ENSSSCG00000006361	PPOX	0.77	8.0E-01	1.18	1E+00	2.12	1.0000
21	ENSSSCG00000020785	DES	0.99	1.0E+00	0.92	1E+00	2.10	1.0000
22	ENSSSCG00000037061	RRP1	0.93	1.0E+00	0.98	1E+00	2.07	1.0000
23	ENSSSCG00000015976	LNPBK	1.22	1.0E+00	0.74	7E-01	2.06	1.0000
24	ENSSSCG00000030798	FUS	1.44	3.9E-01	0.62	1E-01	2.04	1.0000
25	ENSSSCG00000030183	ENSSSCG00000030183	1.11	1.0E+00	0.82	1E+00	2.04	1.0000
26	ENSSSCG00000032176	SMURF2	0.83	1.0E+00	1.11	1E+00	2.03	1.0000
27	ENSSSCG00000006340	UAP1	0.82	9.9E-01	1.12	1E+00	2.03	1.0000
28	ENSSSCG00000029005	KPNA2	1.33	6.9E-01	0.67	3E-01	2.00	1.0000
29	ENSSSCG00000000759	WNT5B	1.32	8.1E-01	0.68	4E-01	2.00	1.0000
30	ENSSSCG00000025698	SERPINE1	2.19	2.3E-04	0.39	3E-06	2.00	1.0000

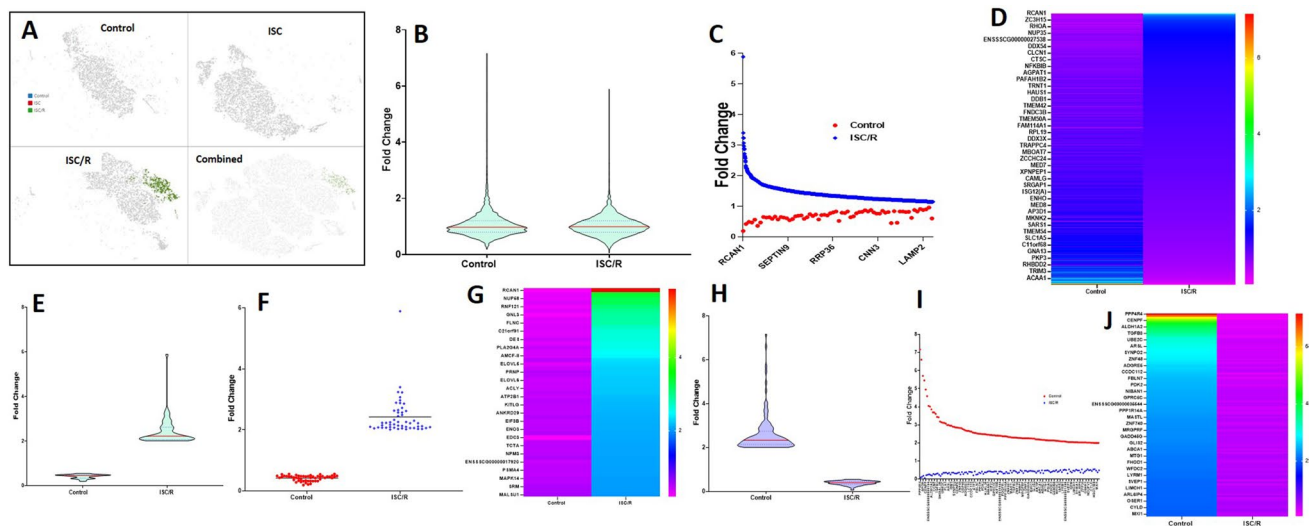


**Fig. 11** Distribution of cell populations and altered genes in Cluster 11: (A) Split view of Control, ISC and ISC/R groups of Cluster 11 cells and combined view of t-SNE plot showing the distribution of cells within the Cluster 11 tending towards the ISC/R group based on the local expression of 4,134 genes. (B) Violin plot for highly expressed 4,134 genes revealing the distribution towards upregulation in ISC/R group. (C) Scatterplot of highly expressed 4,134 genes in ISC/R group showing the upregulation trend compared to control. (D) Heat map of highly altered 4,134 genes ( $FC > 2$ ) revealing the upregulation in ISC/R groups. (E) Violin plot for highly expressed 51 genes revealing the distribution towards upregulation in ISC/R group

compared to control. (F) Scatterplot of highly expressed 51 genes in ISC/R group ( $FC > 2$ ) showing the decreased level of expression in control group where the dotted lines indicate mean FC. (G) Heat map of highly altered 51 genes ( $FC > 2$ ) revealing the upregulation in ISC/R group. (H) Violin plot for highly expressed 126 genes revealing the distribution towards upregulation in Control compared to ISC/R group. (I) Scatterplot of highly expressed 126 genes in Control group showing the minimal level of expression in ISC/R group where the dotted lines indicate mean FC. (J) Heat map of highly altered 126 genes ( $FC > 2$ ) revealing the upregulation in Control compared to ISC/R group

survival, and differentiation of ADMSCs in ischemic tissues improving their therapeutic efficiency [19]. Interestingly, another seminal study reported the critical role of IL-11 in tissue regeneration [38] and the attenuation of

cardiac fibroblasts following MI through IL-11/glycoprotein 130/STAT3 axis [39]. Hence, the cluster 5 represents a subpopulation of EATDS which favors the prevention of inflammation and attenuation of cardiac fibrosis following

**Table 12** The list of genes locally upregulated genes (FC > 2) in control, and ISC/R groups with respect to each other group in Cluster 10 cells

SI/No	Feature ID	Feature Name	Control FC	P-Value	ISC/R	P-Value
Control						
1	ENSSSCG00000002474	PPP4R4	7.17	1.0000	0.09	1.0000
2	ENSSSCG00000008944	NPFFR2	6.61	1.0000	0.13	1.0000
3	ENSSSCG00000003088	APOE	5.71	1.0000	0.19	1.0000
4	ENSSSCG00000016337	ERFE	5.46	1.0000	0.06	1.0000
5	ENSSSCG00000015581	CENPF	4.96	1.0000	0.22	1.0000
6	ENSSSCG00000003439	DHRS3	4.59	1.0000	0.24	1.0000
7	ENSSSCG00000000194	ENSSSCG00000000194	4.05	1.0000	0.27	1.0000
8	ENSSSCG00000017199	TRIM47	4.01	1.0000	0.23	1.0000
9	ENSSSCG00000025578	ALDH1A2	3.86	1.0000	0.20	1.0000
10	ENSSSCG00000017472	IGFBP4	3.70	1.0000	0.29	1.0000
11	ENSSSCG00000026326	CCNF	3.69	1.0000	0.25	1.0000
12	ENSSSCG00000003949	CDC20	3.61	1.0000	0.29	1.0000
13	ENSSSCG00000002385	TGFB3	3.44	1.0000	0.32	1.0000
14	ENSSSCG00000003564	GPATCH3	3.42	1.0000	0.24	1.0000
15	ENSSSCG00000024514	SHISAL2B	3.19	1.0000	0.17	1.0000
16	ENSSSCG00000008002	CIAO3	3.14	1.0000	0.28	1.0000
17	ENSSSCG00000007423	UBE2C	3.12	1.0000	0.35	1.0000
18	ENSSSCG00000005056	DLGAP5	3.11	1.0000	0.35	1.0000
19	ENSSSCG00000026748	PLK1	3.08	1.0000	0.36	1.0000
20	ENSSSCG00000024145	PRR11	2.99	1.0000	0.31	1.0000
21	ENSSSCG00000022129	ARSL	2.99	1.0000	0.35	1.0000
22	ENSSSCG00000026977	TRAIP	2.96	1.0000	0.26	1.0000
23	ENSSSCG00000007073	ISM1	2.95	1.0000	0.36	1.0000
24	ENSSSCG00000017340	DCAKD	2.90	1.0000	0.36	1.0000
25	ENSSSCG00000009111	SYNPO2	2.89	1.0000	0.32	1.0000
26	ENSSSCG00000017446	ENSSSCG00000017446	2.86	1.0000	0.31	1.0000
27	ENSSSCG00000023296	CENPE	2.85	1.0000	0.34	1.0000
28	ENSSSCG00000011732	ENSSSCG00000011732	2.84	1.0000	0.37	1.0000
29	ENSSSCG00000007801	ZNF48	2.83	1.0000	0.26	1.0000
30	ENSSSCG00000009093	BBS7	2.82	1.0000	0.39	1.0000
31	ENSSSCG000000036284	USP46	2.77	1.0000	0.28	1.0000
32	ENSSSCG00000012077	MX1	2.73	1.0000	0.37	1.0000
33	ENSSSCG00000013775	ADGRE5	2.69	1.0000	0.38	1.0000
34	ENSSSCG00000024096	RIPK2	2.67	1.0000	0.30	1.0000
35	ENSSSCG00000021798	LZTS2	2.67	1.0000	0.41	1.0000
36	ENSSSCG000000035653	PGAP2	2.64	1.0000	0.40	1.0000
37	ENSSSCG00000029866	CCDC112	2.63	1.0000	0.38	1.0000
38	ENSSSCG00000006284	C1orf112	2.58	1.0000	0.21	1.0000
39	ENSSSCG00000003201	ATF5	2.56	1.0000	0.43	1.0000
40	ENSSSCG00000010240	DNA2	2.55	1.0000	0.25	1.0000
41	ENSSSCG00000008101	FBLN7	2.53	1.0000	0.27	1.0000
42	ENSSSCG00000014041	ENSSSCG00000014041	2.51	1.0000	0.36	1.0000
43	ENSSSCG00000022758	PECR	2.51	1.0000	0.33	1.0000
44	ENSSSCG000000033453	BST2	2.50	1.0000	0.42	1.0000
45	ENSSSCG00000027198	PDK2	2.49	1.0000	0.29	1.0000
46	ENSSSCG00000034096	DMAPI	2.49	1.0000	0.38	1.0000
47	ENSSSCG00000038285	KLHL36	2.48	1.0000	0.37	1.0000
48	ENSSSCG00000003981	ZFP69B	2.46	1.0000	0.42	1.0000
49	ENSSSCG00000015567	NIBAN1	2.46	1.0000	0.44	1.0000
50	ENSSSCG000000038487	TMPO	2.44	1.0000	0.43	1.0000



**Table 12** (continued)

SI/No	Feature ID	Feature Name	Control FC	P-Value	ISC/R	P-Value
51	ENSSSCG0000004969	KIF23	2.44	1.0000	0.40	1.0000
52	ENSSSCG0000003964	PIIH	2.43	1.0000	0.41	1.0000
53	ENSSSCG00000040989	GPRC5C	2.43	1.0000	0.43	1.0000
54	ENSSSCG00000015862	LIMS2	2.41	1.0000	0.43	1.0000
55	ENSSSCG00000017342	KIF18B	2.41	1.0000	0.30	1.0000
56	ENSSSCG00000027124	ENSSSCG00000027124	2.40	1.0000	0.42	1.0000
57	ENSSSCG00000035544	ENSSSCG00000035544	2.40	1.0000	0.43	1.0000
58	ENSSSCG00000037307	PRC1	2.39	1.0000	0.39	1.0000
59	ENSSSCG00000006988	PDGFRL	2.37	1.0000	0.31	1.0000
60	ENSSSCG00000022177	DIS3L2	2.37	1.0000	0.32	1.0000
61	ENSSSCG00000038077	PPP1R14A	2.37	1.0000	0.40	1.0000
62	ENSSSCG00000038313	ZNF219	2.35	1.0000	0.33	1.0000
63	ENSSSCG00000006627	ZNF687	2.33	1.0000	0.33	1.0000
64	ENSSSCG00000006717	PHGDH	2.33	1.0000	0.47	1.0000
65	ENSSSCG00000011065	MASTL	2.31	1.0000	0.36	1.0000
66	ENSSSCG00000038549	ZFP36L2	2.30	1.0000	0.46	1.0000
67	ENSSSCG00000010816	TGFB2	2.30	1.0000	0.46	1.0000
68	ENSSSCG00000021845	ATXN2L	2.30	1.0000	0.41	1.0000
69	ENSSSCG00000036564	ZNF740	2.29	1.0000	0.34	1.0000
70	ENSSSCG00000001904	CLK3	2.28	1.0000	0.38	1.0000
71	ENSSSCG00000005689	FNBP1	2.28	1.0000	0.49	1.0000
72	ENSSSCG00000004961	ITGA11	2.27	1.0000	0.44	1.0000
73	ENSSSCG00000034441	MRGPRF	2.26	1.0000	0.34	1.0000
74	ENSSSCG00000025588	FJX1	2.26	1.0000	0.46	1.0000
75	ENSSSCG00000027128	LONP1	2.26	1.0000	0.46	1.0000
76	ENSSSCG00000009009	MND1	2.26	1.0000	0.41	1.0000
77	ENSSSCG00000035249	GADD45G	2.26	1.0000	0.45	1.0000
78	ENSSSCG00000009240	ENSSSCG00000009240	2.25	1.0000	0.46	1.0000
79	ENSSSCG00000040486	BIRC5	2.25	1.0000	0.45	1.0000
80	ENSSSCG00000002455	GOLGA5	2.24	1.0000	0.44	1.0000
81	ENSSSCG00000023653	GLIS2	2.24	1.0000	0.43	1.0000
82	ENSSSCG00000010241	TET1	2.21	1.0000	0.35	1.0000
83	ENSSSCG00000026181	AKTIP	2.20	1.0000	0.44	1.0000
84	ENSSSCG00000023727	TRIM37	2.20	1.0000	0.46	1.0000
85	ENSSSCG00000005423	ABCA1	2.19	1.0000	0.35	1.0000
86	ENSSSCG00000017473	TOP2A	2.18	1.0000	0.49	1.0000
87	ENSSSCG00000028010	ABHD3	2.17	1.0000	0.33	1.0000
88	ENSSSCG00000010209	FAM13C	2.17	1.0000	0.47	1.0000
89	ENSSSCG00000029088	MTG1	2.15	1.0000	0.48	1.0000
90	ENSSSCG00000004658	FBN1	2.15	1.0000	0.49	1.0000
91	ENSSSCG00000011870	PDIA5	2.14	1.0000	0.45	1.0000
92	ENSSSCG00000035664	ZBTB45	2.14	1.0000	0.38	1.0000
93	ENSSSCG00000026116	FHOD1	2.14	1.0000	0.41	1.0000
94	ENSSSCG00000024938	SH3BP5	2.14	1.0000	0.45	1.0000
95	ENSSSCG00000012127	GEMIN8	2.14	1.0000	0.44	1.0000
96	ENSSSCG00000023408	SAMD4A	2.12	1.0000	0.50	1.0000
97	ENSSSCG00000033003	WFDC2	2.12	1.0000	0.40	1.0000
98	ENSSSCG00000035827	CTDSPL2	2.11	1.0000	0.44	1.0000
99	ENSSSCG00000010823	IARS2	2.10	1.0000	0.50	1.0000
100	ENSSSCG00000029201	AJUBA	2.09	1.0000	0.39	1.0000
101	ENSSSCG00000007853	LYRM1	2.09	1.0000	0.50	1.0000

Table 12 (continued)

SI/No	Feature ID	Feature Name	Control FC	P-Value	ISC/R	P-Value
102	ENSSSCG00000013752	STX10	2.09	1.0000	0.53	1.0000
103	ENSSSCG00000001398	ENSSSCG00000001398	2.08	1.0000	0.50	1.0000
104	ENSSSCG00000008238	ELMOD3	2.06	1.0000	0.32	1.0000
105	ENSSSCG00000005455	SVEP1	2.05	1.0000	0.54	1.0000
106	ENSSSCG00000027550	PLCD1	2.05	1.0000	0.43	1.0000
107	ENSSSCG00000006105	GEM	2.05	1.0000	0.37	1.0000
108	ENSSSCG00000017670	ENSSSCG00000017670	2.05	1.0000	0.47	1.0000
109	ENSSSCG00000008799	LIMCH1	2.04	1.0000	0.45	1.0000
110	ENSSSCG00000008207	RPIA	2.04	1.0000	0.52	1.0000
111	ENSSSCG00000031053	S100A1	2.04	1.0000	0.48	1.0000
112	ENSSSCG00000017301	TLK2	2.03	1.0000	0.48	1.0000
113	ENSSSCG00000009782	ARL6IP4	2.03	1.0000	0.37	1.0000
114	ENSSSCG00000000202	MCRS1	2.03	1.0000	0.54	1.0000
115	ENSSSCG00000028056	ZFP36	2.03	1.0000	0.34	1.0000
116	ENSSSCG00000018091	ND5	2.03	1.0000	0.42	1.0000
117	ENSSSCG00000022714	OSER1	2.03	1.0000	0.48	1.0000
118	ENSSSCG00000040575	ISG15	2.02	1.0000	0.55	1.0000
119	ENSSSCG00000012896	NDUFV1	2.02	1.0000	0.49	1.0000
120	ENSSSCG00000012172	ACOT9	2.02	1.0000	0.51	1.0000
121	ENSSSCG00000040286	CYLD	2.01	1.0000	0.45	1.0000
122	ENSSSCG00000038929	CEMIP	2.01	1.0000	0.54	1.0000
123	ENSSSCG00000028431	HSD17B4	2.00	1.0000	0.55	1.0000
124	ENSSSCG00000026153	ACAT1	2.00	1.0000	0.47	1.0000
125	ENSSSCG00000022128	MXI1	2.00	1.0000	0.38	1.0000
126	ENSSSCG00000021408	TKT	2.00	1.0000	0.49	1.0000
ISC/R						
1	ENSSSCG00000012050	RCAN1	0.19	1.0000	5.89	1.0000
2	ENSSSCG00000005494	TNC	0.29	1.0000	3.40	1.0000
3	ENSSSCG00000035318	NUP58	0.28	1.0000	3.24	1.0000
4	ENSSSCG00000040725	IL11	0.34	1.0000	3.23	1.0000
5	ENSSSCG00000014800	RNF121	0.26	1.0000	3.07	1.0000
6	ENSSSCG00000031580	LLPH	0.32	1.0000	2.97	1.0000
7	ENSSSCG00000011449	GNL3	0.23	1.0000	2.89	1.0000
8	ENSSSCG00000033786	ENSSSCG00000033786	0.32	1.0000	2.88	1.0000
9	ENSSSCG00000016578	FLNC	0.32	1.0000	2.86	1.0000
10	ENSSSCG00000034156	GTF2F2	0.36	1.0000	2.72	1.0000
11	ENSSSCG00000033025	C21orf91	0.32	1.0000	2.65	1.0000
12	ENSSSCG00000000849	HSP90B1	0.32	1.0000	2.63	1.0000
13	ENSSSCG00000020785	DES	0.41	1.0000	2.62	1.0000
14	ENSSSCG00000006296	ATP1B1	0.33	1.0000	2.57	1.0000
15	ENSSSCG00000023351	PLA2G4A	0.43	1.0000	2.57	1.0000
16	ENSSSCG00000039591	SERINC3	0.38	1.0000	2.49	1.0000
17	ENSSSCG00000008957	AMCF-II	0.37	1.0000	2.45	1.0000
18	ENSSSCG00000024916	DHX36	0.47	1.0000	2.33	1.0000
19	ENSSSCG00000024149	ELOVL5	0.32	1.0000	2.30	1.0000
20	ENSSSCG00000004382	SEC63	0.42	1.0000	2.26	1.0000
21	ENSSSCG00000007039	PRNP	0.49	1.0000	2.26	1.0000
22	ENSSSCG00000013380	ENSSSCG00000013380	0.47	1.0000	2.25	1.0000
23	ENSSSCG00000036236	ELOVL6	0.42	1.0000	2.23	1.0000
24	ENSSSCG00000006089	PTDSS1	0.43	1.0000	2.23	1.0000
25	ENSSSCG00000017421	ACLY	0.43	1.0000	2.22	1.0000

**Table 12** (continued)

SI/No	Feature ID	Feature Name	Control FC	P-Value	ISC/R	P-Value
26	ENSSSCG00000008963	AREG	0.48	1.0000	2.22	1.0000
27	ENSSSCG00000027898	ATP2B1	0.43	1.0000	2.18	1.0000
28	ENSSSCG00000004383	OSTM1	0.51	1.0000	2.17	1.0000
29	ENSSSCG00000035495	KITLG	0.48	1.0000	2.15	1.0000
30	ENSSSCG00000034814	MRTO4	0.47	1.0000	2.14	1.0000
31	ENSSSCG00000003708	ANKRD29	0.46	1.0000	2.13	1.0000
32	ENSSSCG00000024660	ENSSSCG00000024660	0.52	1.0000	2.12	1.0000
33	ENSSSCG000000039390	EIF3B	0.46	1.0000	2.11	1.0000
34	ENSSSCG00000000551	ARNTL2	0.47	1.0000	2.10	1.0000
35	ENSSSCG00000017904	ENO3	0.47	1.0000	2.10	1.0000
36	ENSSSCG00000031639	ZCCHC17	0.50	1.0000	2.09	1.0000
37	ENSSSCG00000001903	EDC3	0.21	1.0000	2.09	1.0000
38	ENSSSCG00000005203	IL33	0.47	1.0000	2.08	1.0000
39	ENSSSCG00000037459	TCTA	0.49	1.0000	2.07	1.0000
40	ENSSSCG00000017306	ITGB3	0.48	1.0000	2.07	1.0000
41	ENSSSCG00000010568	NPM3	0.48	1.0000	2.07	1.0000
42	ENSSSCG00000008497	GPATCH11	0.54	1.0000	2.06	1.0000
43	ENSSSCG00000017920	ENSSSCG00000017920	0.44	1.0000	2.06	1.0000
44	ENSSSCG00000015579	PTGS2	0.48	1.0000	2.06	1.0000
45	ENSSSCG00000036924	PSMA4	0.48	1.0000	2.05	1.0000
46	ENSSSCG00000031109	HILPDA	0.46	1.0000	2.05	1.0000
47	ENSSSCG00000001556	MAPK14	0.49	1.0000	2.03	1.0000
48	ENSSSCG00000009904	DYNLL1	0.49	1.0000	2.03	1.0000
49	ENSSSCG00000027689	SRM	0.54	1.0000	2.03	1.0000
50	ENSSSCG00000001095	GMNN	0.55	1.0000	2.02	1.0000
51	ENSSSCG00000036722	MALSU1	0.55	1.0000	2.01	1.0000

the reperfusion; however, further validations are warranted. Similarly, cluster 7 cells favoring reperfusion revealed the upregulation of IL-11 suggesting a closely related subpopulation of EATDS. The unique functions of these two subpopulations require further research for their application in translational cardiology.

EATDS in the clusters 8 and 9 tending towards ischemia upregulated HSP90B1 and CRELD2, respectively. HSP90B1 has been identified as chaperone for several Toll-like receptors (TLRs) playing crucial role in inflammatory responses and TLR mediated apoptosis following renal ischemia [40, 41]. In addition, CRELD2 regulates activating transcription factor 6 (Atf6) to induce ER-stress resulting in decreased protein translation and increased degradation [42, 43]. However, the potential role of HSP90B1 and CRELD2 in EATDS and their association with ischemic cardiac tissues are yet to be discovered. Similarly, cluster 10 cells favored ischemia with an upregulation of the glycolytic component SLC16A3. Interestingly, SLC16A3 is intimately involved in stem-cell associated hypoxic/ischemic microenvironment especially activating HIF1 $\alpha$  signaling [44]. Importantly, SLC16A3 plays a crucial role in lactate extrusion and facilitates AMPK phosphorylation eliciting protective

responses during cardiac ischemia and myocardial injury [45]. Hence, the cluster 10 subpopulation of EATDS are equipped to withstand and to survive the extreme ischemic insults in the myocardium during/following an injury.

Cluster 11 cells favoring the reperfusion displayed the upregulation of RCAN1 which is a negative regulator for TLR-MyD88-NF- $\kappa$ B signaling mediates through I $\kappa$ B $\alpha$  [46]. Interestingly, RCAN1 elicits protective role against ischemic insults in multiple tissue types including myocardium and brain [47, 48]. The upregulation of RCAN1 in the reperfused cells suggests the protective mechanisms elicited by cluster 11 subpopulation by preventing TLR-driven aggravated inflammation. The regulatory role of RCAN1 in EATDS are largely unknown; however, the identification of RCAN1 + population unveils the possible trans-acting cardioprotective stem cell population.

It has been believed that the epicardium retains the embryonic program to generate mesenchymal progenitor cells secreting paracrine factors to stimulate the growth and survival of cardiomyocytes and promote angiogenesis for repair and regenerative responses. Hence, the epicardium has been considered as a signal generator for cardiac regeneration [49]. Despite a few recent reports [49, 50], minimal

information is available regarding the cellular heterogeneity of epicardial tissue which points the necessity of mapping the subpopulations of epicardial cells. Unfortunately, the information regarding the heterogeneity of EF and EATDS is unavailable in the literature. EF being a repository of translationally worthwhile EATDS for cardiac regeneration, it is relevant to explore the cellular heterogeneity to identify the ideal stem cell subpopulations for improved cardiac healing. As hyperlipidemia is integral to atherosclerosis and IHD, we utilized atherosclerotic Yucatan micro swine model to harvest EATDS which was manipulated in vitro to simulate ischemia and reperfusion. To the best of our knowledge, this is the first report dealing with the heterogeneity of EATDS based on ischemia and reperfusion unveiling 18 unique clusters.

The overall findings regarding the characteristic subpopulations are summarized in Table 13. The outcomes of this study are novel, encouraging potential avenues for phenotyping EATDS for cardiac regeneration. Also, the easiness

of harvesting and possibilities of expansion encourage the application of EATDS in regenerative cardiology. The major focus of this study was to map the unique cell clusters using scRNAseq representing the major EATDS subpopulations and future research is warranted to further characterize these populations for cardiac applications. In addition, the bulk of the obtained data drive us to focus on the upregulated genes based on the treatment status (ischemia or reperfusion) and further emphasis was given only to the highly upregulated genes for deriving the conclusions. However, the data regarding the downregulated genes warrant similar assessment for designing the panel of biomarkers for defining each unique cluster. Importantly, atherosclerotic swine ( $n=3$ ) was used for ensuring the clinical relevance and the cells were pooled for post-isolation culture, simulation of ischemia and reperfusion, and scRNAseq analysis.

The untreated EATDS harvested from hyperlipidemic swine were used control for ensuring the alteration of gene expression was solely due to ischemia and reperfusion. The

**Table 13** Overview of the EATDS phenotypes identified in the clusters based on their differential gene expression and possible mechanism of action (based on published literature)

Cluster	Major genes	Phenotype	Mechanism of action
Cluster 1	H1-0, MGP, DHRS3, TGF $\beta$ 3	Regenerative/protective	Activation, differentiation, and plasticity of stem cells BMP inhibition Prevention of vascular calcification Angiogenesis
Cluster 2	CDC20, MGP	Proliferative Progenitor	Cell cycle progression Cell proliferation Cellular homeostasis
Cluster 3	CCN5	Proliferative Progenitor	Cellular homeostasis
Cluster 4	NREP, RAMP1, ISG15, PICK1	Antifibrotic Cardiac progenitor	Prevention of fibrosis Preservation of stemness
Cluster 5	IL11, RNF121, POCHR	Anti-inflammatory Regenerative/protective Antifibrotic	Activation, proliferation, differentiation, and commitment of various progenitor cells Antiinflammation Attenuation of cardiac fibroblasts
Cluster 6	MYH11, CRELD2, OAS2	Cardiac progenitor	cardiomyocytes activation by NOTCH signaling
Cluster 7	IL11, RNF121, H1.0, HSPA5, MDR/TAP, LMCD1	Anti-inflammatory Regenerative/protective Antifibrotic	Activation, proliferation, differentiation, and commitment of various progenitor cells Antiinflammation Attenuation of cardiac fibroblasts
Cluster 8	HSP90B1, CRELD2, ISG15	Inflammatory	Pro-inflammatory responses TLR mediated apoptosis Decreased protein translation and increased degradation
Cluster 9	ACTA1, CRELD2, MCM3, Myosin XIX	Inflammatory	Pro-inflammatory responses TLR mediated apoptosis Decreased protein translation and increased degradation
Cluster 10	SLC16A3, PRXL2A, ISG15, RNF121, TNC,	Regenerative/protective	HIF1 $\alpha$ signaling Protective responses by AMPK phosphorylation
Cluster 11	RCAN1, PPP4R4, NPFFR2	Regenerative/protective Anti-inflammatory	Prevention of TLR-mediated inflammation

data from normal swine is warranted to investigate the effect of hyperlipidemia/atherosclerosis in EATDS heterogeneity. Additionally, the analysis was based on the number of cells in each cluster and 8 clusters displaying < 1000 cells were exempted from screening which need further analysis. Furthermore, the validation of the gene expression using qRT-PCR is limited as the major focus of this study was to identify EATDS heterogeneity by screening the cell clusters employing the sc-RNAseq analysis. However, further investigations and validations are warranted to confirm the gene expression profiles in the clusters/sub-populations of interest. Additionally, Loupe Browser was solely used for the analysis and batch correction was not performed. However, batch variation has minimal impact as all the samples utilized same 10× chemistry for data generation and followed identical sample preparation protocol. Moreover, the present study focused on differential gene expression to screen the cellular phenotypes where the batch effect is negligible. However, future data analysis warrants batch correction and utilization of computational and statistical programs. Moreover, the gene interactions and prediction/assessment of regenerative pathways using bioinformatics tools using the findings from this study pose additional translational relevance.

To the best of our knowledge, this is the first study unveiling EATDS heterogeneity in hyperlipidemic microswine using single cell genomics. Overall, the study unveiled the existence of subpopulations of EATDS unveiling the regenerative phenotypes and the identification of similar regenerative phenotypes in human system may open novel avenues for MI management. A seminal study demonstrated the conserved cardiac fibroblast subpopulation between porcine and human heart following MI suggesting the possibilities of the co-existence of similar subpopulation of EATDS in human system [51]. Unfortunately, the information regarding such human counterpart of EATDS are unavailable in the literature; however, warrants further investigations for the potential therapeutic interventions. Nevertheless, our findings revealed unique phenotypes of heterogeneous EATDS population which open potent translational avenues for regenerative cardiology in the management of myocardial damage.

## Conclusions

The scRNAseq of EATDS under simulated ischemia and reperfusion revealed 18 unique cell clusters suggesting the existence of heterogeneous phenotypes. Interestingly, the functions of the key upregulated genes screened in the treatment group revealed the cardioprotective phenotypes which elicits diverse mechanism of action including epigenetic regulation of differentiation pathways (Cluster 1), maintenance

of myocardial homeostasis (Cluster 1), maintenance of cell integrity and cell cycle (Clusters 2 and 3), prevention of fibroblast differentiation (Cluster 4), differentiation to myocardial lineage (Cluster 6), anti-inflammatory responses (Clusters 5, 8, and 11), prevention of ER-stress (Cluster 9), and increasing the energy metabolism (Cluster 10). These unique phenotypes of heterogeneous EATDS population warrant further characterization for clinical applications; however, open significant translational opportunities for myocardial regeneration and cardiac management.

**Supplementary Information** The online version contains supplementary material available at <https://doi.org/10.1007/s12015-021-10273-0>.

**Acknowledgements** Authors are grateful to Dr. Hung Long, SC2 Core—Children Hospital Los Angeles, and Dr Anja Bastin and Dr. Elizabeth Collins, 10x genomics, for their technical support in multiple aspects of scRNAseq analysis.

**Authors' Contribution** FT – conceptualization, experiments, data generation and analysis, manuscript preparation, and manuscript edits. DK—conceptualization, data generation and analysis, manuscript preparation, and manuscript edits.

**Funding** The research work of FT is supported by the startup funds from WU and DK Agrawal is supported by research grants R01 HL144125 and R01HL147662 from the National Institutes of Health, USA. The content of this original article is solely the responsibility of the authors and does not necessarily represent the official views of the National Institutes of Health.

**Data Availability** Data with the raw counts matrices and annotation are available upon request from the authors through proper channels.

**Code Availability** NA.

## Declarations

**Ethics Approval and Consent to Participate** NA.

**Consent for Publication** Both the authors have read the manuscript and agreed to publish in CMLS.

**Conflict of Interest** All the authors have read the manuscript and declare no conflict of interest.

**Competing Interests** The authors declare no competing financial and/or non-financial interests or other interests that might be perceived to influence the results and/or discussion reported in this paper. No writing assistance was utilized in the production of this manuscript.

## References

1. Joo, H. J., Kim, J.-H., & Hong, S. J. (2017). Adipose tissue-derived stem cells for myocardial regeneration. *Korean Circulation Journal*, 47(2), 151–159. <https://doi.org/10.4070/kcj.2016.0207>.

2. Thankam, F. G., & Agrawal, D. K. (2020). Infarct zone: A novel platform for exosome trade in cardiac tissue regeneration. *Journal of Cardiovascular Translational Research*. <https://doi.org/10.1007/s12265-019-09952-8>.
3. Lambert, C., Arderiu, G., Bejar, M. T., Crespo, J., Baldellou, M., Juan-Babot, O., & Badimon, L. (2019). Stem cells from human cardiac adipose tissue depots show different gene expression and functional capacities. *Stem Cell Research & Therapy*, *10*(1), 361. <https://doi.org/10.1186/s13287-019-1460-1>.
4. Kim, J.-H., Hong, S. J., Park, C.-Y., Park, J. H., Choi, S.-C., Woo, S.-K., ... Lim, D.-S. (2016). Intramyocardial adipose-derived stem cell transplantation increases pericardial fat with recovery of myocardial function after acute myocardial infarction. *PLoS ONE*, *11*(6), e0158067. <https://doi.org/10.1371/journal.pone.0158067>.
5. Mayfield, A. E., Tilokee, E. L., & Davis, D. R. (2014). Resident cardiac stem cells and their role in stem cell therapies for myocardial repair. *Canadian Journal of Cardiology*, *30*(11), 1288–1298. <https://doi.org/10.1016/j.cjca.2014.03.018>.
6. Wu, Y., Zhang, A., Hamilton, D. J., & Deng, T. (2017). Epicardial fat in the maintenance of cardiovascular health. *Methodist DeBakey Cardiovascular Journal*, *13*(1), 20–24. <https://doi.org/10.14797/mdcj-13-1-20>.
7. Ege, M. R. (2020). Epicardial adipose tissue: Good or bad for cardiac function? *Herz*, *45*(3), 299–299. <https://doi.org/10.1007/s00059-018-4731-1>.
8. Gui, C., Parson, J., & Meyer, G. A. (2021). Harnessing adipose stem cell diversity in regenerative medicine. *APL Bioengineering*, *5*(2), 021501. <https://doi.org/10.1063/5.0038101>.
9. Hou, W., Duan, L., Huang, C., Li, X., Xu, X., Qin, P., ... Jin, W. (2021). Mesenchymal stem cell subpopulations and their heterogeneity of response to inductions revealed by single-cell RNA-seq. *bioRxiv*, 2021.05.07.443197. <https://doi.org/10.1101/2021.05.07.443197>.
10. Thankam, F. G., Ayoub, J. G., Ahmed, M. M. R., Siddique, A., Sanchez, T. C., Peralta, R. A., ... Agrawal, D. K. (2020). Association of hypoxia and mitochondrial damage associated molecular patterns in the pathogenesis of vein graft failure: A pilot study. *Translational Research*. <https://doi.org/10.1016/j.trsl.2020.08.010>.
11. Thankam, F. G., Chandra, I. S., Kovilam, A. N., Diaz, C. G., Volberding, B. T., Dilisio, M. F., ... Agrawal, D. K. (2018). Amplification of mitochondrial activity in the healing response following rotator cuff tendon injury. *Scientific Reports*, *8*(1), 1–14. <https://doi.org/10.1038/s41598-018-35391-7>.
12. Farbehi, N., Patrick, R., Dorison, A., Xaymardan, M., Janbandhu, V., Wystub-Lis, K., ... Harvey, R. P. (n.d.). Single-cell expression profiling reveals dynamic flux of cardiac stromal, vascular and immune cells in health and injury. *eLife*, *8*. <https://doi.org/10.7554/eLife.43882>.
13. Wolmarans, E., Mellet, J., Durandt, C., Joubert, F., & Pepper, M. S. (2021). Single-cell transcriptome analysis of human adipose-derived stromal cells identifies a contractile cell subpopulation. *Stem Cells International*, 2021, e5595172. <https://doi.org/10.1155/2021/5595172>.
14. Wang, W., Gao, D., & Wang, X. (2018). Can single-cell RNA sequencing crack the mystery of cells? *Cell Biology and Toxicology*, *34*(1), 1–6. <https://doi.org/10.1007/s10565-017-9404-y>.
15. Nurzynska, D., Di Meglio, F., Romano, V., Miraglia, R., Sacco, A. M., Latino, F., ... Castaldo, C. (2012). Cardiac primitive cells become committed to a cardiac fate in adult human heart with chronic ischemic disease but fail to acquire mature phenotype: Genetic and phenotypic study. *Basic Research in Cardiology*, *108*(1), 320. <https://doi.org/10.1007/s00395-012-0320-2>.
16. Urbanek, K., Torella, D., Sheikh, F., De Angelis, A., Nurzynska, D., Silvestri, F., ... Anversa, P. (2005). Myocardial regeneration by activation of multipotent cardiac stem cells in ischemic heart failure. *Proceedings of the National Academy of Sciences of the United States of America*, *102*(24), 8692–8697. <https://doi.org/10.1073/pnas.0500169102>.
17. Sebastião, M. J., Serra, M., Pereira, R., Palacios, I., Gomes-Alves, P., & Alves, P. M. (2019). Human cardiac progenitor cell activation and regeneration mechanisms: Exploring a novel myocardial ischemia/reperfusion in vitro model. *Stem Cell Research & Therapy*, *10*(1), 77. <https://doi.org/10.1186/s13287-019-1174-4>.
18. Docshin, P. M., Karpov, A. A., Eyvazova, Sh. D., Puzanov, M. V., Kostareva, A. A., Galagudza, M. M., & Malashicheva, A. B. (2018). Activation of cardiac stem cells in myocardial infarction. *Cell and Tissue Biology*, *12*(3), 175–182. <https://doi.org/10.1134/S1990519X18030045>.
19. Yang, W., Zhang, S., Ou, T., Jiang, H., Jia, D., Qi, Z., ... Ge, J. (2020). Interleukin-11 regulates the fate of adipose-derived mesenchymal stem cells via STAT3 signalling pathways. *Cell Proliferation*, *53*(5), e12771. <https://doi.org/10.1111/cpr.12771>.
20. Okada, T., & Suzuki, H. (2021). The role of tenascin-C in tissue injury and repair after stroke. *Frontiers in Immunology*, *11*, 3553. <https://doi.org/10.3389/fimmu.2020.607587>.
21. Findley, A. S., Monziani, A., Richards, A. L., Rhodes, K., Ward, M. C., Kalita, C. A., & Luca, F. (2021). Functional dynamic genetic effects on gene regulation are specific to particular cell types and environmental conditions. *eLife*, *10*, e67077. <https://doi.org/10.7554/eLife.67077>.
22. Verhelst, J., Hulpiau, P., & Saelens, X. (2013). Mx proteins: Antiviral gatekeepers that restrain the uninvited. *Microbiology and Molecular Biology Reviews : MMBR*, *77*(4), 551–566. <https://doi.org/10.1128/MMBR.00024-13>.
23. Kavanagh, K. L., Jörnvall, H., Persson, B., & Oppermann, U. (2008). Medium- and short-chain dehydrogenase/reductase gene and protein families. *Cellular and Molecular Life Sciences*, *65*(24), 3895. <https://doi.org/10.1007/s00018-008-8588-y>.
24. Jin, X., Chen, C., Li, D., Su, Q., Hang, Y., Zhang, P., & Hu, W. (2017). PRDX2 in myocyte hypertrophy and survival is mediated by TLR4 in acute infarcted myocardium. *Scientific Reports*, *7*(1), 6970. <https://doi.org/10.1038/s41598-017-06718-7>.
25. Han, Y.-H., Jin, M.-H., Jin, Y.-H., Yu, N.-N., Liu, J., Zhang, Y.-Q., ... Sun, H.-N. (2020). Deletion of peroxiredoxin II inhibits the growth of mouse primary mesenchymal stem cells through induction of the G0/G1 cell-cycle arrest and activation of AKT/GSK3β/catenin signaling. *In Vivo*, *34*(1), 133–141. <https://doi.org/10.21873/in vivo.11754>.
26. Di Liegro, C. M., Schiera, G., & Di Liegro, I. (2018). H1.0 linker histone as an epigenetic regulator of cell proliferation and differentiation. *Genes*, *9*(6), 310. <https://doi.org/10.3390/genes9060310>.
27. Chen, E., Yang, L., Ye, C., Zhang, W., Ran, J., Xue, D., ... Hu, Q. (2018). An asymmetric chitosan scaffold for tendon tissue engineering: In vitro and in vivo evaluation with rat tendon stem/progenitor cells. *Acta Biomaterialia*, *73*, 377–387. <https://doi.org/10.1016/j.actbio.2018.04.027>.
28. Torres, C. M., Biran, A., Burney, M. J., Patel, H., Henser-Brownhill, T., Cohen, A.-H. S., ... Scaffidi, P. (2016). The linker histone H1.0 generates epigenetic and functional intratumor heterogeneity. *Science (New York, N.Y.)*, *353*(6307), aaf1644. <https://doi.org/10.1126/science.aaf1644>.
29. Yao, J., Guihard, P. J., Blazquez-Medela, A. M., Guo, Y., Liu, T., Boström, K. I., & Yao, Y. (2016). Matrix Gla protein regulates differentiation of endothelial cells derived from mouse embryonic stem cells. *Angiogenesis*, *19*(1), 1–7. <https://doi.org/10.1007/s10456-015-9484-3>.
30. Feng, Y., Liao, Y., Huang, W., Lai, X., Luo, J., Du, C., ... Zhang, Q. (2018). Mesenchymal stromal cells-derived matrix Gla protein contribute to the alleviation of experimental colitis. *Cell Death & Disease*, *9*(6), 691. <https://doi.org/10.1038/s41419-018-0734-3>.



31. Wei, F.-F., Trenson, S., Monney, P., Yang, W.-Y., Pruijm, M., Zhang, Z.-Y., ... Staessen, J. A. (2018). Epidemiological and histological findings implicate matrix Gla protein in diastolic left ventricular dysfunction. *PLoS ONE*, *13*(3), e0193967. <https://doi.org/10.1371/journal.pone.0193967>.
32. Milliron, H. Y., Weiland, M. J., Kort, E. J., & Jovinge, S. (2019). Isolation of cardiomyocytes undergoing mitosis with complete cytokinesis. *Circulation Research*, *125*(12), 1070–1086. <https://doi.org/10.1161/CIRCRESAHA.119.314908>.
33. Shoji, M., Ueda, M., Nishioka, M., Minato, H., Seki, M., Harada, K., ... Kuzuhara, T. (2019). Jiadifenolide induces the expression of cellular communication network factor (CCN) genes, and CCN2 exhibits neurotrophic activity in neuronal precursor cells derived from human induced pluripotent stem cells. *Biochemical and Biophysical Research Communications*, *519*(2), 309–315. <https://doi.org/10.1016/j.bbrc.2019.09.003>.
34. Li, H., Yao, Z., He, W., Gao, H., Bai, Y., Yang, S., ... Luo, G. (2016). P311 induces the transdifferentiation of epidermal stem cells to myofibroblast-like cells by stimulating transforming growth factor  $\beta$ 1 expression. *Stem Cell Research & Therapy*, *7*, 175. <https://doi.org/10.1186/s13287-016-0421-1>.
35. Tan, J., Peng, X., Luo, G., Ma, B., Cao, C., He, W., ... Wu, J. (2010). Investigating the role of P311 in the hypertrophic scar. *PLoS ONE*, *5*(4), e9995. <https://doi.org/10.1371/journal.pone.0009995>.
36. Plaisance, I., Perruchoud, S., Fernandez-Tenorio, M., Gonzales, C., Ounzain, S., Ruchat, P., ... Pedrazzini, T. (2016). Cardiomyocyte lineage specification in adult human cardiac precursor cells via modulation of enhancer-associated long noncoding RNA expression. *JACC: Basic to Translational Science*, *1*(6), 472–493. <https://doi.org/10.1016/j.jacbts.2016.06.008>.
37. Wang, Y., Niu, Z., Guo, Y., Wang, L., Lin, F., & Zhang, J. (2017). IL-11 promotes the treatment efficacy of hematopoietic stem cell transplant therapy in aplastic anemia model mice through a NF- $\kappa$ B/microRNA-204/thrombopoietin regulatory axis. *Experimental & Molecular Medicine*, *49*(12), e410–e410. <https://doi.org/10.1038/emm.2017.217>.
38. Tsujioka, H., Kunieda, T., Katou, Y., Shirahige, K., Fukazawa, T., & Kubo, T. (2017). interleukin-11 induces and maintains progenitors of different cell lineages during *Xenopus* tadpole tail regeneration. *Nature Communications*, *8*(1), 495. <https://doi.org/10.1038/s41467-017-00594-5>.
39. Obana, M., Maeda, M., Takeda, K., Hayama, A., Mohri, T., Yamashita, T., ... Fujio, Y. (2010). Therapeutic activation of signal transducer and activator of transcription 3 by interleukin-11 ameliorates cardiac fibrosis after myocardial infarction. *Circulation*, *121*(5), 684–691. <https://doi.org/10.1161/CIRCULATIONAHA.109.893677>.
40. Graustein, A. D., Misch, E. A., Musvosvi, M., Shey, M., Shah, J. A., Seshadri, C., ... Hawn, T. R. (2018). Toll-like receptor chaperone HSP90B1 and the immune response to *Mycobacteria*. *PLoS ONE*, *13*(12), e0208940. <https://doi.org/10.1371/journal.pone.0208940>.
41. Ben Mkaddem, S., Pedruzzi, E., Werts, C., Coant, N., Bens, M., Cluzeaud, F., ... Vandewalle, A. (2010). Heat shock protein gp96 and NAD(P)H oxidase 4 play key roles in Toll-like receptor 4-activated apoptosis during renal ischemia/reperfusion injury. *Cell Death & Differentiation*, *17*(9), 1474–1485. <https://doi.org/10.1038/cdd.2010.26>.
42. Kern, P., Balzer, N. R., Bender, F., Frolov, A., Sowa, J.-P., Bonaguro, L., ... Mass, E. (2020). Creld2 function during unfolded protein response is essential for liver metabolism homeostasis. *bioRxiv*, 2020.01.28.923136. <https://doi.org/10.1101/2020.01.28.923136>.
43. Kim, Y., Park, S.-J., Manson, S. R., Molina, C. A. F., Kidd, K., Thiessen-Philbrook, H., ... Chen, Y. M. (n.d.). Elevated urinary CRELD2 is associated with endoplasmic reticulum stress-mediated kidney disease. *JCI Insight*, *2*(23), e92896. <https://doi.org/10.1172/jci.insight.92896>.
44. Lim, K., Lim, K., Price, A., Orr, B., Eberhart, C., & Bar, E. (2014). Inhibition of monocarboxylate transporter-4 depletes stem-like glioblastoma cells and inhibits HIF transcriptional response in a lactate-independent manner. *Oncogene*, *33*(35), 4433–4441. <https://doi.org/10.1038/onc.2013.390>.
45. Zhu, Y., Wu, J., & Yuan, S.-Y. (2013). MCT1 and MCT4 expression during myocardial ischemic-reperfusion injury in the isolated rat heart. *Cellular Physiology and Biochemistry: International Journal of Experimental Cellular Physiology, Biochemistry, and Pharmacology*, *32*(3), 663–674. <https://doi.org/10.1159/000354470>.
46. Pang, Z., Junkins, R. D., Raudonis, R., MacNeil, A. J., McCormick, C., Cheng, Z., & Lin, T.-J. (2018). Regulator of calcineurin 1 differentially regulates TLR-dependent MyD88 and TRIF signaling pathways. *PLoS ONE*, *13*(5), e0197491. <https://doi.org/10.1371/journal.pone.0197491>.
47. Corbalan, J. J., & Kitsis, R. N. (2018). RCAN1–calcineurin axis and the set-point for myocardial damage during ischemia-reperfusion. *Circulation Research*, *122*(6), 796–798. <https://doi.org/10.1161/CIRCRESAHA.118.312787>.
48. Sobrado, M., Ramirez, B. G., Neria, F., Lizasoain, I., Arbones, M. L., Minami, T., ... Cano, E. (2012). Regulator of calcineurin 1 (Rcan1) has a protective role in brain ischemia/reperfusion injury. *Journal of Neuroinflammation*, *9*(1), 48. <https://doi.org/10.1186/1742-2094-9-48>.
49. Hesse, J., Owenier, C., Lautwein, T., Zalfen, R., Weber, J. F., Ding, Z., ... Schrader, J. (2021). Single-cell transcriptomics defines heterogeneity of epicardial cells and fibroblasts within the infarcted murine heart. *eLife*, *10*, e65921. <https://doi.org/10.7554/eLife.65921>.
50. Cui, Y., Zheng, Y., Liu, X., Yan, L., Fan, X., Yong, J., ... Tang, F. (2019). Single-cell transcriptome analysis maps the developmental track of the human heart. *Cell Reports*, *26*(7), 1934–1950.e5. <https://doi.org/10.1016/j.celrep.2019.01.079>.
51. Ruiz-Villalba, A., Romero, J. P., Hernández, S. C., Vilas-Zornoza, A., Fortelny, N., Castro-Labrador, L., ... Prósper, F. (2020). Single-cell rna sequencing analysis reveals a crucial role for CTHRC1 (collagen triple helix repeat containing 1) cardiac fibroblasts after myocardial infarction. *Circulation*, *142*(19), 1831–1847. <https://doi.org/10.1161/CIRCULATIONAHA.119.044557>.

**Publisher's Note** Springer Nature remains neutral with regard to jurisdictional claims in published maps and institutional affiliations.